A problem dependent analysis of SOCP algorithms in noisy compressed sensing

MIHAILO STOJNIC

School of Industrial Engineering
Purdue University, West Lafayette, IN 47907
e-mail: mstojnic@purdue.edu

Abstract

Under-determined systems of linear equations with sparse solutions have been the subject of an extensive research in last several years above all due to results of [9, 10, 21]. In this paper we will consider *noisy* under-determined linear systems. In a breakthrough [10] it was established that in *noisy* systems for any linear level of under-determinedness there is a linear sparsity that can be *approximately* recovered through an SOCP (second order cone programming) optimization algorithm so that the approximate solution vector is (in an ℓ_2-norm sense) guaranteed to be no further from the sparse unknown vector than a constant times the noise. In our recent work [53] we established an alternative framework that can be used for statistical performance analysis of the SOCP algorithms. To demonstrate how the framework works we then showed in [53] how one can use it to precisely characterize the *generic* (worst-case) performance of the SOCP. In this paper we present a different set of results that can be obtained through the framework of [53]. The results will relate to *problem dependent* performance analysis of SOCP's. We will consider specific types of unknown sparse vectors and characterize the SOCP performance when used for recovery of such vectors. We will also show that our theoretical predictions are in a solid agreement with the results one can get through numerical simulations.

Index Terms: Noisy systems of linear equations; SOCP; ℓ_1-optimization; compressed sensing.

1 Introduction

In recent years there has been an enormous interest in studying under-determined systems of linear equations with sparse solutions. With potential applications ranging from high-dimensional geometry, image reconstruction, single-pixel camera design, decoding of linear codes, channel estimation in wireless communications, to machine learning, data-streaming algorithms, DNA micro-arrays, magneto-encephalography etc. (see, e.g. [3, 8, 11, 18, 26, 38, 42, 46–49, 56, 65, 67] and references therein) studying these systems seems to be of substantial theoretical/practical importance in a variety of different area. In this paper we study mathematical aspects of under-determined systems and put an emphasis on theoretical analysis of particular algorithms used for solving them.

In its simplest form solving an under-determined system of linear equations amounts to finding a, say, k-sparse $\mathbf{x}$ such that

$$A\mathbf{x}=\mathbf{y} \tag{1}$$

where A is an $m\times n$ ($m<n$) matrix and $\mathbf{y}$ is an $m\times 1$ vector (see Figure 1; here and in the rest of the

paper, under k-sparse vector we assume a vector that has at most k nonzero components). Of course, the assumption will be that such an $\mathbf{x}$ exists. To make writing in the rest of the paper easier, we will assume the so-called *linear* regime, i.e. we will assume that $k=\beta n$ and that the number of equations is $m=\alpha n$ where α and β are constants independent of n (more on the non-linear regime, i.e. on the regime when m is larger than linearly proportional to k can be found in e.g. [17, 30, 31]).

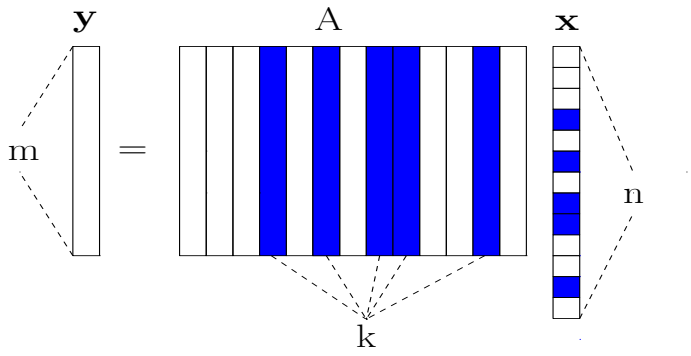

Figure 1: Model of a linear system; vector $\mathbf{x}$ is k-sparse

Clearly, if $k\leq\frac{m}{2}$ the solution is unique and can be found through an exhaustive search. However, in the linear regime that we have just assumed above (and will consider throughout the paper) the exhaustive search is clearly of exponential complexity. Instead one can of course design algorithms of much lower complexity while sacrificing on the recovery abilities, i.e. on the recoverable size of the nonzero portion of vector $\mathbf{x}$. Various algorithms have been introduced and analyzed in recent years throughout the literature from those that relate to the parallel design of matrix A and the recovery algorithms (see, e.g. [1, 34, 35, 39, 45, 68]) to those that assume only the design of the recovery algorithms (see, e.g. [10, 19, 21, 25, 43, 44, 62, 63]). If one restricts to the algorithms of polynomial complexity and allows for the design of A then the results from [1, 39, 45] that guarantee recovery of *any* k-sparse $\mathbf{x}$ in (1) for any $0<\alpha\leq 1$ and any $\beta\leq\frac{\alpha}{2}$ are essentially optimal. On the other hand, if one restricts to the algorithms of polynomial complexity and does not allow for the parallel design of A then the results of [10, 21] established that for any $\alpha>0$ there still exists a $\beta>0$ such that any $k=\beta n$-sparse $\mathbf{x}$ in (1) can be recovered via a polynomial time *Basis pursuit* (BP) algorithm.

Since the BP algorithm is fairly closely related to what we will be presenting later in the paper we will now briefly introduce it (we will often refer to it as the ℓ_1-optimization concept; a slight modification/adaptation of it will actually be the main topic of this paper). Variations of the standard ℓ_1-optimization from e.g. [12, 16, 51] as well as those from [28, 32, 50] related to ℓ_q-optimization, $0<q<1$, are possible as well; moreover they can all be incorporated in what we will present below. The ℓ_1-optimization concept suggests that one can maybe find the k-sparse $\mathbf{x}$ in (1) by solving the following ℓ_1-norm minimization problem

$$\begin{aligned} \min \quad & \|\mathbf{x}\|_1 \\ \text{subject to} \quad & A\mathbf{x}=\mathbf{y}. \end{aligned} \tag{2}$$

As mentioned above the results from [10, 21] were instrumental in theoretical characterization of (2) and its popularization in sparse recovery and even more so in generating an unprecedented interest in sparse recovery algorithms. The main reason is of course the quality of the results achieved in [10,21]. Namely, [10] established that for any $\alpha>0$ there is a $\beta>0$ such that the solution of (2) is the $k=\beta n$-sparse $\mathbf{x}$ in (1). In a statistical and large dimensional context in [21] and later in [55, 57] for any given value of α the exact value of the maximum possible β was determined.

The above sparse recovery scenario is in a sense idealistic. Namely, it assumes that $\mathbf{y}$ in (2) was obtained through (1). On other hand in many applications only a *noisy* version of $A\mathbf{x}$ may be available for $\mathbf{y}$ (this is especially so in measuring type of applications) see, e.g. [10, 33, 66] (another somewhat related version of "imperfect" linear systems are the under-determined systems with the so-called approximately sparse solutions; more in this direction can be found in e.g. [10, 59]). When that happens one has the following equivalent to (1) (see, Figure 2)

$$\mathbf{y} = A\mathbf{x} + \mathbf{v}, \tag{3}$$

where $\mathbf{v}$ is an $m \times 1$ so-called noise vector (the so-called ideal case presented above is of course a special case of the noisy one given in (3)). Finding the k-sparse $\mathbf{x}$ in (3) is now incredibly hard. In fact it is pretty much

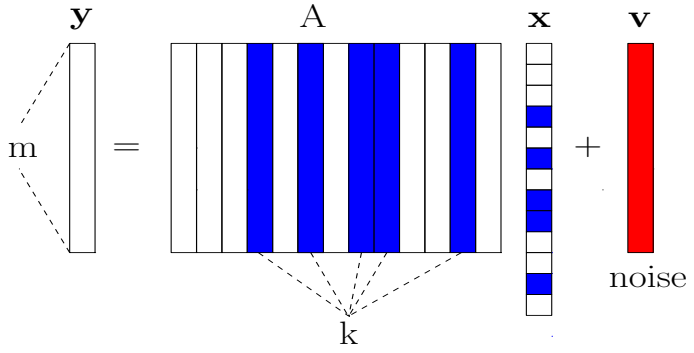

Figure 2: Model of a linear system; vector $\mathbf{x}$ is k-sparse

impossible. Basically, one is looking for a k-sparse $\mathbf{x}$ such that (3) holds and on top of that $\mathbf{v}$ is unknown. Although the problem is hard there are various heuristics throughout the literature that one can use to solve it approximately. Majority of these heuristics are based on appropriate generalizations of the corresponding algorithms one would use in the noiseless case. Thinking along the same lines as in the noiseless case one can distinguish two scenarios depending on the availability of the freedom to choose/design A. If one has the freedom to design A then one can adapt the corresponding noiseless algorithms to the noisy scenario as well (more on this can be found in e.g. [5]). However, in this paper we mostly focus on the scenario where one has no control over A. In such a scenario one can again make a parallel to the noiseless case and look at e.g. CoSAMP algorithm from [43] or Subspace pursuit from [20]. Essentially, in a statistical context, these algorithms can provably recover a linear sparsity while maintaining the approximation error proportional to the norm-2 of the noise vector which is pretty much a benchmark of what is currently known. These algorithms are in a way perfected noisy generalizations of the so-called *Orthogonal matching pursuit* (OMP) algorithms.

On the other hand in this paper we will focus on generalizations of BP that can handle the noisy case. To introduce a bit or tractability in finding the k-sparse $\mathbf{x}$ in (3) one usually assumes certain amount of knowledge about either $\mathbf{x}$ or $\mathbf{v}$. As far as the tractability assumptions on $\mathbf{v}$ are concerned one typically (and possibly fairly reasonably in applications of interest) assumes that $\|\mathbf{v}\|_2$ is bounded (or highly likely to be bounded) from above by a certain known quantity. The following second-order cone programming (SOCP) analogue to (or say noisy generalization of) (2) is one of the approaches that utilizes such an assumption (more on this approach and its variations can be found in e.g. [10])

$$\begin{aligned} \min_{\mathbf{x}} \quad & \|\mathbf{x}\|_1 \\ \text{subject to} \quad & \|\mathbf{y} - A\mathbf{x}\|_2 \leq r_{socp} \end{aligned} \tag{4}$$

where r_{socp} is a quantity such that $\|\mathbf{v}\|_2 \leq r_{socp}$ (or r_{socp} is a quantity such that $\|\mathbf{v}\|_2 \leq r_{socp}$ is say highly

likely). For example, in [10] a statistical context is assumed and based on the statistics of $\mathbf{v}$, r_{socp} was chosen such that $\|\mathbf{v}\|_2 \leq r_{socp}$ happens with overwhelming probability (as usual, under overwhelming probability we in this paper assume a probability that is no more than a number exponentially decaying in n away from 1). Given that (4) is now among few almost standard choices when it comes to finding an approximation to the k-sparse $\mathbf{x}$ in (3), the literature on its properties is vast (see, e.g. [10, 24, 33, 61] and references therein). We here briefly mention only what we consider to be the most influential work on this topic in recent years. Namely, in [10] the authors analyzed performance of (4) and showed a result similar in flavor to the one that holds in the ideal - noiseless - case. In a nutshell the following was shown in [10]: let $\mathbf{x}$ be a βn-sparse vector such that (3) holds and let $\mathbf{x}_{socp}$ be the solution of (4). Then

$$\|\mathbf{x}_{socp} - \mathbf{x}\|_2 \leq C r_{socp} \tag{5}$$

where β is a constant independent of n and C is a constant independent of n and of course dependent on α and β. This result in a sense establishes a noisy equivalent to the fact that a linear sparsity can be recovered from an under-determined system of linear equations. In an informal language, it states that a linear sparsity can be *approximately* recovered in polynomial time from a noisy under-determined system with the norm of the recovery error guaranteed to be within a constant multiple of the noise norm (as mentioned above, the same was also established later in [43] for CoSAMP and in [20] for Subspace pursuit). Establishing such a result is, of course, a feat in its own class, not only because of its technical contribution but even more so because of the amount of interest that it generated in the field.

In our recent work [53] we designed a framework for performance analysis of the SOCP algorithm from (4). We then went further in [53] and showed how the framework practically works through a precise characterization of the *generic* (worst-case) performance of the SOCP from (4). In this paper we will again focus on the general framework developed in [53]. This time though we will focus on the *problem dependent* performance analysis of the SOCP. In other words, we will consider specific types of unknown sparse vectors $\mathbf{x}$ in (3) and provide a performance analysis of the SOCP when applied for recovery of such vectors.

Before going into the details of the SOCP approach we should also mention that the SOCP algorithms are of course not the only possible generalizations (adaptations) of ℓ_1 optimization to the noisy case. For example, LASSO algorithms (more on these algorithms can be found in e.g. [7, 14, 15, 41, 60, 64] as well as in recent developments [4, 22, 52]) are a very successful alternative. In our recent work [52] we established a nice connection between some of the algorithms from the LASSO group and certain SOCP algorithms and showed that with respect to certain performance measure they could be equivalent. Besides the LASSO algorithms the so-called Dantzig selector introduced in [13] is another alternative to the SOCP algorithms that is often encountered in the literature (more on the Dantzig selector as well as on its relation to the LASSO or SOCP algorithms can be found in e.g. [2, 6, 27, 29, 36, 37, 40]). Depending on the scenarios they are to be applied in each of these algorithms can have certain advantages/disadvantages over the other ones. A simple (general) characterization of these advantages/disadvanatges does not seem easy to us. In a rather informal language one could say that LASSO and SOCP are expected to perform better (i.e. to provide a solution vector that is under various metrics closer to the unknown one) in a larger set of different scenarios but as quadratic programs could be slower than the Dantzig selector which happens to be a linear program. Of course, whether LASSO or SOCP algorithms are indeed going to be slower or not or how much larger would be a set of different scenarios where they are expected to perform better are interesting/important questions. While clearly of interest answering these questions certainly goes way beyond the scope of the present paper and we will not pursue it here any further.

Before we proceed with the exposition we briefly summarize the organization of the rest of the paper. In Section 2, we recall on a set of powerful results presented in [53] and discuss further how they can be utilized to analyze the problem dependent performance of the SOCP from (4). The results that we will present in Section 2 will relate to the so-called general sparse signals $\tilde{\mathbf{x}}$. In Section 3 we will show how

these results from Section 2 that relate to the general sparse vectors $\tilde{\mathbf{x}}$ can be specialized further so they cover the so-called signed vectors $\mathbf{x}$. Finally, in Section 4 we will discuss obtained results.

2 SOCP's problem dependent performance – general $\mathbf{x}$

In this section we first recall on the basic properties of the statistical SOCP's performance analysis framework developed in [53]. We will then show how the framework can be used to characterize the SOCP from (4) in certain situations when the SOCP's performance substantially depends on $\tilde{\mathbf{x}}$.

2.1 Basic properties of the SOCP's framework

Before proceeding further we will now first state major assumptions that will be in place throughout the paper (clearly, since we will be utilizing the framework of [53] a majority of these assumptions was already present in [53]). Namely, as mentioned above, we will consider noisy under-determined systems of linear equations. The systems will be defined by a random matrix A where the elements of A are i.i.d. standard normal random variables. Also, we will assume that the elements of $\mathbf{v}$ are i.i.d. Gaussian random variables with zero mean and variance σ. $\tilde{\mathbf{x}}$ will be assumed to be the original $\mathbf{x}$ in (3) that we are trying to recover (or a bit more precisely approximately recover). We will assume that $\tilde{\mathbf{x}}$ is *any* k-sparse vector with a given fixed location of its nonzero elements and a given fixed combination of their signs. Due to assumed statistics the analysis (and the performance of (4)) will clearly be irrelevant with respect to what particular location and what particular combination of signs of nonzero elements are chosen. We will therefore for the simplicity of the exposition and without loss of generality assume that the components $\mathbf{x}_1, \mathbf{x}_2, \ldots, \mathbf{x}_{n-k}$ of $\mathbf{x}$ are equal to zero and the components $\mathbf{x}_{n-k+1}, \mathbf{x}_{n-k+2}, \ldots, \mathbf{x}_n$ of $\mathbf{x}$ are greater than or equal to zero. Moreover, throughout the paper we will call such an $\mathbf{x}$ k-sparse and positive. In a more formal way we will set

$$\begin{aligned} &\tilde{\mathbf{x}}_1 = \tilde{\mathbf{x}}_2 = \cdots = \tilde{\mathbf{x}}_{n-k} = 0 \\ &\tilde{\mathbf{x}}_{n-k+1} \geq 0, \tilde{\mathbf{x}}_{n-k+1} \geq 0, \ldots, \tilde{\mathbf{x}}_n \geq 0. \end{aligned} \tag{6}$$

We also now take the opportunity to point out a rather obvious detail. Namely, the fact that $\tilde{\mathbf{x}}$ is positive is assumed for the purpose of the analysis. However, this fact is not known *a priori* and is not available to the solving algorithm (this will of course change in Section 3).

Before proceeding further we will introduce a few definitions that will be useful in formalizing/presenting our results as well as in conducting the entire analysis. Following what was done in [53] let us define the optimal value of a slightly changed objective of (4) in the following way

$$\begin{aligned} f_{obj}(\sigma, \tilde{\mathbf{x}}, A, \mathbf{v}, r_{socp}) = \min_{\mathbf{x}} \quad & \|\mathbf{x}\|_1 - \|\tilde{\mathbf{x}}\|_1 \\ \text{subject to} \quad & \|\mathbf{y} - A\mathbf{x}\|_2 \leq r_{socp}. \end{aligned} \tag{7}$$

To make writing easier we will instead of $f_{obj}(\sigma, \tilde{\mathbf{x}}, A, \mathbf{v}, r_{socp})$ write just f_{obj}. A similar convention will be applied to few other functions throughout the paper. On many occasions, though, (especially where we deem it as substantial to the presentation) we will also keep all (or a majority of) arguments of the corresponding functions.

Also let $\mathbf{x}_{socp}$ be the solution of (4) (or the solution of (7)) and let $\mathbf{w}_{socp} \in R^n$ be the so-called error vector defined in the following way

$$\mathbf{w}_{socp} = \mathbf{x}_{socp} - \tilde{\mathbf{x}}. \tag{8}$$

Our main goal in this paper will then boil down to various characterizations of $\mathbf{w}_{socp}$ and f_{obj}. Throughout the paper we will heavily rely on the following theorem from [53] that provides a general characterization

of $\mathbf{w}_{socp}$ and f_{obj}.

Theorem 1. *([53] — SOCP's performance characterization) Let* $\mathbf{v}$ *be an* $n \times 1$ *vector of i.i.d. zero-mean variance* σ^2 *Gaussian random variables and let* A *be an* $m \times n$ *matrix of i.i.d. standard normal random variables. Further, let* $\mathbf{g}$ *and* $\mathbf{h}$ *be* $m \times 1$ *and* $n \times 1$ *vectors of i.i.d. standard normals, respectively and let* $\mathbf{z}$ *be* $n \times 1$ *vector of all ones. Consider a* k*-sparse* $\tilde{\mathbf{x}}$ *defined in (6) and a* $\mathbf{y}$ *defined in (3) for* $\mathbf{x} = \tilde{\mathbf{x}}$*. Let the solution of (4) be* $\mathbf{x}_{socp}$ *and let the so-called error vector of the SOCP from (4) be* $\mathbf{w}_{socp} = \mathbf{x}_{socp} - \tilde{\mathbf{x}}$*. Let* r_{socp} *in (4) be a positive scalar. Let* n *be large and let constants* $\alpha = \frac{m}{n}$ *and* $\beta_w = \frac{k}{n}$ *be below the following so-called* fundamental *characterization of* ℓ_1 *optimization*

$$(1-\beta_w)\frac{\sqrt{\frac{2}{\pi}}e^{-(erfinv(\frac{1-\alpha_w}{1-\beta_w}))^2}}{\alpha_w} - \sqrt{2}erfinv(\frac{1-\alpha_w}{1-\beta_w}) = 0. \tag{9}$$

Consider the following optimization problem:

$$\begin{aligned} \xi_{prim}(\sigma, \mathbf{g}, \mathbf{h}, \tilde{\mathbf{x}}, r_{socp}) = \max_{\nu,\lambda} \quad & \sigma\sqrt{\|\mathbf{g}\|_2^2\nu^2 - \|\nu\mathbf{h} + \mathbf{z} - \lambda\|_2^2} - \sum_{i=n-k+1}^{n} \lambda_i \tilde{\mathbf{x}}_i - \nu r_{socp} \\ \textit{subject to} \quad & \nu \geq 0 \\ & 0 \leq \lambda_i \leq 2, 1 \leq i \leq n. \end{aligned} \tag{10}$$

Let $\hat{\nu}$ *and* $\hat{\lambda}$ *be the solution of (10). Set*

$$\|\hat{\mathbf{w}}\|_2 = \sigma\frac{\|\hat{\nu}\mathbf{h} + \mathbf{z} - \hat{\lambda}\|_2}{\sqrt{\|\mathbf{g}\|_2^2\hat{\nu}^2 - \|\hat{\nu}\mathbf{h} + \mathbf{z} - \hat{\lambda}\|_2^2}}. \tag{11}$$

Then:

$$\begin{aligned} P(\|\tilde{\mathbf{x}} + \mathbf{w}_{socp}\|_1 - \|\tilde{\mathbf{x}}\|_1 \in (E\xi_{prim}(\sigma, \mathbf{g}, \mathbf{h}, \tilde{\mathbf{x}}, r_{socp})) - \epsilon_1^{(socp)}|E\xi_{prim}(\sigma, \mathbf{g}, \mathbf{h}, \tilde{\mathbf{x}}, r_{socp}))|, \\ E\xi_{prim}(\sigma, \mathbf{g}, \mathbf{h}, \tilde{\mathbf{x}}, r_{socp})) + \epsilon_1^{(socp)}|E\xi_{prim}(\sigma, \mathbf{g}, \mathbf{h}, \tilde{\mathbf{x}}, r_{socp}))|) = 1 - e^{-\epsilon_2^{(socp)}n} \end{aligned} \tag{12}$$

and

$$P((1-\epsilon_1^{(socp)})E\|\hat{\mathbf{w}}\|_2 \leq \|\mathbf{w}_{socp}\|_2 \leq (1+\epsilon_1^{(socp)})E\|\hat{\mathbf{w}}\|_2) = 1 - e^{-\epsilon_2^{(socp)}n}, \tag{13}$$

where $\epsilon_1^{(socp)} > 0$ *is an arbitrarily small constant and* $\epsilon_2^{(socp)}$ *is a constant dependent on* $\epsilon_1^{(socp)}$ *and* σ *but independent of* n*.*

Proof. Presented in [53]. □

Remark: A pair (α, β_w) lies below the fundamental characterization (9) if $\alpha > \alpha_w$ and α_w and β_w are such that (9) holds.

2.2 Problem dependent properties of the framework

To facilitate the exposition that will follow we similarly to what was done in [53, 54, 57] set

$$\bar{\mathbf{h}} = [|\mathbf{h}|_{(1)}^{(1)}, |\mathbf{h}|_{(2)}^{(2)}, \ldots, |\mathbf{h}|_{(n-k)}^{(n-k)}, \mathbf{h}_{n-k+1}^{(k)}, \mathbf{h}_{n-k+2}^{(k-1)}, \ldots, \mathbf{h}_n^{(1)}]^T, \tag{14}$$

where $[|\mathbf{h}|_{(1)}^{(1)}, |\mathbf{h}|_{(2)}^{(2)}, \ldots, |\mathbf{h}|_{(n-k)}^{(n-k)}]$ are the magnitudes of $[\mathbf{h}_1, \mathbf{h}_2, \ldots, \mathbf{h}_{n-k}]$ sorted in increasing order and $[\mathbf{h}_{n-k+1}^{(k)}, \mathbf{h}_{n-k+2}^{(k-1)}, \ldots, \mathbf{h}_n^{(1)}]$ are the elements of $[-\mathbf{h}_{n-k+1}, -\mathbf{h}_{n-k+2}, \ldots, -\mathbf{h}_n]$ sorted in decreasing order

(possible ties in the sorting processes are of course broken arbitrarily). One can then rewrite the optimization problem from (10) in the following way

$$\begin{aligned}\xi_{prim}(\sigma,\mathbf{g},\mathbf{h},\tilde{\mathbf{x}},r_{socp}) = \max_{\nu,\lambda} \quad & \sigma\sqrt{\|\mathbf{g}\|_2^2\nu^2 - \|\nu\bar{\mathbf{h}}-\mathbf{z}+\lambda\|_2^2} - \sum_{i=n-k+1}^{n}\lambda_i\tilde{\mathbf{x}}_i - \nu r_{socp} \\ \text{subject to} \quad & \nu \geq 0 \\ & 0 \leq \lambda_i \leq 1, 1 \leq i \leq n-k \\ & 0 \leq \lambda_i \leq 2, n-k+1 \leq i \leq n. \end{aligned} \tag{15}$$

In what follows we will restrict our attention to a specific class of unknown vectors $\tilde{\mathbf{x}}$. Namely, we will consider vectors $\tilde{\mathbf{x}}$ that have amplitude of the nonzero components equal to x_{mag}. In the noiseless case these problem instances are typically the hardest to solve (at least as long as one uses the ℓ_1 optimization from (2)). We will again emphasize that the fact that magnitudes of the nonzero elements of $\tilde{\mathbf{x}}$ are x_{mag} is not known a priori and can not be used in the solving algorithm (i.e. one can not add constraints that would exploit this knowledge in optimization problem (4)). It is just that we will consider how the SOCP from (4) behaves when used to solve problem instances generated by such an $\tilde{\mathbf{x}}$. Also, for such an $\tilde{\mathbf{x}}$ (15) can be rewritten in the following way

$$\begin{aligned}\xi^{(dep)}_{prim}(\sigma,\mathbf{g},\mathbf{h},x_{mag},r_{socp}) = \max_{\nu,\lambda} \quad & \sigma\sqrt{\|\mathbf{g}\|_2^2\nu^2 - \|\nu\bar{\mathbf{h}}-\mathbf{z}+\lambda\|_2^2} - x_{mag}\sum_{i=n-k+1}^{n}\lambda_i - \nu r_{socp} \\ \text{subject to} \quad & \nu \geq 0 \\ & 0 \leq \lambda_i \leq 1, 1 \leq i \leq n-k \\ & 0 \leq \lambda_i \leq 2, n-k+1 \leq i \leq n. \end{aligned} \tag{16}$$

Now, let ν_{dep} and $\lambda^{(dep)}$ be the solution of (16). Then analogously to (11) we can set

$$\|\mathbf{w}_{dep}\|_2 = \sigma\frac{\|\nu_{dep}\bar{\mathbf{h}}-\mathbf{z}+\lambda^{(dep)}\|_2}{\sqrt{\|\mathbf{g}\|_2^2\nu_{dep}^2 - \|\nu_{dep}\bar{\mathbf{h}}-\mathbf{z}+\lambda^{(dep)}\|_2^2}}, \tag{17}$$

In what follows we will determine $\|\mathbf{w}_{dep}\|_2$ and $\xi^{(dep)}_{prim}(\sigma,\mathbf{g},\mathbf{h},x_{mag},r_{socp})$ or more precisely their concentrating points $E\|\mathbf{w}_{dep}\|_2$ and $E\xi^{(dep)}_{prim}(\sigma,\mathbf{g},\mathbf{h},x_{mag},r_{socp})$. All other parameters such as ν_{dep}, $\lambda^{(dep)}$ can (and some of them will) be computed through the framework as well. We do however mention right here that what we present below assumes a fair share of familiarity with the techniques introduced in our earlier papers [52,53,57]. To shorten the exposition we will skip many details presented in those papers and present only the key differences.

We proceed by following the line of thought presented in [53, 57]. Since $\lambda^{(dep)}$ is the solution of (16) there will be parameters c_1, c_2, and c_3 such that

$$\lambda^{(dep)} = [\lambda^{(dep)}_1, \lambda^{(dep)}_2, \ldots, \lambda^{(dep)}_{c_1}, 0, 0, \ldots, 0, \lambda^{(dep)}_{c_2+1}, \lambda^{(dep)}_{c_2+2}, \ldots, \lambda^{(dep)}_{n-c_3}, 2, 2, \ldots, 2]$$

and obviously $c_1 \leq n-k$, $n-k \leq c_2 \leq n$, and $0 \leq c_3 \leq n-c_2$. At this point let us assume that these parameters are known and fixed. Then following [53, 57] the optimization problem from (16) can be

rewritten in the following way

$$\begin{aligned}\xi_{prim}(\sigma,\mathbf{g},\mathbf{h},\tilde{\mathbf{x}},r_{socp}) = \max_{\nu,\lambda_{c_1+1:n}} \quad & \sigma\sqrt{\|\mathbf{g}\|_2^2\nu^2 - \|\nu\bar{\mathbf{h}}_{c_1+1:n} - \mathbf{z}_{c_1+1:n} + \lambda_{c_1+1:n}\|_2^2} - x_{mag}\sum_{i=n-k+1}^{n}\lambda_i - \nu r_{socp} \\ \text{subject to} \quad & \nu \geq 0 \\ & 0 \leq \lambda_i \leq 2, c_2 \leq i \leq n-c_3 \\ & \lambda_i = 2, n-c_3+1 \leq i \leq n \\ & \lambda_i = 0, c_1+1 \leq i \leq n-k. \end{aligned} \tag{18}$$

To make writing of what will follow somewhat easier we set

$$\xi^{(obj)} = \sigma\sqrt{\|\mathbf{g}\|_2^2\nu^2 - \|\nu\bar{\mathbf{h}}_{c_1+1:n} - \mathbf{z}_{c_1+1:n} + \lambda_{c_1+1:n}\|_2^2} - x_{mag}\sum_{i=n-k+1}^{n}\lambda_i - \nu r_{socp}. \tag{19}$$

We then proceed by solving the optimization in (18) over ν and $\lambda_{c_1+1:n}$. To do so we first look at the derivatives with respect to $\lambda_i, c_2+1 \leq i \leq n-c_3$, of the objective in (18). Computing the derivatives and equalling them to zero gives

$$\begin{aligned} & \frac{d\xi^{(obj)}}{d\lambda_i} = 0, c_2+1 \leq i \leq n-c_3 \\ \iff \quad & \sigma\frac{-(\nu\bar{\mathbf{h}}_i - \mathbf{z}_i + \lambda_i)}{\sqrt{\|\mathbf{g}\|_2^2\nu^2 - \|\nu\bar{\mathbf{h}}_{c_1+1:n} - \mathbf{z}_{c_1+1:n} + \lambda_{c_1+1:n}\|_2^2}} - x_{mag} = 0, c_2+1 \leq i \leq n-c_3 \\ \iff \quad & \lambda_i - \mathbf{z}_i + \nu\bar{\mathbf{h}}_i = -\frac{x_{mag}}{\sigma}\sqrt{\|\mathbf{g}\|_2^2\nu^2 - \|\nu\bar{\mathbf{h}}_{c_1+1:n} - \mathbf{z}_{c_1+1:n} + \lambda_{c_1+1:n}\|_2^2}, c_2+1 \leq i \leq n-c_3 \\ \iff \quad & \lambda_i = -\frac{x_{mag}}{\sigma}\sqrt{\|\mathbf{g}\|_2^2\nu^2 - \|\nu\bar{\mathbf{h}}_{c_1+1:n} - \mathbf{z}_{c_1+1:n} + \lambda_{c_1+1:n}\|_2^2} + \mathbf{z}_i - \nu\bar{\mathbf{h}}_i, c_2+1 \leq i \leq n-c_3. \end{aligned} \tag{20}$$

From the second to last line in the above equation one then has

$$\begin{aligned}(\lambda_i - \mathbf{z}_i + \nu\bar{\mathbf{h}}_i)^2 = \frac{x_{mag}^2}{\sigma^2}(&\|\mathbf{g}\|_2^2\nu^2 - \|\nu\bar{\mathbf{h}}_{c_1+1:c_2} - \mathbf{z}_{c_1+1:c_2} + \lambda_{c_1+1:c_2}\|_2^2 \\ &- \|\nu\bar{\mathbf{h}}_{c_2+1:n-c_3} - \mathbf{z}_{c_2+1:n-c_3}\|_2^2 - \|\nu\bar{\mathbf{h}}_{n-c_3+1:n} + \mathbf{z}_{n-c_3+1:n}\|_2^2)\end{aligned} \tag{21}$$

and after an easy algebraic transformation

$$(\lambda_i - \mathbf{z}_i + \nu\bar{\mathbf{h}}_i)^2 = \frac{x_{mag}^2}{\sigma^2 + (n-c_2-c_3)x_{mag}^2}(\|\mathbf{g}\|_2^2\nu^2 - \|\nu\bar{\mathbf{h}}_{c_1+1:c_2} - \mathbf{z}_{c_1+1:c_2}\|_2^2 - \|\nu\bar{\mathbf{h}}_{n-c_3+1:n} + \mathbf{z}_{n-c_3+1:n}\|_2^2). \tag{22}$$

Using (22) we further have

$$\begin{aligned}
&\sqrt{\|\mathbf{g}\|_2^2\nu^2 - \|\nu\bar{\mathbf{h}}_{c_1+1:n} - \mathbf{z}_{c_1+1:n} + \lambda_{c_1+1:n}\|_2^2} \\
&= \sqrt{\|\mathbf{g}\|_2^2\nu^2 - \|\nu\bar{\mathbf{h}}_{c_1+1:c_2} - \mathbf{z}_{c_1+1:c_2}\|_2^2 - \|\nu\bar{\mathbf{h}}_{c_2+1:n-c_3} - \mathbf{z}_{c_2+1:n-c_3} + \lambda_{c_2+1:n-c_3}\|_2^2 - \|\nu\bar{\mathbf{h}}_{n-c_3+1:n} + \mathbf{z}_{n-c_3+1:n}\|_2^2} \\
&= \frac{\sigma}{\sqrt{\sigma^2 + (n-c_3-c_2)x_{mag}^2}}\sqrt{\|\mathbf{g}\|_2^2\nu^2 - \|\nu\bar{\mathbf{h}}_{c_1+1:c_2} - \mathbf{z}_{c_1+1:c_2}\|_2^2 - \|\nu\bar{\mathbf{h}}_{n-c_3+1:n} + \mathbf{z}_{n-c_3+1:n}\|_2^2}.
\end{aligned} \tag{23}$$

Plugging the value for λ_i from (18) in (19) gives

$$\begin{aligned}
\xi^{(obj)} &= \sigma\sqrt{\|\mathbf{g}\|_2^2\nu^2 - \|\nu\bar{\mathbf{h}}_{c_1+1:n} - \mathbf{z}_{c_1+1:n} + \lambda_{c_1+1:n}\|_2^2} - x_{mag}\sum_{i=n-k+1}^{n}\lambda_i - \nu r_{socp} \\
&= \frac{\sigma^2 + (n-c_3-c_2)x_{mag}^2}{\sigma}\sqrt{\|\mathbf{g}\|_2^2\nu^2 - \|\nu\bar{\mathbf{h}}_{c_1+1:n} - \mathbf{z}_{c_1+1:n} + \lambda_{c_1+1:n}\|_2^2} \\
&- x_{mag}(n-c_3-c_2) + \nu x_{mag}\sum_{i=c_2+1}^{n-c_3}\bar{\mathbf{h}}_i - 2c_3x_{mag} - \nu r_{socp}.
\end{aligned} \tag{24}$$

Combining (23) and (24) we finally obtain

$$\begin{aligned}
\xi^{(obj)} &= \sqrt{\sigma^2 + (n-c_3-c_2)x_{mag}^2}\sqrt{\|\mathbf{g}\|_2^2\nu^2 - \|\nu\bar{\mathbf{h}}_{c_1+1:c_2} - \mathbf{z}_{c_1+1:c_2}\|_2^2 - \|\nu\bar{\mathbf{h}}_{n-c_3+1:n} + \mathbf{z}_{n-c_3+1:n}\|_2^2} \\
&- \nu(r_{socp} - x_{mag}\sum_{i=c_2+1}^{n-c_3}\bar{\mathbf{h}}_i) - x_{mag}(n-c_3-c_2) - 2c_3x_{mag}.
\end{aligned} \tag{25}$$

Equalling the derivative of $\xi^{(obj)}$ with respect to ν to zero further gives

$$\begin{aligned}
&\frac{d\xi^{(obj)}}{d\nu} = 0 \\
\iff\ &\frac{\nu(\|\mathbf{g}\|_2^2 - \sum_{i=c_1+1}^{c_2}\bar{\mathbf{h}}_i^2 - \sum_{i=n-c_3+1}^{n}\bar{\mathbf{h}}_i^2) + \bar{\mathbf{h}}_{c_1+1:c_2}^T\mathbf{z}_{c_1+1:c_2} - \bar{\mathbf{h}}_{n-c_3+1:n}^T\mathbf{z}_{n-c_3+1:n}}{(\sqrt{\sigma^2 + (n-c_3-c_2)x_{mag}^2})^{-1}\sqrt{\|\mathbf{g}\|_2^2\nu^2 - \|\nu\bar{\mathbf{h}}_{c_1+1:c_2} - \mathbf{z}_{c_1+1:c_2}\|_2^2 - \|\nu\bar{\mathbf{h}}_{n-c_3+1:n} + \mathbf{z}_{n-c_3+1:n}\|_2^2}} \\
&-(r_{socp} - x_{mag}\sum_{i=c_2+1}^{n-c_3}\bar{\mathbf{h}}_i) = 0.
\end{aligned} \tag{26}$$

Let

$$\begin{aligned}
s_{dep} &= \bar{\mathbf{h}}_{c_1+1:c_2}^T \mathbf{z}_{c_1+1:c_2} - \bar{\mathbf{h}}_{n-c_3+1:n}^T \mathbf{z}_{n-c_3+1:n} \\
d_{dep} &= \sum_{i=c_1+1}^{c_2} \bar{\mathbf{h}}_i^2 + \sum_{i=n-c_3+1}^{n} \bar{\mathbf{h}}_i^2 \\
r_{dep} &= r_{socp} - x_{mag} \sum_{i=c_2+1}^{n-c_3} \bar{\mathbf{h}}_i \\
a_{dep} &= \frac{\|\mathbf{g}\|_2^2 - (\sum_{i=c_1+1}^{c_2} \bar{\mathbf{h}}_i^2 + \sum_{i=n-c_3+1}^{n} \bar{\mathbf{h}}_i^2)}{\sqrt{\sigma^2 + (n-c_3-c_2)x_{mag}^2}^{-1} r_{dep}} = \frac{\sqrt{\sigma^2 + (n-c_3-c_2)x_{mag}^2}(\|\mathbf{g}\|_2^2 - d_{dep})}{r_{dep}} \\
b_{dep} &= \frac{\bar{\mathbf{h}}_{c_1+1:c_2}^T \mathbf{z}_{c_1+1:c_2} - \bar{\mathbf{h}}_{n-c_3+1:n}^T \mathbf{z}_{n-c_3+1:n}}{\sqrt{\sigma^2 + (n-c_3-c_2)x_{mag}^2}^{-1} r_{dep}} = \frac{\sqrt{\sigma^2 + (n-c_3-c_2)x_{mag}^2} s_{dep}}{r_{dep}}.
\end{aligned} \tag{27}$$

Then combining (26) and (27) one obtains

$$(a_{dep}\nu + b_{dep})^2 = \|\mathbf{g}\|_2^2 \nu^2 - \|\nu \bar{\mathbf{h}}_{c_1+1:c_2} - \mathbf{z}_{c_1+1:c_2}\|_2^2 - \|\nu \bar{\mathbf{h}}_{n-c_3+1:n} + \mathbf{z}_{n-c_3+1:n}\|_2^2. \tag{28}$$

After solving (28) over ν we have

$$\nu = \frac{-(a_{dep}b_{dep} - s_{dep}) - \sqrt{(a_{dep}b_{dep} - s_{dep})^2 - (b_{dep}^2 + \|\mathbf{z}_{c_1+1:c_2}\|_2^2 + \|\mathbf{z}_{n-c_3+1:n}\|_2^2)(a_{dep}^2 - \|\mathbf{g}\|_2^2 + d_{dep})}}{a_{dep}^2 - \|\mathbf{g}\|_2^2 + d_{dep}}. \tag{29}$$

Following what was done in [53, 57], we have that a combination of (20) and (29) gives the following three equations that can be used to determine c_1, c_2, and c_3 (the equations are rather inequalities; since we will assume a large dimensional scenario we will instead of any of the inequalities below write an equality; this will make writing much easier).

$$\begin{aligned}
\nu \bar{\mathbf{h}}_{c_2} - \mathbf{z}_{c_2} + \frac{x_{mag}}{\sigma} \sqrt{\|\mathbf{g}\|_2^2 \nu^2 - \|\nu \bar{\mathbf{h}}_{c_1+1:n} - \mathbf{z}_{c_1+1:n} + \lambda_{c_1+1:n}\|_2^2} &= 0 \\
\nu \bar{\mathbf{h}}_{n-c_3} + \mathbf{z}_{n-c_3} + \frac{x_{mag}}{\sigma} \sqrt{\|\mathbf{g}\|_2^2 \nu^2 - \|\nu \bar{\mathbf{h}}_{c_1+1:n} - \mathbf{z}_{c_1+1:n} + \lambda_{c_1+1:n}\|_2^2} &= 0 \\
\bar{\mathbf{h}}_{c_1} \frac{-(a_{dep}b_{dep} - s_{dep}) - \sqrt{(a_{dep}b_{dep} - s_{dep})^2 - (b_{dep}^2 + \|\mathbf{z}_{c_1+1:c_2}\|_2^2 + \|\mathbf{z}_{n-c_3+1:n}\|_2^2)(a_{dep}^2 - \|\mathbf{g}\|_2^2 + d_{dep})}}{a_{dep}^2 - \|\mathbf{g}\|_2^2 + d_{dep}} &= 1.
\end{aligned} \tag{30}$$

The last term that appears on the right hand side of the first two of the above equations can be further

simplified based on (23) in the following way

$$\sqrt{\|\mathbf{g}\|_2^2\nu^2 - \|\nu\bar{\mathbf{h}}_{c_1+1:n} - \mathbf{z}_{c_1+1:n} + \lambda_{c_1+1:n}\|_2^2} = \frac{\sigma\sqrt{\|\mathbf{g}\|_2^2\nu^2 - \|\nu\bar{\mathbf{h}}_{c_1+1:c_2} - \mathbf{z}_{c_1+1:c_2}\|_2^2 - \|\nu\bar{\mathbf{h}}_{n-c_3+1:n} + \mathbf{z}_{n-c_3+1:n}\|_2^2}}{\sqrt{\sigma^2 + (n-c_3-c_2)x_{mag}^2}}$$
$$= \frac{\sigma\sqrt{\|\mathbf{g}\|_2^2\nu^2 - \nu^2 d_{dep} + 2\nu s_{dep} - (\|\mathbf{z}_{c_1+1:c_2}\|_2^2 + \|\mathbf{z}_{n-c_3+1:n}\|_2^2)}}{\sqrt{\sigma^2 + (n-c_3-c_2)x_{mag}^2}} = \frac{\sigma\sqrt{\|\mathbf{g}\|_2^2\nu^2 - \nu^2 d_{dep} + 2\nu s_{dep} - (c_2 - c_1 + c_3)}}{\sqrt{\sigma^2 + (n-c_3-c_2)x_{mag}^2}}, \tag{31}$$

where we of course recognized that $\|\mathbf{z}_{c_1+1:c_2}\|_2^2 + \|\mathbf{z}_{n-c_3+1:n}\|_2^2 = c_2 - c_1 + c_3$. Combining (27) and (31) one can then simplify the equations from (30) in the following way

$$\begin{aligned}
\nu\bar{\mathbf{h}}_{c_2} - \mathbf{z}_{c_2} + \frac{x_{mag}}{\sqrt{\sigma^2 + (n-c_3-c_2)x_{mag}^2}}\sqrt{\|\mathbf{g}\|_2^2\nu^2 - \nu^2 d_{dep} + 2\nu s_{dep} - (c_2 - c_1 + c_3)} &= 0 \\
\nu\bar{\mathbf{h}}_{n-c_3} + \mathbf{z}_{n-c_3} + \frac{x_{mag}}{\sqrt{\sigma^2 + (n-c_3-c_2)x_{mag}^2}}\sqrt{\|\mathbf{g}\|_2^2\nu^2 - \nu^2 d_{dep} + 2\nu s_{dep} - (c_2 - c_1 + c_3)} &= 0 \\
\bar{\mathbf{h}}_{c_1}\frac{-(a_{dep}b_{dep} - s_{dep}) - \sqrt{(a_{dep}b_{dep} - s_{dep})^2 - (b_{dep}^2 + (c_2 - c_1 + c_3))(a_{dep}^2 - \|\mathbf{g}\|_2^2 + d_{dep})}}{a_{dep}^2 - \|\mathbf{g}\|_2^2 + d_{dep}} &= 1.
\end{aligned} \tag{32}$$

Let $\widehat{c_1}$, $\widehat{c_2}$, and $\widehat{c_3}$ be the solution of (32). Then

$$\nu_{dep} = \frac{-(\widehat{a_{dep}}\widehat{b_{dep}} - \widehat{s_{dep}}) - \sqrt{(\widehat{a_{dep}}\widehat{b_{dep}} - \widehat{s_{dep}})^2 - (\widehat{b_{dep}}^2 + (\widehat{c_2} - \widehat{c_1} + \widehat{c_3}))(\widehat{a_{dep}}^2 - \|\mathbf{g}\|_2^2 + \widehat{d_{dep}})}}{\widehat{a_{dep}}^2 - \|\mathbf{g}\|_2^2 + \widehat{d_{dep}}}, \tag{33}$$

where $\widehat{s_{dep}}$, $\widehat{d_{dep}}$, $\widehat{a_{dep}}$, and $\widehat{b_{dep}}$ are s_{dep}, d_{dep}, a_{dep}, and b_{dep} from (27) computed with $\widehat{c_1}$, $\widehat{c_2}$, and $\widehat{c_3}$. From (17) one then has

$$\|\mathbf{w}_{dep}\|_2 = \sigma\frac{\|\nu_{dep}\bar{\mathbf{h}}_{\widehat{c_1}+1:n} - \mathbf{z}_{\widehat{c_1}+1:n} + \lambda^{(dep)}_{\widehat{c_1}+1:n}\|_2}{\sqrt{\|\mathbf{g}\|_2^2\nu_{dep}^2 - \|\nu_{dep}\bar{\mathbf{h}}_{\widehat{c_1}+1:n} - \mathbf{z}_{\widehat{c_1}+1:n} + \lambda^{(dep)}_{\widehat{c_1}+1:n}\|_2^2}}. \tag{34}$$

Combining (31) and (34) one further has

$$\|\mathbf{w}_{dep}\|_2 = \sigma\frac{\sqrt{\|\mathbf{g}\|_2^2\nu_{dep}^2(n - \widehat{c_3} - \widehat{c_2})\frac{x_{mag}^2}{\sigma^2} + \nu_{dep}^2\widehat{d_{dep}} - 2\nu\widehat{s_{dep}} + (\widehat{c_2} - \widehat{c_1} + \widehat{c_3})}}{\sqrt{\|\mathbf{g}\|_2^2\nu_{dep}^2 - \nu_{dep}^2\widehat{d_{dep}} + 2\nu_{dep}\widehat{s_{dep}} - (\widehat{c_2} - \widehat{c_1} + \widehat{c_3})}}. \tag{35}$$

Combination of (33) and (35) is conceptually enough to determine $\|\mathbf{w}_{dep}\|_2$ (and then afterwards easily $E\xi^{(dep)}_{prim}(\sigma, \mathbf{g}, \mathbf{h}, x_{mag}, r_{socp})$). What is left to be done is a computation of all unknown quantities that appear in (33) and (35). We will below show how that can be done. As mentioned earlier what we will present substantially relies on what was shown in [53,57] and we assume a familiarity with the procedures presented there.

The first thing to resolve is (32). Since all random quantities concentrate we will be dealing (as in

[53,57]) with the expected values. To compute the solution of (32), $\widehat{c_1}$, $\widehat{c_2}$, and $\widehat{c_3}$, we will need the following expected values

$$E\|\mathbf{g}\|_2^2, E\|\bar{\mathbf{h}}_{c_1+1:n-k}\|_2^2, E\|\bar{\mathbf{h}}_{n-k+1:c_2}\|_2^2, E\|\bar{\mathbf{h}}_{n-c_3+1:n}\|_2^2,$$
$$E(\bar{\mathbf{h}}_{c_1+1:n-k}^T\mathbf{z}_{c_1+1:n-k}), E(\bar{\mathbf{h}}_{n-k+1:c_2}^T\mathbf{z}_{n-k+1:c_2}), E(\bar{\mathbf{h}}_{n-c_3+1:n}^T\mathbf{z}_{n-c_3+1:n}). \tag{36}$$

Clearly, since components of $\mathbf{g}$ are i.i.d. standard normals one easily has

$$E\|\mathbf{g}\|_2^2 = m. \tag{37}$$

Let $c_1 = (1-\theta_1)n$, $c_2 = \theta_2 n$, and $c_3 = \theta_3 n$ where θ_1, θ_2, and θ_3 are constants independent of n. Then as shown in [53, 57]

$$\lim_{n\to\infty}\frac{E\|\bar{\mathbf{h}}_{c_1+1:n-k}\|_2^2}{n} = \frac{1-\beta_w}{\sqrt{2\pi}}\left(2\frac{\sqrt{2(\text{erfinv}(\frac{1-\theta_1}{1-\beta_w}))^2}}{e^{(\text{erfinv}(\frac{1-\theta_1}{1-\beta_w}))^2}}\right)+\theta_1-\beta_w. \tag{38}$$

where we of course recall that $\beta_w = \frac{k}{n}$. Also, as shown in [53, 57]

$$\lim_{n\to\infty}\frac{E\|\bar{\mathbf{h}}_{n-k+1:c_2}\|_2^2}{n} = \frac{\beta_w}{\sqrt{2\pi}}\left(\frac{\sqrt{2}\text{erfinv}(2\frac{1-\theta_2}{\beta_w}-1)}{e^{(\text{erfinv}(2\frac{1-\theta_2}{\beta_w}-1))^2}}\right)+\theta_2-1+\beta_w, \tag{39}$$

and

$$\lim_{n\to\infty}\frac{E\|\bar{\mathbf{h}}_{n-c_3+1:n}\|_2^2}{n} = \frac{\beta_w}{\sqrt{2\pi}}\left(\frac{\sqrt{2}\text{erfinv}(2\frac{\beta_w-\theta_3}{\beta_w}-1)}{e^{(\text{erfinv}(2\frac{\beta_w-\theta_3}{\beta_w}-1))^2}}\right)+\theta_3, \tag{40}$$

Following further what was established in [53, 57] we have

$$\begin{aligned}
\lim_{n\to\infty}\frac{E(\bar{\mathbf{h}}_{c_1+1:n-k}^T\mathbf{z}_{c_1+1:n-k})}{n} &= \left((1-\beta_w)\sqrt{\frac{2}{\pi}}e^{-(\text{erfinv}(\frac{1-\theta_1}{1-\beta_w}))^2}\right)\\
\lim_{n\to\infty}\frac{E(\bar{\mathbf{h}}_{n-k+1:c_2}^T\mathbf{z}_{n-k+1:c_2})}{n} &= \left(\beta_w\sqrt{\frac{1}{2\pi}}e^{-(\text{erfinv}(2\frac{1-\theta_2}{\beta_w}-1))^2}\right)\\
\lim_{n\to\infty}\frac{E(\bar{\mathbf{h}}_{n-c_3+1:n}^T\mathbf{z}_{n-c_3+1:n})}{n} &= -\left(\beta_w\sqrt{\frac{1}{2\pi}}e^{-(\text{erfinv}(2\frac{\beta_w-\theta_3}{\beta_w}-1))^2}\right).
\end{aligned} \tag{41}$$

From (41) we also have

$$\lim_{n\to\infty}\frac{E(\sum_{i=c_2+1}^{n-c_3}\bar{\mathbf{h}}_i)}{n} = \left(\beta_w\sqrt{\frac{1}{2\pi}}e^{-(\text{erfinv}(2\frac{\beta_w-\theta_3}{\beta_w}-1))^2}\right)-\left(\beta_w\sqrt{\frac{1}{2\pi}}e^{-(\text{erfinv}(2\frac{1-\theta_2}{\beta_w}-1))^2}\right). \tag{42}$$

The only other thing that we will need in order to be able to compute $\widehat{c_1}$, $\widehat{c_2}$, and $\widehat{c_3}$ (besides the expectations from (36)) are the following inequalities related to the behavior of $\bar{\mathbf{h}}_{c_1}$, $\bar{\mathbf{h}}_{c_2}$, and $\bar{\mathbf{h}}_{c_3}$. Again, as shown

in [53, 57]

$$\begin{aligned} P(\sqrt{2}\text{erfinv}((1+\epsilon_1^{\bar{\mathbf{h}}_{c_1}})(\frac{1-\theta_1}{1-\beta_w})) \leq \bar{\mathbf{h}}_{c_1}) &\leq e^{-\epsilon_2^{\bar{\mathbf{h}}_{c_1}} n} \\ P(\sqrt{2}\text{erfinv}((1+\epsilon_1^{\bar{\mathbf{h}}_{c_2}})(2\frac{1-\theta_2}{\beta_w}-1)) \leq \bar{\mathbf{h}}_{c_2}) &\leq e^{-\epsilon_2^{\bar{\mathbf{h}}_{c_2}} n} \\ P(-\sqrt{2}\text{erfinv}((1+\epsilon_1^{\bar{\mathbf{h}}_{c_3}})(2\frac{\beta_w-\theta_3}{\beta_w}-1)) \leq \bar{\mathbf{h}}_{n-c_3}) &\leq e^{-\epsilon_2^{\bar{\mathbf{h}}_{n-c_3}} n}. \end{aligned} \tag{43}$$

where $\epsilon_1^{\bar{\mathbf{h}}_{c_1}} > 0$, $\epsilon_1^{\bar{\mathbf{h}}_{c_2}} > 0$, and $\epsilon_1^{\bar{\mathbf{h}}_{n-c_3}} > 0$ are arbitrarily small constants and $\epsilon_2^{\bar{\mathbf{h}}_{c_1}}$, $\epsilon_2^{\bar{\mathbf{h}}_{c_2}}$, and $\epsilon_2^{\bar{\mathbf{h}}_{n-c_3}}$ are constants dependent on $\epsilon_1^{\bar{\mathbf{h}}_{c_1}}$, $\epsilon_1^{\bar{\mathbf{h}}_{c_2}}$, and $\epsilon_1^{\bar{\mathbf{h}}_{n-c_3}}$, respectively, but independent of n (essentially one only needs the direction of inequalities as in (43); however, a similar reverse inequalities hold as well).

At this point we have all the necessary ingredients to determine $\widehat{c_1}$, $\widehat{c_2}$, and $\widehat{c_3}$ and consequently ν_{dep}, $\|\mathbf{w}_{dep}\|_2$, and $\xi_{prim}^{(dep)}(\sigma, \mathbf{g}, \mathbf{h}, x_{mag}, r_{socp})$. We of course recall that in a random setup that we consider quantities $\widehat{c_1}$, $\widehat{c_2}$, $\widehat{c_3}$, ν_{dep}, $\|\mathbf{w}_{dep}\|_2$, and $\xi_{prim}^{(dep)}(\sigma, \mathbf{g}, \mathbf{h}, x_{mag}, r_{socp})$ can not really be determined. Instead what we will be determining are their concentrating points. The following theorem then provides a systematic way of doing so.

Theorem 2. *Assume the setup of Theorem 1. Let the nonzero components of $\tilde{\mathbf{x}}$ have magnitude x_{mag} and let $\bar{\mathbf{h}}$ be as defined in (14). Further, let $r_{socp}^{(sc)} = \lim_{n\to\infty} \frac{r_{socp}}{\sqrt{n}}$ and $x_{mag}^{(sc)} = \lim_{n\to\infty} \frac{x_{mag}}{\sqrt{n}}$. Also, let ν_{dep}, $\|\mathbf{w}_{dep}\|_2$, and $\xi_{prim}^{(dep)}(\sigma, \mathbf{g}, \mathbf{h}, x_{mag}, r_{socp})$ be as defined in and right after (16). Let $\alpha = \frac{m}{n}$ and $\beta_w = \frac{k}{n}$ be fixed. Consider the following*

$$\begin{aligned} S(\theta_1,\theta_2,\theta_3) = \lim_{n\to\infty}\frac{Es_{dep}}{n} = &\left((1-\beta_w)\sqrt{\frac{2}{\pi}}e^{-(\textit{erfinv}(\frac{1-\theta_1}{1-\beta_w}))^2}\right) + \left(\beta_w\sqrt{\frac{1}{2\pi}}e^{-(\textit{erfinv}(2\frac{1-\theta_2}{\beta_w}-1))^2}\right) \\ &+ \left(\beta_w\sqrt{\frac{1}{2\pi}}e^{-(\textit{erfinv}(2\frac{\beta_w-\theta_3}{\beta_w}-1))^2}\right) \end{aligned}$$

$$\begin{aligned} D(\theta_1,\theta_2,\theta_3) = \lim_{n\to\infty}\frac{Ed_{dep}}{n} = &\frac{1-\beta_w}{\sqrt{2\pi}}\left(2\frac{\sqrt{2(\textit{erfinv}(\frac{1-\theta_1}{1-\beta_w}))^2}}{e^{(\textit{erfinv}(\frac{1-\theta_1}{1-\beta_w}))^2}}\right) + \theta_1 - \beta_w \\ &+ \frac{\beta_w}{\sqrt{2\pi}}\left(\frac{\sqrt{2}\textit{erfinv}(2\frac{1-\theta_2}{\beta_w}-1)}{e^{(\textit{erfinv}(2\frac{1-\theta_2}{\beta_w}-1))^2}}\right) + \theta_2 - 1 + \beta_w + \frac{\beta_w}{\sqrt{2\pi}}\left(\frac{\sqrt{2}\textit{erfinv}(2\frac{1-\theta_3}{\beta_w}-1)}{e^{(\textit{erfinv}(2\frac{\beta_w-\theta_3}{\beta_w}-1))^2}}\right) + \theta_3 \end{aligned}$$

$$R(\theta_2,\theta_3) = \lim_{n\to\infty}\frac{Er_{dep}}{\sqrt{n}} = r_{socp}^{(sc)} - x_{mag}^{(sc)}\left(\left(\beta_w\sqrt{\frac{1}{2\pi}}e^{-(\textit{erfinv}(2\frac{\beta_w-\theta_3}{\beta_w}-1))^2}\right) - \left(\beta_w\sqrt{\frac{1}{2\pi}}e^{-(\textit{erfinv}(2\frac{1-\theta_2}{\beta_w}-1))^2}\right)\right)$$

$$\begin{aligned}
A(\theta_1,\theta_2,\theta_3) &= \lim_{n\to\infty}\frac{Ea_{dep}}{\sqrt{n}}=\frac{\sqrt{\sigma^2+(1-\theta_3-\theta_2)(x_{mag}^{(sc)})^2}(\alpha-D(\theta_1,\theta_2,\theta_3))}{R(\theta_2,\theta_3)}\\
B(\theta_1,\theta_2,\theta_3) &= \lim_{n\to\infty}\frac{Eb_{dep}}{\sqrt{n}}=\frac{\sqrt{\sigma^2+(1-\theta_3-\theta_2)(x_{mag}^{(sc)})^2}S(\theta_1,\theta_2,\theta_3)}{R(\theta_2,\theta_3)}\\
F(\theta_1) &= \sqrt{2}\mathit{erfinv}(\frac{1-\theta_1}{1-\beta_w})\\
G(\theta_2) &= \sqrt{2}\mathit{erfinv}(2\frac{1-\theta_2}{\beta_w}-1)\\
H(\theta_3) &= \sqrt{2}\mathit{erfinv}(2\frac{\beta-\theta_3}{\beta_w}-1). \qquad (44)
\end{aligned}$$

Set

$$N(\theta_1,\theta_2,\theta_3)=\frac{-(A(\theta_1,\theta_2,\theta_3)B(\theta_1,\theta_2,\theta_3)-S(\theta_1,\theta_2,\theta_3))}{A(\theta_1,\theta_2,\theta_3)^2-\alpha+D(\theta_1,\theta_2,\theta_3)}$$
$$-\frac{\sqrt{(A(\theta_1,\theta_2,\theta_3)B(\theta_1,\theta_2,\theta_3)-S(\theta_1,\theta_2,\theta_3))^2-(B(\theta_1,\theta_2,\theta_3)^2+\theta_1+\theta_2+\theta_3-1)(A(\theta_1,\theta_2,\theta_3)^2-\alpha+D(\theta_1,\theta_2,\theta_3))}}{A(\theta_1,\theta_2,\theta_3)^2-\alpha+D(\theta_1,\theta_2,\theta_3)}.$$

Let the triplet ($\widehat{\theta_1}$, $\widehat{\theta_2}$, $\widehat{\theta_3}$) be the solution of the following three equations

$$\begin{aligned}
N(\theta_1,\theta_2,\theta_3)G(\theta_2)+\frac{x_{mag}^{(sc)}\sqrt{N(\theta_1,\theta_2,\theta_3)^2(\alpha^2-D(\theta_1,\theta_2,\theta_3))+2N(\theta_1,\theta_2,\theta_3)S(\theta_1,\theta_2,\theta_3)-(\theta_1+\theta_2+\theta_3-1)}}{\sqrt{\sigma^2+(1-\theta_3-\theta_2)(x_{mag}^{(sc)})^2}} &= 1\\
N(\theta_1,\theta_2,\theta_3)H(\theta_3)-\frac{x_{mag}^{(sc)}\sqrt{N(\theta_1,\theta_2,\theta_3)^2(\alpha^2-D(\theta_1,\theta_2,\theta_3))+2N(\theta_1,\theta_2,\theta_3)S(\theta_1,\theta_2,\theta_3)-(\theta_1+\theta_2+\theta_3-1)}}{\sqrt{\sigma^2+(1-\theta_3-\theta_2)(x_{mag}^{(sc)})^2}} &= 1\\
F(\theta_1)N(\theta_1,\theta_2,\theta_3) &= 1. \qquad (45)
\end{aligned}$$

Then the concentrating points of ν_{dep}, $\|\mathbf{w}_{dep}\|_2$, and $\xi_{prim}^{(dep)}(\sigma,\mathbf{g},\mathbf{h},x_{mag},r_{socp})$ can be determined as

$$E\nu_{dep}=N(\widehat{\theta_1},\widehat{\theta_2},\widehat{\theta_3})$$

$$E\|\mathbf{w}_{dep}\|_2=\sigma\frac{\sqrt{N(\widehat{\theta_1},\widehat{\theta_2},\widehat{\theta_3})^2(\alpha(1-\widehat{\theta_3}-\widehat{\theta_2})\frac{(x_{mag}^{(sc)})^2}{\sigma^2}+D(\widehat{\theta_1},\widehat{\theta_2},\widehat{\theta_3}))-2N(\widehat{\theta_1},\widehat{\theta_2},\widehat{\theta_3})S(\widehat{\theta_1},\widehat{\theta_2},\widehat{\theta_3})+(\widehat{\theta_1}+\widehat{\theta_2}+\widehat{\theta_3}-1)}}{\sqrt{N(\widehat{\theta_1},\widehat{\theta_2},\widehat{\theta_3})^2(\alpha-D(\widehat{\theta_1},\widehat{\theta_2},\widehat{\theta_3}))+2N(\widehat{\theta_1},\widehat{\theta_2},\widehat{\theta_3})S(\widehat{\theta_1},\widehat{\theta_2},\widehat{\theta_3})-(\widehat{\theta_1}+\widehat{\theta_2}+\widehat{\theta_3}-1)}}$$

$$\lim_{n\to\infty}\frac{E\xi_{prim}^{(dep)}(\sigma,\mathbf{g},\mathbf{h},x_{mag},r_{socp})}{\sqrt{n}}=\sigma\frac{\sqrt{N(\widehat{\theta_1},\widehat{\theta_2},\widehat{\theta_3})^2(\alpha-D(\widehat{\theta_1},\widehat{\theta_2},\widehat{\theta_3}))+2N(\widehat{\theta_1},\widehat{\theta_2},\widehat{\theta_3})S(\widehat{\theta_1},\widehat{\theta_2},\widehat{\theta_3})-(\widehat{\theta_1}+\widehat{\theta_2}+\widehat{\theta_3}-1)}}{\sqrt{1+(1-\widehat{\theta_2}-\widehat{\theta_3})\frac{(x_{mag}^{(sc)})^2}{\sigma^2}}}$$
$$-N(\widehat{\theta_1},\widehat{\theta_2},\widehat{\theta_3})r_{socp}^{(sc)}. \qquad (46)$$

Proof. Follows from Theorem 1 based on the discussion presented above and a combination of (27), (32), (33), and (35). □

The results from the above theorem can be used to compute parameters of interest in our derivation for particular values of β_w, α, σ, x_{mag}, and r_{socp}. In the following subsection we will present a collection of such results.

2.2.1 Theoretical predictions

In this subsection we present the theoretical predictions one can get based on the result of the previous sections. We will split the presentation of the results into several parts.

1) $\frac{E\|\mathbf{w}_{dep}\|_2}{\sigma}=\frac{E\|\mathbf{w}_{socp}\|_2}{\sigma}$ ***as a function of*** $x_{mag}^{(sc)}$

To present this portion (as well as several others that will follow) of theoretical results we will look at three regimes: 1) low α-, medium α-, and high α-regime. For each of the regimes we will show the theoretical results for $\frac{E\|\mathbf{w}_{dep}\|_2}{\sigma}=\frac{E\|\mathbf{w}_{socp}\|_2}{\sigma}$ as a function of $x_{mag}^{(sc)}$. We will take $\alpha=0.3$ as a representative of the low α-regime, $\alpha=0.5$ as a representative of the medium α-regime, and $\alpha=0.7$ as a representative of the high α-regime. We will consider $r_{socp}=r_{socp}^{(opt)}=\sigma\sqrt{\frac{\alpha n}{1+\rho^2}}$. For each of the α-regimes we will look at two different sub-regimes: low β_w- and high β_w-regime (which based on results from [53] is equivalent to low ρ- and high ρ-regimes). For each of these two sub-regimes β_w will be selected based on the curves obtained in [53] (or those obtained in [52]) in the following way. In the low β_w sub-regime we will set $\rho=2$ and $r_{socp}=r_{socp}^{(opt)}=\sigma\sqrt{\frac{\alpha n}{5}}$ whereas in the high β_w sub-regime we will set $\rho=3$ and $r_{socp}=r_{socp}^{(opt)}=\sigma\sqrt{\frac{\alpha n}{10}}$. At the same time from [53] we will have $r_{socp}=r_{socp}^{(opt)}=\sigma\sqrt{(\alpha-\alpha_w)n}$ where α_w and β_w are such that (9) holds (we also recall on [53] where it was reasoned that the low β regime is selected so that the pair (α,β_w) is well below the fundamental characterization (9) whereas the high β regime is selected so that the pair (α,β_w) is closer to the fundamental characterization (9)). The values for $\frac{E\|\mathbf{w}_{dep}\|_2}{\sigma}=\frac{E\|\mathbf{w}_{socp}\|_2}{\sigma}$ one can then get through the results of Theorem 2 for such (α,β_w) pairs, $r_{socp}^{(opt)}$ are shown in Figure 3 as functions of $x_{mag}^{(sc)}$. As can be seen from Figure 3, the values of $\frac{E\|\mathbf{w}_{dep}\|_2}{\sigma}=\frac{E\|\mathbf{w}_{socp}\|_2}{\sigma}$ converge to ρ as

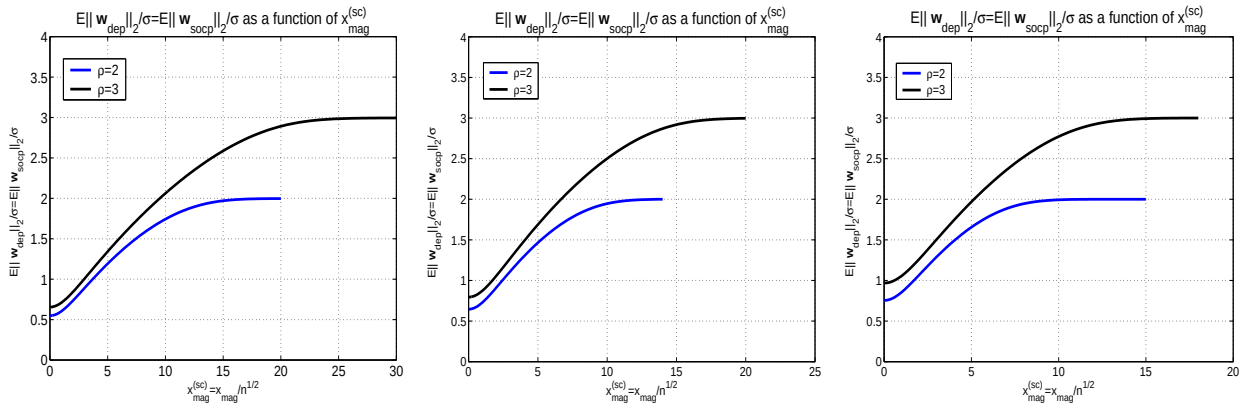

Figure 3: $\frac{E\|\mathbf{w}_{dep}\|_2}{\sigma}=\frac{E\|\mathbf{w}_{socp}\|_2}{\sigma}$ as a function of $x_{mag}^{(sc)}$; $r_{socp}=\sqrt{\frac{\alpha n}{1+\rho^2}}$; left — $\alpha=0.3$, center — $\alpha=0.5$, right — $\alpha=0.7$

$x_{mag}^{(sc)}$ increases. This is of course in agreement with [53] where it was demonstrated that for $r_{socp}^{(opt)}$ one has $\rho=\frac{\|\mathbf{w}_{socp}\|_2}{\sigma}$ with overwhelming probability. Another interesting observation one can make is that the convergence is "faster" (or happens for smaller $x_{mag}^{(sc)}$) for larger α.

2) $\frac{Ef_{obj}}{\sqrt{n}}=\frac{E\xi_{prim}^{(dep)}(\sigma,\mathbf{g},\mathbf{h},x_{mag},r_{socp})}{\sqrt{n}}$ ***as a function of*** $x_{mag}^{(sc)}$

Similarly to what was discussed above (and is related to $\|\mathbf{w}_{socp}\|_2$ and $\|\mathbf{w}_{dep}\|_2$) one can determine

the concentrating points of f_{obj} and $\xi_{prim}^{(dep)}$ also as functions of $x_{mag}^{(sc)}$. To present these results we restrict ourselves to the medium α-regime, or in other words to $\alpha = 0.5$. As above we again choose $r_{socp} = r_{socp}^{(opt)} = \sigma\sqrt{\frac{\alpha n}{1+\rho^2}}$ and consider low $\rho = 2$- and high $\rho = 3$- regime. The obtained results are shown in Figure 4. As can be seen from Figure 4 $\frac{Ef_{obj}}{\sqrt{n}}$ is larger for larger ρ.

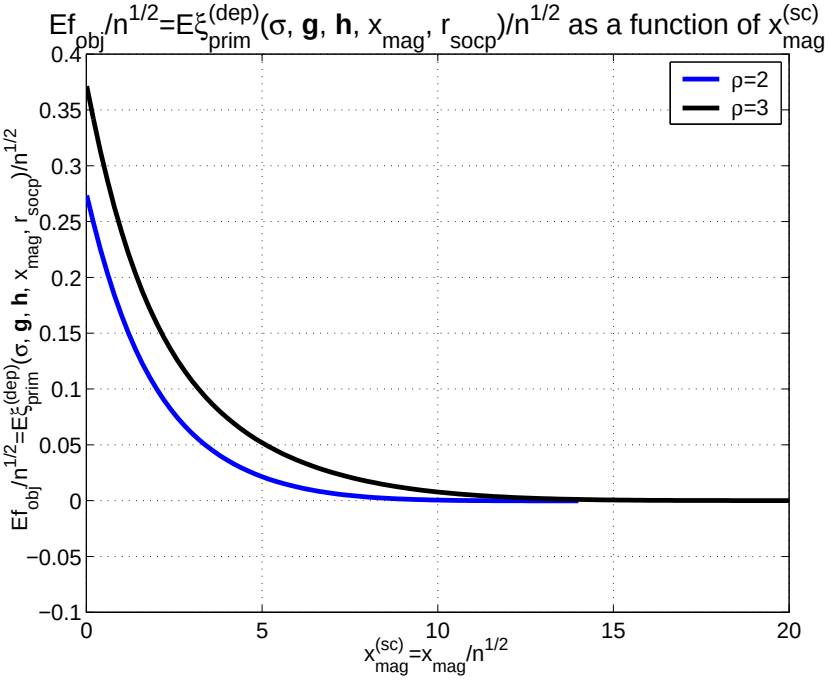

Figure 4: $\frac{Ef_{obj}}{\sqrt{n}} = \frac{E\xi_{prim}^{(dep)}(\sigma,\mathbf{g},\mathbf{h},x_{mag},r_{socp})}{\sqrt{n}}$ as a function of $x_{mag}^{(sc)}$; $r_{socp} = \sqrt{\frac{\alpha n}{1+\rho^2}}$; $\alpha = 0.5$

3) $\frac{E\|\mathbf{w}_{dep}\|_2}{\sigma} = \frac{E\|\mathbf{w}_{socp}\|_2}{\sigma}$ ***as a function of*** $x_{mag}^{(sc)}$***; varying*** r_{socp}

Another interesting set of results relates to possible variations in the r_{socp} that can be used in (4). The results that we presented above assume an optimal choice for r_{socp} (in a sense defined in [53]). Namely, they assume that for a fixed pair (α, β_w) one chooses $r_{socp} = r_{socp}^{(opt)} = \sigma\sqrt{(\alpha - \alpha_w)n}$ where α_w and β_w are such that (9) holds. In the worst-case scenario (or in the generic scenario as we referred to it in [53]) one has that choice $r_{socp}^{(opt)}$ offers the minimal norm-2 of the error vector. However, such a scenario assumes particular $\tilde{\mathbf{x}}$'s which leaves a possibility that for a wide range of other $\tilde{\mathbf{x}}$'s the performance of the SOCP from (4) in the ℓ_2 norm of the error vector sense can be more favorable. Of course as shown in Figure (3) this indeed happens to be the case. On the other hand that also leaves an option that one can possibly choose a different r_{socp} and get say a smaller norm-2 of the error vector for various different $\tilde{\mathbf{x}}$. Below we present a few results in this direction.

We will consider again only the medium or $\alpha = 0.5$ regime. For two different values of ρ, $r_{socp} = r_{socp}^{(opt)}$, and β_w we presented the results for $\frac{E\|\mathbf{w}_{dep}\|_2}{\sigma} = \frac{E\|\mathbf{w}_{socp}\|_2}{\sigma}$ in Figure 3. In addition to that we now in Figure 5 show similar results one can get through Theorem 2 for two different choices of r_{socp}. To be more precise, for $\rho = 2$ we choose the same α and β_w as in Figure and only vary r_{socp} over $\{\sigma\sqrt{0.05\alpha n}, \sigma\sqrt{0.2\alpha n}\sigma\sqrt{0.6\alpha n}\}$. Clearly, choice $\sigma\sqrt{0.05\alpha n}$ is smaller than $r_{socp}^{(opt)} = \sigma\sqrt{0.2\alpha n}$ whereas choice $\sigma\sqrt{0.6\alpha n}$ is larger than $r_{socp}^{(opt)} = \sigma\sqrt{0.2\alpha n}$. On the other hand for $\rho = 3$ we choose the same α and β_w as we have chose for $\rho = 3$ in Figure 3 and vary r_{socp} but this time over $\{\sigma\sqrt{0.05\alpha n}, \sigma\sqrt{0.1\alpha n}\sigma\sqrt{0.5\alpha n}\}$. Again, clearly, choice

$\sigma\sqrt{0.05\alpha n}$ is smaller than $r_{socp}^{(opt)} = \sigma\sqrt{0.1\alpha n}$ whereas choice $\sigma\sqrt{0.6\alpha n}$ is larger than $r_{socp}^{(opt)} = \sigma\sqrt{0.2\alpha n}$. It is rather obvious but we mention for the completeness that the middle r_{socp} choices for both, $\rho = 2$ and $\rho = 3$, cases correspond to the center plot in Figure 3. We make two interesting observations related to the

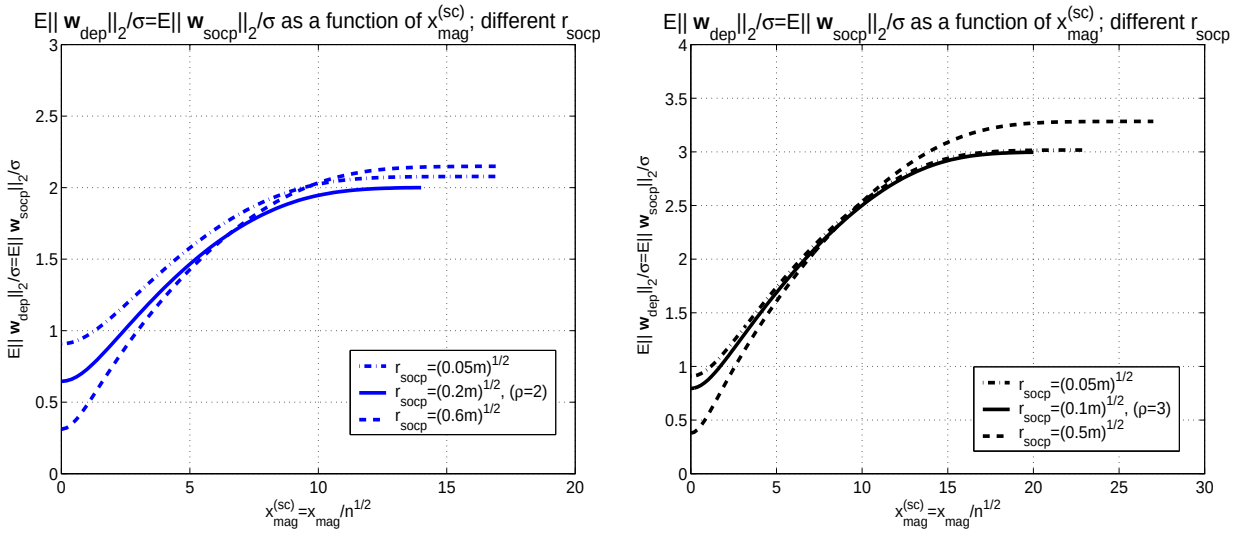

Figure 5: $\frac{E\|\mathbf{w}_{dep}\|_2}{\sigma} = \frac{E\|\mathbf{w}_{socp}\|_2}{\sigma}$ as a function of $x_{mag}^{(sc)}$ for different r_{socp}; left — $\rho = 2$, $r_{socp} \in \{\sigma\sqrt{0.05\alpha n}, \sigma\sqrt{0.2\alpha n}\sigma\sqrt{0.6\alpha n}\}$; right — $\rho = 3$, $r_{socp} \in \{\sigma\sqrt{0.05\alpha n}, \sigma\sqrt{0.1\alpha n}\sigma\sqrt{0.5\alpha n}\}$

results presented in Figure 5. The first one is that Figure 5 suggests that if r_{socp} is smaller than $r_{socp}^{(opt)}$ then $\frac{E\|\mathbf{w}_{socp}\|_2}{\sigma}$ could be larger than the one that can be obtained for $r_{socp}^{(opt)}$. This actually happens to be the case. A reasoning similar to the one presented in Section 2.4.2 in [53] can show that this is indeed true. Moreover, not only is it true for the $\tilde{\mathbf{x}}$ considered in Theorem 2 but it is actually true for any $\tilde{\mathbf{x}}$. We skip the details of this simple exercise, though. The second observation is that if r_{socp} is larger than $r_{socp}^{(opt)}$ then for certain $\tilde{\mathbf{x}}$ (but of course not for all of them and certainly not for the worst-case or the generic one) $\frac{E\|\mathbf{w}_{socp}\|_2}{\sigma}$ could be smaller than the one that can be obtained for $r_{socp}^{(opt)}$. This of course suggests that a choice of r_{socp} larger than $r_{socp}^{(opt)}$ could be more favorable in certain applications and for a particular measure of performance. However, if one has no a priori available knowledge about $\tilde{\mathbf{x}}$ then adapting r_{socp} beyond $r_{socp}^{(opt)}$ would be hard.

4) $\frac{Ef_{obj}}{\sqrt{n}} = \frac{E\xi_{prim}^{(dep)}(\sigma,\mathbf{g},\mathbf{h},x_{mag},r_{socp})}{\sqrt{n}}$ ***as a function of*** $x_{mag}^{(sc)}$***; varying*** r_{socp}

Similarly to what was done above in part 2) one can also determine the theoretical predictions for $\frac{Ef_{obj}}{\sqrt{n}} = \frac{E\xi_{prim}^{(dep)}}{\sqrt{n}}$ for a varying r_{socp}. As in parts 2) and 3) above, we restrict our attention only to the medium $\alpha = 0.5$ regime. We also assume exactly the same scenarios as in part 3). The obtained results are shown in Figure 6. As in part 2) Figure 6 shows that $\frac{Ef_{obj}}{\sqrt{n}}$ is larger for larger ρ. On the other hand it also shows that $\frac{Ef_{obj}}{\sqrt{n}}$ decreases as r_{socp} increases. This also follows rather trivially by the use of arguments from Section 2.4.2. We skip this easy exercise as well.

We conducted massive numerical experiments and found that the results one can get through them are in a firm agreement (as they should be) with what the presented theory predicts. In the next subsection we present a sample of the results obtained through the conducted numerical experiments.

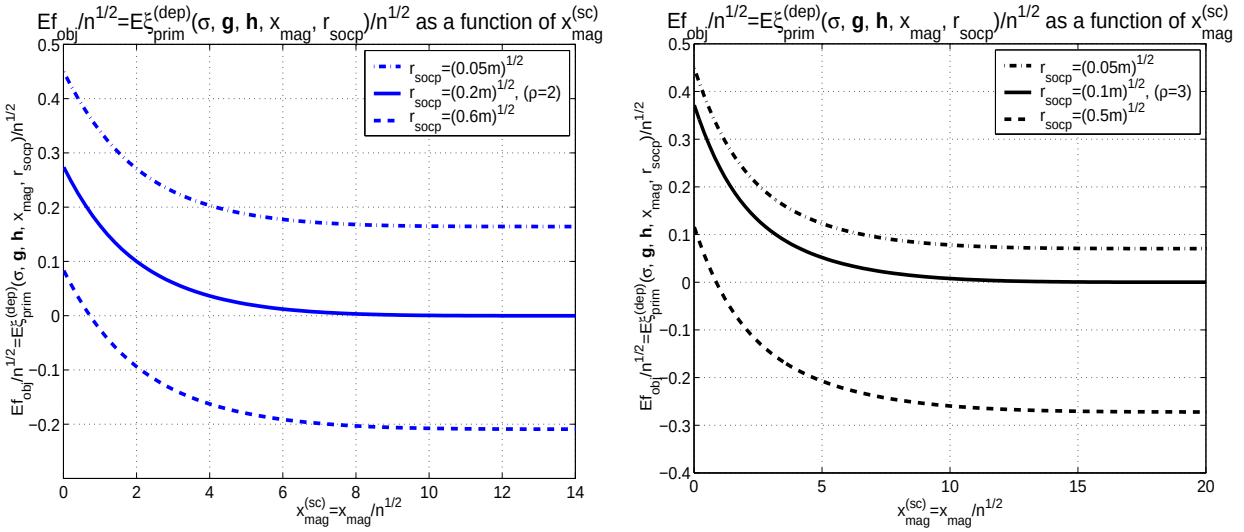

Figure 6: $\frac{Ef_{obj}}{\sqrt{n}} = \frac{E\xi^{(dep)}_{prim}(\sigma,\mathbf{g},\mathbf{h},x_{mag},r_{socp})}{\sqrt{n}}$ as a function of $x^{(sc)}_{mag}$ for different r_{socp}; left — $\rho = 2$, $r_{socp} \in \{\sigma\sqrt{0.05\alpha n}, \sigma\sqrt{0.2\alpha n}\sigma\sqrt{0.6\alpha n}\}$; right — $\rho = 3$, $r_{socp} \in \{\sigma\sqrt{0.05\alpha n}, \sigma\sqrt{0.1\alpha n}\sigma\sqrt{0.5\alpha n}\}$

2.2.2 Numerical experiments

Similarly to what was done in the previous subsection, we will split the presentation of the numerical results in several parts. The numerical results that we will present below are obtained by running the SOCP from (4). To demonstrate the precision of our technique we will in parallel show the results obtained by running (16). To make scaling simpler in all our numerical experiments we set $\sigma = 1$.

1) $\frac{E\|\mathbf{w}_{dep}\|_2}{\sigma}$ ***and*** $\frac{E\|\mathbf{w}_{socp}\|_2}{\sigma}$ ***as functions of*** $x^{(sc)}_{mag}$

In this part we will show the numerical results that correspond to the theoretical ones given in part 1) in the previous subsection. To shorten a bit the exposition we will restrict our attention again only on the medium or $\alpha = 0.5$ regime. We then set all other parameters as in the center plot of Figure 3 (these parameters are of course different depending if we are considering $\rho = 2$ or $\rho = 3$; below we will consider both of them).

a) Low (α, β_w) *regime,* $\rho = 2$

We first consider the $\rho = 2$ scenario. As mentioned above in our experiments we set $\alpha = 0.5$, $r_{socp} = \sqrt{\frac{\alpha n}{1+\rho^2}} = \sqrt{0.2\alpha n}$, and (as shown in [53]) β_w such that (α_w, β_w) satisfy (9) and $\alpha_w = \frac{\rho^2}{1+\rho^2}\alpha$. We then ran (4) 300 times with $n = 800$ for various $x^{(sc)}_{mag}$. In parallel we ran (16) for the exact same parameters with only one difference; namely we ran (16) with $n = 2000$. The obtained results for $\frac{E\|\mathbf{w}_{socp}\|_2}{\sigma}$ and $\frac{E\|\mathbf{w}_{dep}\|_2}{\sigma}$ are shown on the left-hand and right-hand side of Figure 7, respectively (given our assumption that $\sigma = 1$ $\frac{E\|\mathbf{w}_{dep}\|_2}{\sigma}$ and $\frac{E\|\mathbf{w}_{socp}\|_2}{\sigma}$ are of course just $E\|\mathbf{w}_{dep}\|_2$ and $E\|\mathbf{w}_{socp}\|_2$, respectively). We also show in Figure 7 the corresponding theoretical predictions obtained in the previous subsection.

b) High (α, β_w) *regime,* $\rho = 3$

We also conducted a set of experiments in the so-called "high" (α, β_w) regime. We used exactly the same parameters as in low (α, β_w) except that we changed ρ from 2 to 3. Consequently we chose $r_{socp} = \sqrt{0.1\alpha n}$ and β_w such that (α_w, β_w) satisfy (9) and $\alpha_w = \frac{\rho^2}{1+\rho^2}\alpha$. As above we ran 300 times each (4) and (16). We ran (4) with $n = 800$ and (16) with $n = 2000$. The numerical results obtained for $\rho = 3$ together with the theoretical predictions are again shown in Figure 7. From Figure 7 we observe a solid agreement between the theoretical predictions and the results obtained through numerical experiments.

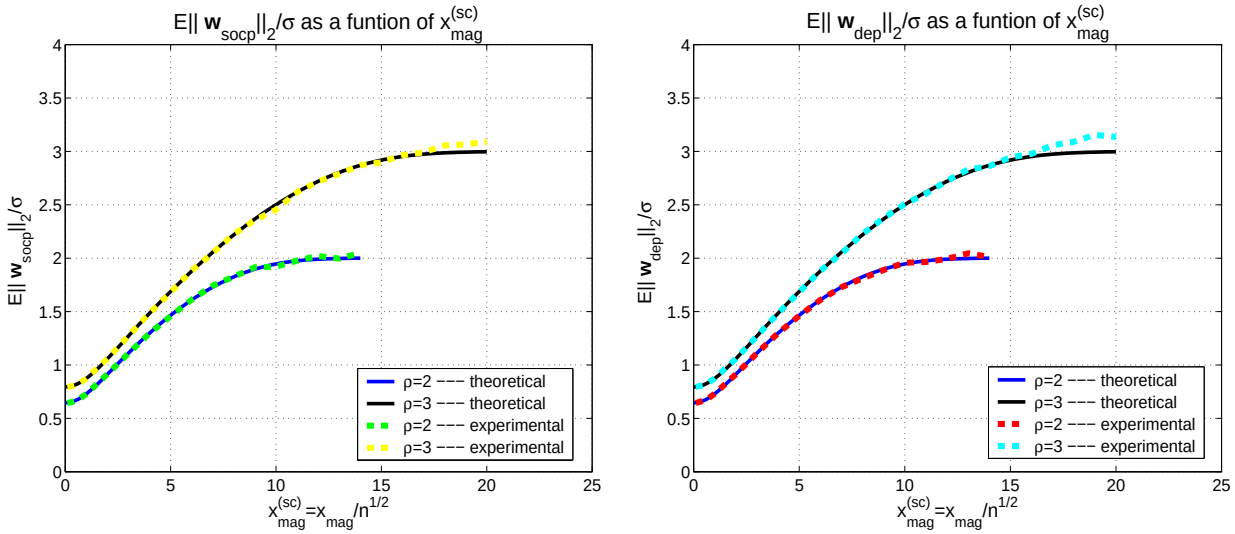

Figure 7: Experimental results for $\frac{E\|\mathbf{w}_{socp}\|_2}{\sigma}$ and $\frac{E\|\mathbf{w}_{dep}\|_2}{\sigma}$ as a function of $x_{mag}^{(sc)}$; $\rho = 2$, $r_{socp} = \sqrt{0.2\alpha n}$; $\rho = 3$, $r_{socp} = \sqrt{0.1\alpha n}$; left — SOCP from (4), right — (16)

2) $\frac{Ef_{obj}}{\sqrt{n}}$ ***and*** $\frac{E\xi_{prim}^{(dep)}(\sigma,\mathbf{g},\mathbf{h},x_{mag},r_{socp})}{\sqrt{n}}$ ***as functions of*** $x_{mag}^{(sc)}$

In this part we will show the numerical results that correspond to the theoretical ones given in part 2) in the previous subsection. We then set all parameters as in Figure 3 (these parameters are exactly the same as in experiments whose results we just presented above). Of course we again distinguish two cases: $\rho = 2$ and $\rho = 3$. For both $\rho = 2$ and $\rho = 3$ we ran 300 times each, (4) and (16) and again we ran (4) with $n = 800$ and (16) with $n = 2000$. The numerical results that we obtained for $\frac{Ef_{obj}}{\sqrt{n}}$ and $\frac{E\xi_{prim}^{(dep)}(\sigma,\mathbf{g},\mathbf{h},x_{mag},r_{socp})}{\sqrt{n}}$ are shown in Figure 8. We again observe a solid agreement between the theoretical predictions and the results

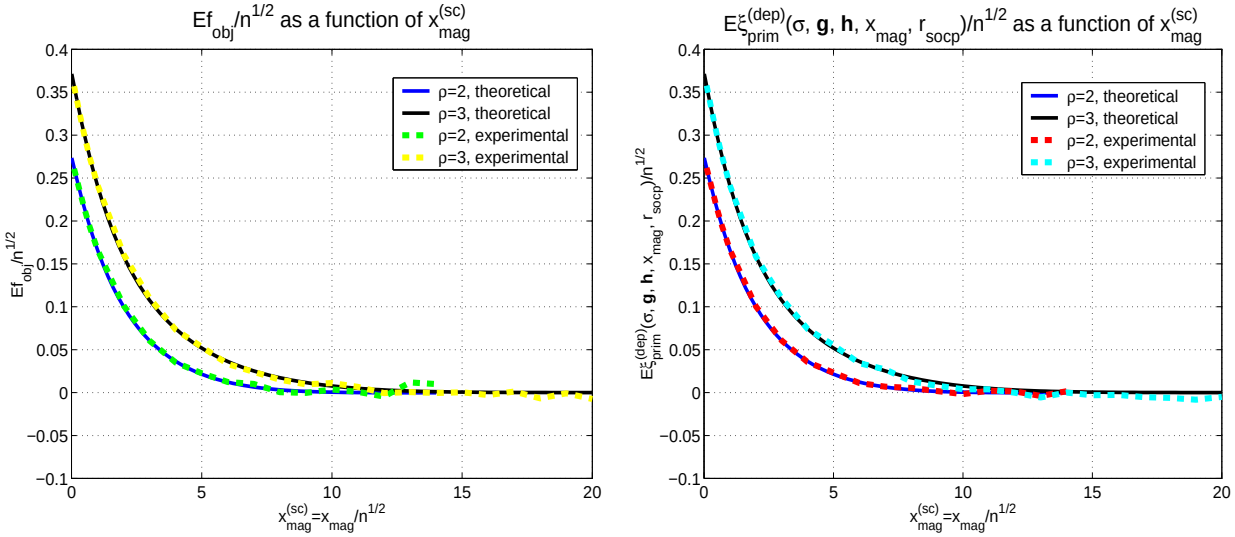

Figure 8: Experimental results for $\frac{Ef_{obj}}{\sqrt{n}}$ and $\frac{E\xi_{prim}^{(dep)}(\sigma,\mathbf{g},\mathbf{h},x_{mag},r_{socp})}{\sqrt{n}}$ as a function of $x_{mag}^{(sc)}$; $\rho = 2$, $r_{socp} = \sqrt{0.2\alpha n}$; $\rho = 3$, $r_{socp} = \sqrt{0.1\alpha n}$; left — SOCP from (4); right — (16)

obtained through numerical experiments.

3) $\frac{E\|\mathbf{w}_{dep}\|_2}{\sigma}$ and $\frac{E\|\mathbf{w}_{socp}\|_2}{\sigma}$ as functions of $x_{mag}^{(sc)}$; varying r_{socp}

In this part we will show the numerical results that correspond to the theoretical ones given in part 3) in the previous subsection. These results relate to possible variations in the r_{socp} that can be used in (4). We then set all other parameters as in Figure 5 (these parameters are of course again different depending if we are considering $\rho = 2$ or $\rho = 3$).

a) Low (α, β_w) regime, $\rho = 2$

We first consider the $\rho = 2$ scenario. As in part 1) of this subsection we set $\alpha = 0.5$ and choose β_w as in part 1). However, differently from part 1) we now consider two different possibilities for r_{socp}, namely $r_{socp} = \sqrt{0.05\alpha n}$ and $r_{socp} = \sqrt{0.6\alpha n}$. We then ran (4) 300 times with $n = 800$ for various $x_{mag}^{(sc)}$. In parallel we ran (16) with $n = 2000$. The obtained results for $\frac{E\|\mathbf{w}_{socp}\|_2}{\sigma}$ and $\frac{E\|\mathbf{w}_{dep}\|_2}{\sigma}$ are shown on the left-hand and right-hand side of Figure 9, respectively (again, given our assumption that $\sigma = 1$ $\frac{E\|\mathbf{w}_{dep}\|_2}{\sigma}$ and $\frac{E\|\mathbf{w}_{socp}\|_2}{\sigma}$ are of course just $E\|\mathbf{w}_{dep}\|_2$ and $E\|\mathbf{w}_{socp}\|_2$, respectively). We also show in Figure 9 the corresponding theoretical predictions obtained in the previous subsection.

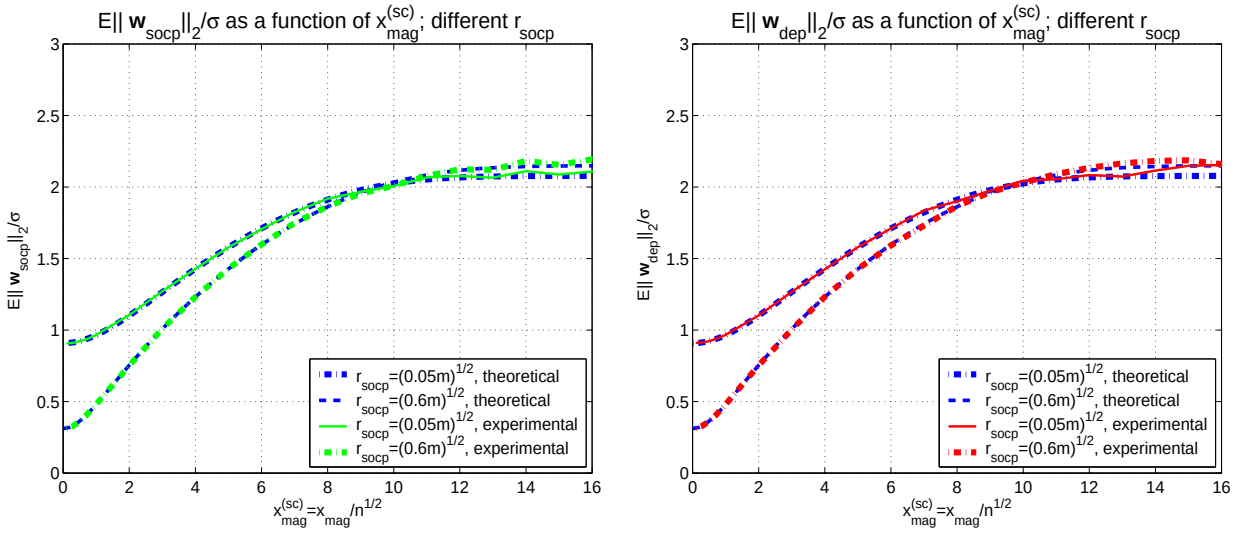

Figure 9: Experimental results for $\frac{E\|\mathbf{w}_{socp}\|_2}{\sigma}$ and $\frac{E\|\mathbf{w}_{dep}\|_2}{\sigma}$ as a function of $x_{mag}^{(sc)}$; $\rho = 2$; $r_{socp} \in \{\sqrt{0.05\alpha n}, \sqrt{0.6\alpha n}\}$; left — SOCP from (4), right — (16)

b) High (α, β_w) regime, $\rho = 3$

We also consider the $\rho = 3$ scenario. As above, we set $\alpha = 0.5$ and choose β_w as in part 1) of this subsection. Everything else remain the same as in $\rho = 2$ case except the way we vary r_{socp}. This time we consider (as in part 3) of the previous section when $\rho = 3$ case was considered) $r_{socp} = \sqrt{0.05\alpha n}$ and $r_{socp} = \sqrt{0.5\alpha n}$. As usual (4) was run 300 times with $n = 800$ for various $x_{mag}^{(sc)}$. In parallel we ran (16) with $n = 2000$. The obtained numerical results for $\frac{Ef_{obj}}{\sqrt{n}}$ and $\frac{E\xi_{prim}^{(dep)}(\sigma,\mathbf{g},\mathbf{h},x_{mag},r_{socp})}{\sqrt{n}}$ as well as the corresponding theoretical predictions obtained in the previous subsection are shown on the left-hand and right-hand side of Figure 10, respectively. We again observe a solid agreement between the theoretical predictions and the results obtained through numerical experiments. Small glitches that happen in large $x_{mag}^{(sc)}$ regime could have been fixed by choosing a larger n. We purposely chose a smaller n to show that results are fairly good even when n is not very large. In fact, even a smaller n than the one we have chosen would work quite fine.

4) $\frac{Ef_{obj}}{\sqrt{n}}$ and $\frac{E\xi_{prim}^{(dep)}(\sigma,\mathbf{g},\mathbf{h},x_{mag},r_{socp})}{\sqrt{n}}$ as functions of $x_{mag}^{(sc)}$; varying r_{socp}

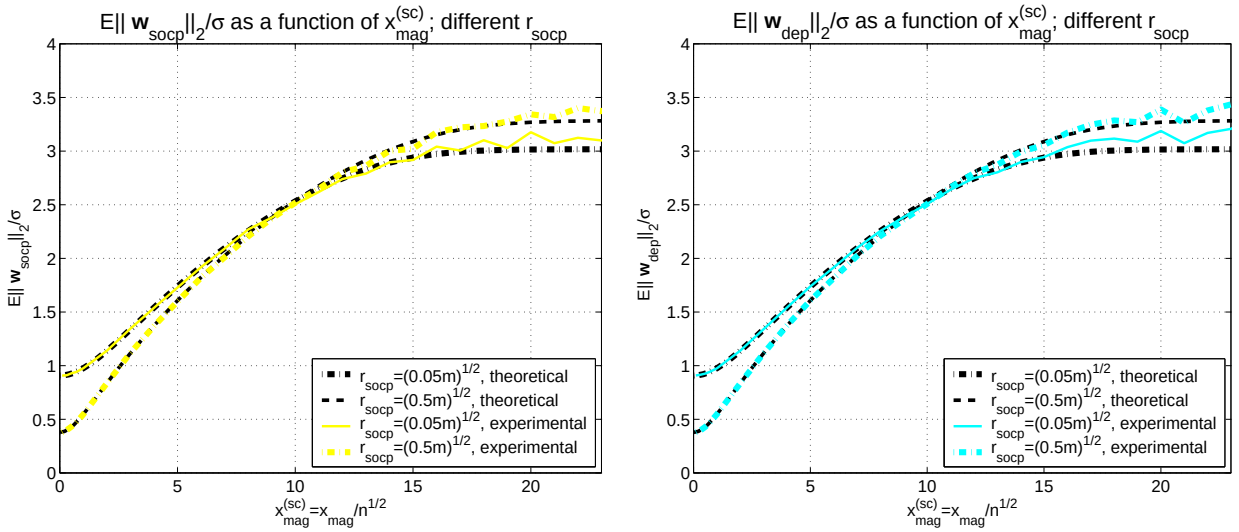

Figure 10: Experimental results for $\frac{E\|\mathbf{w}_{socp}\|_2}{\sigma}$ and $\frac{E\|\mathbf{w}_{dep}\|_2}{\sigma}$ as a function of $x_{mag}^{(sc)}$; $\rho = 3$; $r_{socp} \in \{\sqrt{0.05\alpha n}, \sqrt{0.5\alpha n}\}$; left — SOCP from (4), right — (16)

In this part we will show the numerical results that correspond to the theoretical ones given in part 4) in the previous subsection. These results relate to behavior of $\frac{Ef_{obj}}{\sqrt{n}}$ and $\frac{E\xi_{prim}^{(dep)}(\sigma,\mathbf{g},\mathbf{h},x_{mag},r_{socp})}{\sqrt{n}}$ when one varies r_{socp} in (4). We again consider $\rho = 2$ or $\rho = 3$.

a) Low (α, β_w) regime, $\rho = 2$

The setup that we consider is exactly the same as the one considered in part 3a) of this subsection. We set $\alpha = 0.5$, choose β_w as in part 1), and considered two different possibilities for r_{socp}, namely $r_{socp} = \sqrt{0.05\alpha n}$ and $r_{socp} = \sqrt{0.6\alpha n}$. The obtained results for $\frac{Ef_{obj}}{\sqrt{n}}$ and $\frac{E\xi_{prim}^{(dep)}(\sigma,\mathbf{g},\mathbf{h},x_{mag},r_{socp})}{\sqrt{n}}$ are shown on the left-hand and right-hand side of Figure 11, respectively. The corresponding theoretical predictions obtained in the previous subsection are also shown in Figure 11.

b) High (α, β_w) regime, $\rho = 3$

The setup that we consider is exactly the same as the one considered in part 3b) of this subsection. We set $\alpha = 0.5$, choose β_w as in part 1), and considered two different possibilities for r_{socp}, namely $r_{socp} = \sqrt{0.05\alpha n}$ and $r_{socp} = \sqrt{0.5\alpha n}$. The obtained results for $\frac{E\|\mathbf{w}_{socp}\|_2}{\sigma}$ and $\frac{E\|\mathbf{w}_{dep}\|_2}{\sigma}$ are shown on the left-hand and right-hand side of Figure 12, respectively. The corresponding theoretical predictions obtained in the previous subsection are also shown in Figure 12. We again observe a solid agreement between the theoretical predictions and the results obtained through numerical experiments.

3 SOCP's problem dependent performance – signed x

In this section we show how the SOCP's problem dependent performance analysis developed in the previous section can be specialized to the case when signals are *a priori* known to have nonzero components of certain sign.

3.1 Basic properties of the SOCP's framework

All major assumptions stated at the beginning of the previous section will continue to hold in this section as well; namely, we will continue to consider matrices A with i.i.d. standard normal random variables; elements

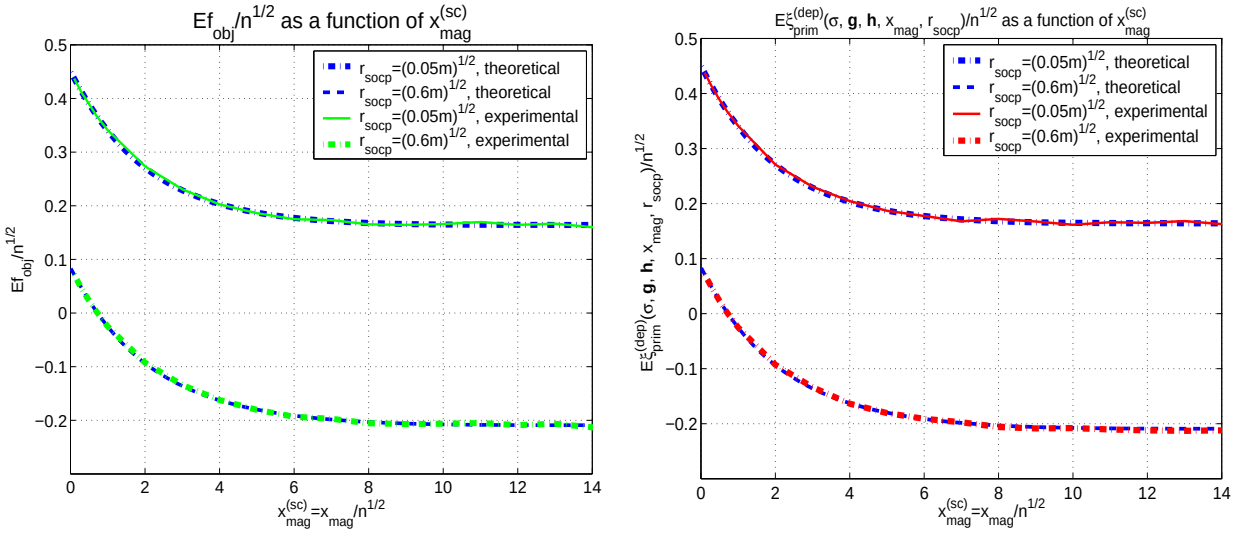

Figure 11: Experimental results for $\frac{Ef_{obj}}{\sqrt{n}}$ and $\frac{E\xi_{prim}^{(dep)}(\sigma,\mathbf{g},\mathbf{h},x_{mag},r_{socp})}{\sqrt{n}}$ as a function of $x_{mag}^{(sc)}$; $\rho=2$; $r_{socp}\in\{\sqrt{0.05\alpha n},\sqrt{0.6\alpha n}\}$; left — SOCP from (4), right — (16)

of $\mathbf{v}$ will again be i.i.d. Gaussian random variables with zero mean and variance σ. The main difference, though, comes in the definition of $\tilde{\mathbf{x}}$. We will in this section assume that $\tilde{\mathbf{x}}$ is the original $\mathbf{x}$ in (3) that we are trying to recover and that it is *any* k-sparse vector with a given fixed location of its nonzero elements and with a priori known signs of its elements. Given the statistical context, it will be fairly easy to see later on that everything that we will present in this section will be irrelevant with respect to what particular location and what particular combination of signs of nonzero elements are chosen. We therefore for the simplicity of the exposition and without loss of generality assume that the components $\mathbf{x}_1,\mathbf{x}_2,\dots,\mathbf{x}_{n-k}$ of $\mathbf{x}$ are equal to zero and that the remaining components of $\mathbf{x}$, $\mathbf{x}_{n-k+1},\mathbf{x}_{n-k+2},\dots,\mathbf{x}_n$, are greater than or equal to zero. However, differently from what was assumed in the previous section, we now assume that this information is *a priori* known. That essentially means that this information is also known to the solving algorithm. Then instead of (4) one can consider its a better ("signed") version

$$\begin{aligned}\min_{\mathbf{x}} \quad & \|\mathbf{x}\|_1 \\ \text{subject to} \quad & \|\mathbf{y}-A\mathbf{x}\|_2\leq r_{socp+} \\ & \mathbf{x}_i\geq 0, 1\leq i\leq n.\end{aligned} \tag{47}$$

Also, one should again note that r_{socp+} in (47) is a parameter that critically impacts the outcome of any SOCP type of algorithm (again, for different r_{socp+}'s one will have different SOCP's). The analysis that we will present assumes a general r_{socp+}. However, we do mention right here that problem (47) is not feasible for all choices of $\tilde{\mathbf{x}}$, α, β_w^+, σ, and r_{socp+}. Unless mentioned otherwise what we present below assumes that $\tilde{\mathbf{x}}$, α, β_w^+, σ, and r_{socp+} are such that (47) is feasible with overwhelming probability. For example, as discussed in [53], a statistical choice $r_{socp+}>\sigma\sqrt{m}$ guarantees feasibility with overwhelming probability. Of course, there are other choices of parameters $\tilde{\mathbf{x}}$, α, β_w^+, σ, and r_{socp+} that guarantee feasibility as well. Towards the end of this section we will mention some of them and address this general question of feasibility in more detail.

Given the positivity of $\mathbf{x}_i, 1\leq i\leq n$, one can, of course, replace ℓ_1 norm in the objective of (47) by the sum of all elements of $\mathbf{x}$. However, to maintain visual similarity between what we will present in this section and what we presented in Section 2 we will keep the ℓ_1 norm in the objective. Along the same lines,

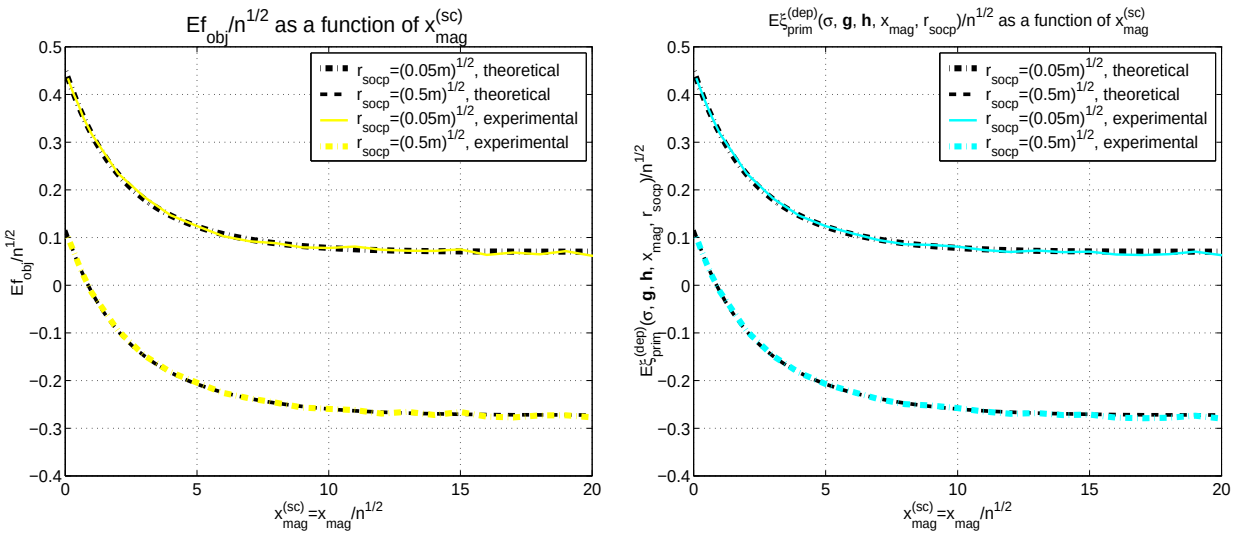

Figure 12: Experimental results for $\frac{Ef_{obj}}{\sqrt{n}}$ and $\frac{E\xi^{(dep)}_{prim}(\sigma,\mathbf{g},\mathbf{h},x_{mag},r_{socp})}{\sqrt{n}}$ as a function of $x^{(sc)}_{mag}$; $\rho = 3$; $r_{socp} \in \{\sqrt{0.05\alpha n}, \sqrt{0.5\alpha n}\}$; left — SOCP from (4), right — (16)

in what follows we will try to mimic the procedure presented in the previous section as much as possible. On such a path we will skip all the obvious parallels and emphasize the points that are different.

As a first step in making the presentation of the "signed" case as parallel as possible to the presentation of the "general" case we will again introduce a few definitions that will turn out to be helpful in what follows. First, let us define the optimal value of a slightly changed objective from (47) in the following way

$$\begin{aligned} f_{obj+} = \min_{\mathbf{x}} \quad & \|\mathbf{x}\|_1 - \|\tilde{\mathbf{x}}\|_1 \\ \text{subject to} \quad & \|\mathbf{y} - A\mathbf{x}\|_2 \leq r_{socp+} \\ & \mathbf{x}_i \geq 0, 1 \leq i \leq n. \end{aligned} \tag{48}$$

As in the previous section, f_{obj+} is clearly a function of $\sigma, \tilde{\mathbf{x}}, A, \mathbf{v}$, and r_{socp+}. To make writing easier we will adopt the same convention as in Section 2 and omit them. Also let $\mathbf{x}_{socp+}$ be the solution of (47) (or the solution of (48)) and let $\mathbf{w}_{socp+} \in R^n$ be the so-called error vector defined in the following way

$$\mathbf{w}_{socp+} = \mathbf{x}_{socp+} - \tilde{\mathbf{x}}. \tag{49}$$

As in Section 2 our main goal in this section will be to provide various characterizations of $\mathbf{w}_{socp+}$ and f_{obj+}. Throughout the paper we will heavily rely on the following theorem from [53] that provides a general characterization of $\mathbf{w}_{socp+}$ and f_{obj+}.

Theorem 3. *([53] — SOCP's performance characterization; signed* $\mathbf{x}$*) Let* $\mathbf{v}$ *be an* $n \times 1$ *vector of i.i.d. zero-mean variance* σ^2 *Gaussian random variables and let* A *be an* $m \times n$ *matrix of i.i.d. standard normal random variables. Further, let* $\mathbf{g}$ *and* $\mathbf{h}$ *be* $m \times 1$ *and* $n \times 1$ *vectors of i.i.d. standard normals, respectively and let* $\mathbf{z}$ *be* $n \times 1$ *vector of all ones. Consider a* k*-sparse* $\tilde{\mathbf{x}}$ *defined in (6) and a* $\mathbf{y}$ *defined in (3) for* $\mathbf{x} = \tilde{\mathbf{x}}$*. Let the solution of (47) be* $\mathbf{x}_{socp+}$ *and let the so-called error vector of the SOCP from (47) be* $\mathbf{w}_{socp+} = \mathbf{x}_{socp+} - \tilde{\mathbf{x}}$*. Let* r_{socp+} *in (47) be a positive scalar. Let* n *be large and let constants* $\alpha = \frac{m}{n}$ *and*

$\beta_w^+ = \frac{k}{n}$ *be below the following so-called* signed fundamental *characterization of* ℓ_1 *optimization*

$$(1-\beta_w^+)\frac{\sqrt{\frac{1}{2\pi}}e^{-(\mathit{erfinv}(2\frac{1-\alpha_w^+}{1-\beta_w^+}-1))^2}}{\alpha_w^+} - \sqrt{2}\mathit{erfinv}(2\frac{1-\alpha_w^+}{1-\beta_w^+}-1) = 0. \tag{50}$$

Furthermore, let $\tilde{\mathbf{x}}$*,* α*,* β_w^+*,* σ*, and* r_{socp+} *be such that (47) is feasible with overwhelming probability and* $E\xi_{prim+}(\sigma, \mathbf{g}, \mathbf{h}, \tilde{\mathbf{x}}, r_{socp+})$ *defined below is finite. Consider the following optimization problem:*

$$\begin{aligned}\xi_{prim+}(\sigma, \mathbf{g}, \mathbf{h}, \tilde{\mathbf{x}}, r_{socp+}) = \max_{\nu,\lambda} \quad & \sigma\sqrt{\|\mathbf{g}\|_2^2\nu^2 - \|\nu\mathbf{h}+\mathbf{z}-\lambda\|_2^2} - \sum_{i=n-k+1}^{n}\lambda_i\tilde{\mathbf{x}}_i - \nu r_{socp+} \\ \textit{subject to} \quad & \nu \geq 0 \\ & \lambda_i \geq 0, 1 \leq i \leq n.\end{aligned} \tag{51}$$

Let $\widehat{\nu^+}$ *and* $\widehat{\lambda^+}$ *be the solution of (51). Set*

$$\|\widehat{\mathbf{w}^+}\|_2 = \sigma\frac{\|\widehat{\nu^+}\mathbf{h}+\mathbf{z}-\widehat{\lambda^+}\|_2}{\sqrt{\|\mathbf{g}\|_2^2\widehat{\nu^+}^2 - \|\widehat{\nu^+}\mathbf{h}+\mathbf{z}-\widehat{\lambda^+}\|_2^2}}. \tag{52}$$

Then:

$$\begin{aligned}P(\|\tilde{\mathbf{x}}+\mathbf{w}_{socp+}\|_1 - \|\tilde{\mathbf{x}}\|_1 \in (E\xi_{prim+}(\sigma, \mathbf{g}, \mathbf{h}, \tilde{\mathbf{x}}, r_{socp+})) - \epsilon_1^{(socp)}|E\xi_{prim+}(\sigma, \mathbf{g}, \mathbf{h}, \tilde{\mathbf{x}}, r_{socp+}))|, \\ E\xi_{prim+}(\sigma, \mathbf{g}, \mathbf{h}, \tilde{\mathbf{x}}, r_{socp+})) + \epsilon_1^{(socp)}|E\xi_{prim+}(\sigma, \mathbf{g}, \mathbf{h}, \tilde{\mathbf{x}}, r_{socp+}))|) = 1 - e^{-\epsilon_2^{(socp)}n}\end{aligned} \tag{53}$$

and

$$P((1-\epsilon_1^{(socp)})E\|\widehat{\mathbf{w}^+}\|_2 \leq \|\mathbf{w}_{socp+}\|_2 \leq (1+\epsilon_1^{(socp)})E\|\widehat{\mathbf{w}^+}\|_2) = 1 - e^{-\epsilon_2^{(socp)}n}, \tag{54}$$

where $\epsilon_1^{(socp)} > 0$ *is an arbitrarily small constant and* $\epsilon_2^{(socp)}$ *is a constant dependent on* $\epsilon_1^{(socp)}$ *and* σ *but independent of* n*.*

Proof. Presented in [53]. □

Remark: A pair (α, β_w^+) lies below the signed fundamental characterization (50) if $\alpha > \alpha_w^+$ and α_w^+ and β_w^+ are such that (50) holds.

3.2 Problem dependent properties of the framework

To facilitate the exposition that will follow we similarly to what was done in Section 2 (and earlier in [53, 54, 57]) set

$$\bar{\mathbf{h}}^+ = [\mathbf{h}_{(1)}^{(1)}, \mathbf{h}_{(2)}^{(2)}, \ldots, \mathbf{h}_{(n-k)}^{(n-k)}, \mathbf{h}_{n-k+1}^{(k)}, \mathbf{h}_{n-k+2}^{(k-1)}, \ldots, \mathbf{h}_n^{(1)}]^T, \tag{55}$$

where $[\mathbf{h}_{(1)}^{(1)}, \mathbf{h}_{(2)}^{(2)}, \ldots, \mathbf{h}_{(n-k)}^{(n-k)}]$ are the elements of $[-\mathbf{h}_1, -\mathbf{h}_2, \ldots, -\mathbf{h}_{n-k}]$ sorted in increasing order and $[\mathbf{h}_{n-k+1}^{(k)}, \mathbf{h}_{n-k+2}^{(k-1)}, \ldots, \mathbf{h}_n^{(1)}]$ are the elements of $[-\mathbf{h}_{n-k+1}, -\mathbf{h}_{n-k+2}, \ldots, -\mathbf{h}_n]$ sorted in decreasing order (possible ties in the sorting processes are of course broken arbitrarily). One can then rewrite the optimization

problem from (51) in the following way

$$\begin{aligned}\xi_{prim+}(\sigma,\mathbf{g},\mathbf{h},\tilde{\mathbf{x}},r_{socp+}) = \max_{\nu,\lambda} \quad & \sigma\sqrt{\|\mathbf{g}\|_2^2\nu^2 - \|\nu\bar{\mathbf{h}}^+ - \mathbf{z} + \lambda\|_2^2} - \sum_{i=n-k+1}^{n}\lambda_i\tilde{\mathbf{x}}_i - \nu r_{socp+} \\ \text{subject to} \quad & \nu \geq 0 \\ & \lambda_i \geq 0, 1 \leq i \leq n. \end{aligned} \tag{56}$$

In what follows we will restrict our attention to a specific class of unknown vectors $\tilde{\mathbf{x}}$. Namely, we will consider vectors $\tilde{\mathbf{x}}$ that have amplitude of the nonzero components equal to x_{mag}. In the noiseless case these problem instances are typically the hardest to solve (at least as long as one uses the signed version of the ℓ_1 optimization from (2)). We will again emphasize that the fact that magnitudes of the nonzero elements of $\tilde{\mathbf{x}}$ are x_{mag} is not known a priori and can not be used in the solving algorithm (i.e. one can not add constraints that would exploit this knowledge in optimization problem (47)). It is just that we will consider how the SOCP from (47) behaves when used to solve problem instances generated by such an $\tilde{\mathbf{x}}$. Also, for such an $\tilde{\mathbf{x}}$ (56) can be rewritten in the following way

$$\begin{aligned}\xi^{(dep)}_{prim+}(\sigma,\mathbf{g},\mathbf{h},x_{mag},r_{socp+}) = \max_{\nu,\lambda} \quad & \sigma\sqrt{\|\mathbf{g}\|_2^2\nu^2 - \|\nu\bar{\mathbf{h}}^+ - \mathbf{z} + \lambda\|_2^2} - x_{mag}\sum_{i=n-k+1}^{n}\lambda_i - \nu r_{socp+} \\ \text{subject to} \quad & \nu \geq 0 \\ & \lambda_i \geq 0, 1 \leq i \leq n. \end{aligned} \tag{57}$$

Now, let ν_{dep+} and $\lambda^{(dep+)}$ be the solution of (57). Then analogously to (52) we can set

$$\|\mathbf{w}_{dep+}\|_2 = \sigma\frac{\|\nu_{dep+}\bar{\mathbf{h}}^+ - \mathbf{z} + \lambda^{(dep+)}\|_2}{\sqrt{\|\mathbf{g}\|_2^2\nu_{dep+}^2 - \|\nu_{dep+}\bar{\mathbf{h}}^+ - \mathbf{z} + \lambda^{(dep+)}\|_2^2}}, \tag{58}$$

In what follows we will determine $\|\mathbf{w}_{dep+}\|_2$ and $\xi^{(dep)}_{prim+}(\sigma,\mathbf{g},\mathbf{h},x_{mag},r_{socp+})$ or more precisely their concentrating points $E\|\mathbf{w}_{dep+}\|_2$ and $E\xi^{(dep)}_{prim+}(\sigma,\mathbf{g},\mathbf{h},x_{mag},r_{socp+})$. All other parameters such as ν_{dep+}, $\lambda^{(dep+)}$ can (and some of them will) be computed through the framework as well.

We proceed by following the line of thought presented in Section 2 and earlier in [53,57]. Since $\lambda^{(dep+)}$ is the solution of (57) there will be parameters c_1^+ and c_2^+ such that

$$\lambda^{(dep+)} = [\lambda_1^{(dep+)},\lambda_2^{(dep+)},\ldots,\lambda_{c_1^+}^{(dep+)},0,0,\ldots,0,\lambda_{c_2^+ +1}^{(dep+)},\lambda_{c_2^+ +2}^{(dep+)},\ldots,\lambda_n^{(dep+)}]$$

and obviously $c_1^+ \leq n-k$ and $n-k \leq c_2^+ \leq n$. At this point let us assume that these parameters are known and fixed. Then following [53,57] as well as what was presented in Section 2 the optimization problem from (57) can be rewritten in the following way

$$\begin{aligned}\xi_{prim+}(\sigma,\mathbf{g},\mathbf{h},\tilde{\mathbf{x}},r_{socp+}) = \max_{\nu,\lambda_{c_1^+ +1:n}} \quad & \sigma\sqrt{\|\mathbf{g}\|_2^2\nu^2 - \|\nu\bar{\mathbf{h}}^+_{c_1^+ +1:n} - \mathbf{z}_{c_1^+ +1:n} + \lambda_{c_1^+ +1:n}\|_2^2} - x_{mag}\sum_{i=n-k+1}^{n}\lambda_i - \nu r_{socp+} \\ \text{subject to} \quad & \nu \geq 0 \\ & \lambda_i \geq 0, c_2^+ + 1 \leq i \leq n \\ & \lambda_i = 0, c_1^+ + 1 \leq i \leq c_2^+. \end{aligned} \tag{59}$$

To make writing of what will follow somewhat easier we set

$$\xi^{(obj+)} = \sigma\sqrt{\|\mathbf{g}\|_2^2\nu^2 - \|\nu\bar{\mathbf{h}}^+_{c_1^++1:n} - \mathbf{z}_{c_1^++1:n} + \lambda_{c_1^++1:n}\|_2^2} - x_{mag}\sum_{i=n-k+1}^{n}\lambda_i - \nu r_{socp+}. \tag{60}$$

Similarly to what was done in Section 2 we then proceed by solving the optimization in (59) over ν and $\lambda_{c_1^++1:n}$. To do so we first look at the derivatives with respect to $\lambda_i, c_2^+ + 1 \leq i \leq n$, of the objective in (59). Computing the derivatives and equalling them to zero gives

$$\begin{aligned}
&\frac{d\xi^{(obj+)}}{d\lambda_i} = 0, c_2^+ + 1 \leq i \leq n \\
\iff \quad & \sigma\frac{-(\nu\bar{\mathbf{h}}_i^+ - \mathbf{z}_i + \lambda_i)}{\sqrt{\|\mathbf{g}\|_2^2\nu^2 - \|\nu\bar{\mathbf{h}}^+_{c_1^++1:n} - \mathbf{z}_{c_1^++1:n} + \lambda_{c_1^++1:n}\|_2^2}} - x_{mag} = 0, c_2^+ + 1 \leq i \leq n \\
\iff \quad & \lambda_i - \mathbf{z}_i + \nu\bar{\mathbf{h}}_i^+ = -\frac{x_{mag}}{\sigma}\sqrt{\|\mathbf{g}\|_2^2\nu^2 - \|\nu\bar{\mathbf{h}}^+_{c_1^++1:n} - \mathbf{z}_{c_1^++1:n} + \lambda_{c_1^++1:n}\|_2^2}, c_2^+ + 1 \leq i \leq n \\
\iff \quad & \lambda_i = -\frac{x_{mag}}{\sigma}\sqrt{\|\mathbf{g}\|_2^2\nu^2 - \|\nu\bar{\mathbf{h}}^+_{c_1^++1:n} - \mathbf{z}_{c_1^++1:n} + \lambda_{c_1^++1:n}\|_2^2} + \mathbf{z}_i - \nu\bar{\mathbf{h}}_i^+, c_2^+ + 1 \leq i \leq n.
\end{aligned} \tag{61}$$

From the second to last line in the above equation one then has

$$(\lambda_i - \mathbf{z}_i + \nu\bar{\mathbf{h}}_i^+)^2 = \frac{x_{mag}^2}{\sigma^2}(\|\mathbf{g}\|_2^2\nu^2 - \|\nu\bar{\mathbf{h}}^+_{c_1^++1:c_2^+} - \mathbf{z}_{c_1^++1:c_2^+} + \lambda_{c_1^++1:c_2^+}\|_2^2 - \|\nu\bar{\mathbf{h}}_{c_2^++1:n} - \mathbf{z}_{c_2^++1:n} + \lambda_{c_2^++1:n}\|_2^2)$$

and after an easy algebraic transformation

$$(\lambda_i - \mathbf{z}_i + \nu\bar{\mathbf{h}}_i^+)^2 = \frac{x_{mag}^2}{\sigma^2 + (n - c_2^+)x_{mag}^2}(\|\mathbf{g}\|_2^2\nu^2 - \|\nu\bar{\mathbf{h}}^+_{c_1^++1:c_2^+} - \mathbf{z}_{c_1^++1:c_2^+}\|_2^2). \tag{62}$$

Using (62) we further have

$$\sqrt{\|\mathbf{g}\|_2^2\nu^2 - \|\nu\bar{\mathbf{h}}^+_{c_1^++1:n} - \mathbf{z}_{c_1^++1:n} + \lambda_{c_1^++1:n}\|_2^2} = \frac{\sigma}{\sqrt{\sigma^2 + (n - c_2^+)x_{mag}^2}}\sqrt{\|\mathbf{g}\|_2^2\nu^2 - \|\nu\bar{\mathbf{h}}^+_{c_1^++1:c_2^+} - \mathbf{z}_{c_1^++1:c_2^+}\|_2^2}. \tag{63}$$

Plugging the value for λ_i from (59) in (60) gives

$$\begin{aligned}
\xi^{(obj+)} &= \sigma\sqrt{\|\mathbf{g}\|_2^2\nu^2 - \|\nu\bar{\mathbf{h}}^+_{c_1^++1:n} - \mathbf{z}_{c_1^++1:n} + \lambda_{c_1^++1:n}\|_2^2} - x_{mag}\sum_{i=n-k+1}^{n}\lambda_i - \nu r_{socp+} \\
&= \frac{\sigma^2 + (n - c_2^+)x_{mag}^2}{\sigma}\sqrt{\|\mathbf{g}\|_2^2\nu^2 - \|\nu\bar{\mathbf{h}}^+_{c_1^++1:n} - \mathbf{z}_{c_1^++1:n} + \lambda_{c_1^++1:n}\|_2^2} \\
&- x_{mag}(n - c_2^+) + \nu x_{mag}\sum_{i=c_2^++1}^{n}\bar{\mathbf{h}}_i^+ - \nu r_{socp+}.
\end{aligned} \tag{64}$$

Combining (63) and (64) we finally obtain the following "signed" analogue to (25)

$$\xi^{(obj+)} = \sqrt{\sigma^2 + (n - c_2^+)x_{mag}^2}\sqrt{\|\mathbf{g}\|_2^2\nu^2 - \|\nu\bar{\mathbf{h}}^+_{c_1^+ + 1:c_2^+} - \mathbf{z}_{c_1^+ + 1:c_2^+}\|_2^2} - \nu(r_{socp+} - x_{mag}\sum_{i=c_2^+ + 1}^{n}\bar{\mathbf{h}}_i^+) - x_{mag}(n - c_2^+). \tag{65}$$

Equalling the derivative of $\xi^{(obj+)}$ with respect to ν to zero further gives

$$\begin{aligned} & \frac{d\xi^{(obj+)}}{d\nu} = 0 \\ \iff \quad & \frac{\nu(\|\mathbf{g}\|_2^2 - \sum_{i=c_1^+ + 1}^{c_2^+}(\bar{\mathbf{h}}_i^+)^2) + (\bar{\mathbf{h}}^+_{c_1^+ + 1:c_2^+})^T\mathbf{z}_{c_1^+ + 1:c_2^+}}{(\sqrt{\sigma^2 + (n - c_2^+)x_{mag}^2})^{-1}\sqrt{\|\mathbf{g}\|_2^2\nu^2 - \|\nu\bar{\mathbf{h}}^+_{c_1^+ + 1:c_2^+} - \mathbf{z}_{c_1^+ + 1:c_2^+}\|_2^2}} - (r_{socp+} - x_{mag}\sum_{i=c_2^+ + 1}^{n}\bar{\mathbf{h}}_i^+) = 0. \end{aligned} \tag{66}$$

Let

$$\begin{aligned} s_{dep+} &= (\bar{\mathbf{h}}^+_{c_1^+ + 1:c_2^+})^T\mathbf{z}_{c_1^+ + 1:c_2^+} \\ d_{dep+} &= \sum_{i=c_1 + 1}^{c_2}(\bar{\mathbf{h}}_i^+)^2 \\ r_{dep+} &= r_{socp+} - x_{mag}\sum_{i=c_2 + 1}^{n}\bar{\mathbf{h}}_i^+ \\ a_{dep+} &= \frac{\|\mathbf{g}\|_2^2 - (\sum_{i=c_1 + 1}^{c_2}(\bar{\mathbf{h}}_i^+)^2)}{\sqrt{\sigma^2 + (n - c_2^+)x_{mag}^2}^{-1}r_{dep+}} = \frac{\sqrt{\sigma^2 + (n - c_2^+)x_{mag}^2}(\|\mathbf{g}\|_2^2 - d_{dep+})}{r_{dep+}} \\ b_{dep+} &= \frac{(\bar{\mathbf{h}}^+_{c_1^+ + 1:c_2^+})^T\mathbf{z}_{c_1^+ + 1:c_2^+}}{\sqrt{\sigma^2 + (n - c_2^+)x_{mag}^2}^{-1}r_{dep+}} = \frac{\sqrt{\sigma^2 + (n - c_2^+)x_{mag}^2}s_{dep+}}{r_{dep+}}. \end{aligned} \tag{67}$$

Then combining (66) and (67) one obtains

$$(a_{dep+}\nu + b_{dep+})^2 = \|\mathbf{g}\|_2^2\nu^2 - \|\nu\bar{\mathbf{h}}^+_{c_1^+ + 1:c_2^+} - \mathbf{z}_{c_1^+ + 1:c_2^+}\|_2^2. \tag{68}$$

After solving (68) over ν we have

$$\nu = \frac{-(a_{dep+}b_{dep+} - s_{dep+}) - \sqrt{(a_{dep+}b_{dep+} - s_{dep+})^2 - (b_{dep+}^2 + \|\mathbf{z}_{c_1^+ + 1:c_2^+}\|_2^2)(a_{dep+}^2 - \|\mathbf{g}\|_2^2 + d_{dep+})}}{a_{dep+}^2 - \|\mathbf{g}\|_2^2 + d_{dep+}}. \tag{69}$$

Following what was done in Section 2 and earlier in [53, 57], we have that a combination of (61) and (69)

gives the following two equations that can be used to determine c_1 and c_2.

$$\begin{aligned} \nu\bar{\mathbf{h}}^+_{c_2^+} - \mathbf{z}_{c_2^+} + \frac{x_{mag}}{\sigma}\sqrt{\|\mathbf{g}\|_2^2\nu^2 - \|\nu\bar{\mathbf{h}}^+_{c_1^+:n} - \mathbf{z}_{c_1^+:n} + \lambda_{c_1^+:n}\|_2^2} &= 0 \\ \bar{\mathbf{h}}^+_{c_1^+}\frac{-(a_{dep+}b_{dep+} - s_{dep+}) - \sqrt{(a_{dep+}b_{dep+} - s_{dep+})^2 - (b_{dep+}^2 + \|\mathbf{z}_{c_1^+:c_2^+}\|_2^2)(a_{dep+}^2 - \|\mathbf{g}\|_2^2 + d_{dep+})}}{a_{dep+}^2 - \|\mathbf{g}\|_2^2 + d_{dep+}} &= 1. \end{aligned} \tag{70}$$

The last term that appears on the right hand side of the first of the above equations can be further simplified based on (63) in the following way

$$\sqrt{\|\mathbf{g}\|_2^2\nu^2 - \|\nu\bar{\mathbf{h}}^+_{c_1^+:n} - \mathbf{z}_{c_1^+:n} + \lambda_{c_1^+:n}\|_2^2} = \frac{\sigma\sqrt{\|\mathbf{g}\|_2^2\nu^2 - \nu^2 d_{dep+} + 2\nu s_{dep+} - (c_2^+ - c_1^+)}}{\sqrt{\sigma^2 + (n - c_2^+)x_{mag}^2}}, \tag{71}$$

where we of course recognized that $\|\mathbf{z}_{c_1^+:c_2^+}\|_2^2 = c_2^+ - c_1^+$. Combining (67) and (71) one can then simplify the equations from (70) in the following way

$$\begin{aligned} \nu\bar{\mathbf{h}}^+_{c_2^+} - \mathbf{z}_{c_2^+} + \frac{x_{mag}}{\sqrt{\sigma^2 + (n - c_2^+)x_{mag}^2}}\sqrt{\|\mathbf{g}\|_2^2\nu^2 - \nu^2 d_{dep+} + 2\nu s_{dep+} - (c_2^+ - c_1^+)} &= 0 \\ \bar{\mathbf{h}}^+_{c_1^+}\frac{-(a_{dep+}b_{dep+} - s_{dep+}) - \sqrt{(a_{dep+}b_{dep+} - s_{dep+})^2 - (b_{dep+}^2 + (c_2^+ - c_1^+))(a_{dep+}^2 - \|\mathbf{g}\|_2^2 + d_{dep+})}}{a_{dep+}^2 - \|\mathbf{g}\|_2^2 + d_{dep+}} &= 1. \end{aligned} \tag{72}$$

Let $\widehat{c_1^+}$ and $\widehat{c_2^+}$ be the solution of (72). Then

$$\nu_{dep+} = \frac{-(\widehat{a_{dep+}}\widehat{b_{dep+}} - \widehat{s_{dep+}}) - \sqrt{(\widehat{a_{dep+}}\widehat{b_{dep+}} - \widehat{s_{dep+}})^2 - (\widehat{b_{dep+}}^2 + (\widehat{c_2} - \widehat{c_1}))(\widehat{a_{dep+}}^2 - \|\mathbf{g}\|_2^2 + \widehat{d_{dep+}})}}{\widehat{a_{dep+}}^2 - \|\mathbf{g}\|_2^2 + \widehat{d_{dep+}}}, \tag{73}$$

where $\widehat{s_{dep+}}$, $\widehat{d_{dep+}}$, $\widehat{a_{dep+}}$, and $\widehat{b_{dep+}}$ are s_{dep+}, d_{dep+}, a_{dep+}, and b_{dep+} from (67) computed with $\widehat{c_1}$ and $\widehat{c_2}$. From (58) one then has

$$\|\mathbf{w}_{dep+}\|_2 = \sigma\frac{\|\nu_{dep+}\bar{\mathbf{h}}^+_{\widehat{c_1^+}:n} - \mathbf{z}_{\widehat{c_1^+}:n} + \lambda^{(dep+)}_{\widehat{c_1^+}:n}\|_2}{\sqrt{\|\mathbf{g}\|_2^2\nu_{dep+}^2 - \|\nu_{dep+}\bar{\mathbf{h}}^+_{\widehat{c_1^+}:n} - \mathbf{z}_{\widehat{c_1^+}:n} + \lambda^{(dep+)}_{\widehat{c_1^+}:n}\|_2^2}}. \tag{74}$$

Combining (71) and (74) one further has

$$\|\mathbf{w}_{dep+}\|_2 = \sigma\frac{\sqrt{\|\mathbf{g}\|_2^2\nu_{dep+}^2(n - \widehat{c_2^+})\frac{x_{mag}^2}{\sigma^2} + \nu_{dep+}^2\widehat{d_{dep+}} - 2\nu\widehat{s_{dep+}} + (\widehat{c_2^+} - \widehat{c_1^+})}}{\sqrt{\|\mathbf{g}\|_2^2\nu_{dep+}^2 - \nu_{dep+}^2\widehat{d_{dep+}} + 2\nu_{dep+}\widehat{s_{dep+}} - (\widehat{c_2^+} - \widehat{c_1^+})}}. \tag{75}$$

Combination of (73) and (75) is conceptually enough to determine $\|\mathbf{w}_{dep+}\|_2$ (and then afterwards easily $E\xi^{(dep)}_{prim+}(\sigma, \mathbf{g}, \mathbf{h}, x_{mag}, r_{socp+})$). The part that remains though is a computation of all unknown quantities that appear in (73) and (75). We will below show how that can be done. In doing so we as usual substantially

rely on what was shown in [53, 57] and assume a familiarity with the procedures presented there.

The first thing to resolve is (72). Since all random quantities concentrate we will be dealing (as in [53, 57]) with the expected values. To compute the solution of (72), $\widehat{c_1}$ and $\widehat{c_2}$, we will need the following expected values

$$E\|\mathbf{g}\|_2^2, E\|\bar{\mathbf{h}}^+_{c_1^+ +1:n-k}\|_2^2, E\|\bar{\mathbf{h}}^+_{n-k+1:c_2^+}\|_2^2, E((\bar{\mathbf{h}}^+_{c_1^+ +1:n-k})^T\mathbf{z}_{c_1^+ +1:n-k}), E((\bar{\mathbf{h}}^+_{n-k+1:c_2^+})^T\mathbf{z}_{n-k+1:c_2^+}). \tag{76}$$

As in Section 2 we easily have

$$E\|\mathbf{g}\|_2^2 = m. \tag{77}$$

Let $c_1^+ = (1-\theta_1^+)n$ and $c_2^+ = \theta_2^+ n$ where θ_1^+ and θ_2^+ are constants independent of n. Then as shown in [53, 57]

$$\lim_{n\rightarrow\infty}\frac{E\|\bar{\mathbf{h}}^+_{c_1^+ +1:n-k}\|_2^2}{n} = \frac{1-\beta_w^+}{\sqrt{2\pi}}\left(\frac{\sqrt{2}(\text{erfinv}(2\frac{1-\theta_1^+}{1-\beta_w^+}-1))}{e^{(\text{erfinv}(2\frac{1-\theta_1^+}{1-\beta_w^+}-1))^2}}\right)+\theta_1^+-\beta_w^+. \tag{78}$$

where we of course recall that $\beta_w^+ = \frac{k}{n}$. Also, as in Section 2 and earlier in [53, 57] we have

$$\lim_{n\rightarrow\infty}\frac{E\|\bar{\mathbf{h}}^+_{n-k+1:c_2^+}\|_2^2}{n} = \frac{\beta_w^+}{\sqrt{2\pi}}\left(\frac{\sqrt{2}\text{erfinv}(2\frac{1-\theta_2^+}{\beta_w^+}-1)}{e^{(\text{erfinv}(2\frac{1-\theta_2^+}{\beta_w^+}-1))^2}}\right)+\theta_2^+-1+\beta_w^+. \tag{79}$$

Following further what was established in [53, 57] we have

$$\begin{aligned}\lim_{n\rightarrow\infty}\frac{E((\bar{\mathbf{h}}^+_{c_1^+ +1:n-k})^T\mathbf{z}_{c_1^+ +1:n-k})}{n} &= \left((1-\beta_w^+)\sqrt{\frac{1}{2\pi}}e^{-(\text{erfinv}(2\frac{1-\theta_1^+}{1-\beta_w^+}-1))^2}\right)\\ \lim_{n\rightarrow\infty}\frac{E((\bar{\mathbf{h}}^+_{n-k+1:c_2^+})^T\mathbf{z}_{n-k+1:c_2^+})}{n} &= \left(\beta_w^+\sqrt{\frac{1}{2\pi}}e^{-(\text{erfinv}(2\frac{1-\theta_2^+}{\beta_w^+}-1))^2}\right).\end{aligned} \tag{80}$$

From (80) we also have

$$\lim_{n\rightarrow\infty}\frac{E(\sum_{i=c_2+1}^n\bar{\mathbf{h}}_i^+)}{n} = -\left(\beta_w^+\sqrt{\frac{1}{2\pi}}e^{-(\text{erfinv}(2\frac{1-\theta_2^+}{\beta_w^+}-1))^2}\right). \tag{81}$$

The only other thing that we will need in order to be able to compute $\widehat{c_1^+}$ and $\widehat{c_2^+}$ (besides the expectations from (76)) are the following inequalities related to the behavior of $\bar{\mathbf{h}}^+_{c_1^+}$ and $\bar{\mathbf{h}}^+_{c_2^+}$. Again, as shown in [53, 57]

$$\begin{aligned}P(\sqrt{2}\text{erfinv}((1+\epsilon_1^{\bar{\mathbf{h}}^+_{c_1^+}})(2\frac{1-\theta_1^+}{1-\beta_w^+}-1)) \leq \bar{\mathbf{h}}^+_{c_1^+}) &\leq e^{-\epsilon_2^{\bar{\mathbf{h}}^+_{c_1^+}}n}\\ P(\sqrt{2}\text{erfinv}((1+\epsilon_1^{\bar{\mathbf{h}}^+_{c_2^+}})(2\frac{1-\theta_2^+}{\beta_w^+}-1)) \leq \bar{\mathbf{h}}^+_{c_2^+}) &\leq e^{-\epsilon_2^{\bar{\mathbf{h}}^+_{c_2^+}}n}.\end{aligned} \tag{82}$$

where $\epsilon_1^{\bar{\mathbf{h}}^+_{c_1^+}} > 0$ and $\epsilon_1^{\bar{\mathbf{h}}^+_{c_2^+}} > 0$ are arbitrarily small constants and $\epsilon_2^{\bar{\mathbf{h}}^+_{c_1^+}}$ and $\epsilon_2^{\bar{\mathbf{h}}^+_{c_2^+}}$ are constants dependent on $\epsilon_1^{\bar{\mathbf{h}}^+_{c_1^+}}$ and $\epsilon_1^{\bar{\mathbf{h}}^+_{c_2^+}}$, respectively, but independent of n.

At this point we have all the necessary ingredients to determine $\widehat{c_1^+}$ and $\widehat{c_2^+}$ and consequently ν_{dep+}, $\|\mathbf{w}_{dep+}\|_2$, and $\xi_{prim+}^{(dep)}(\sigma,\mathbf{g},\mathbf{h},x_{mag},r_{socp+})$, or to be more precise their concentrating points. The following theorem then provides a systematic way of doing so.

Theorem 4. *Assume the setup of Theorem 3. Let the nonzero components of $\tilde{\mathbf{x}}$ have magnitude x_{mag} and let $\bar{\mathbf{h}}^+$ be as defined in (55). Further, let $r_{socp+}^{(sc)}=\lim_{n\rightarrow\infty}\frac{r_{socp+}}{\sqrt{n}}$ and $x_{mag}^{(sc)}=\lim_{n\rightarrow\infty}\frac{x_{mag}}{\sqrt{n}}$. Also, let ν_{dep+}, $\|\mathbf{w}_{dep+}\|_2$, and $\xi_{prim+}^{(dep)}(\sigma,\mathbf{g},\mathbf{h},x_{mag},r_{socp+})$ be as defined in and right after (57). Let $\alpha=\frac{m}{n}$ and $\beta_w^+=\frac{k}{n}$ be fixed. Consider the following*

$$S(\theta_1^+,\theta_2^+)=\lim_{n\rightarrow\infty}\frac{Es_{dep+}}{n}=\left((1-\beta_w^+)\sqrt{\frac{1}{2\pi}}e^{-(\mathit{erfinv}(2\frac{1-\theta_1^+}{1-\beta_w^+}-1))^2}\right)+\left(\beta_w^+\sqrt{\frac{1}{2\pi}}e^{-(\mathit{erfinv}(2\frac{1-\theta_2^+}{\beta_w^+}-1))^2}\right)$$

$$D(\theta_1^+,\theta_2^+)=\lim_{n\rightarrow\infty}\frac{Ed_{dep+}}{n}=\frac{1-\beta_w^+}{\sqrt{2\pi}}\left(\frac{\sqrt{2}(\mathit{erfinv}(2\frac{1-\theta_1^+}{1-\beta_w^+}-1))}{e^{(\mathit{erfinv}(2\frac{1-\theta_1^+}{1-\beta_w^+}-1))^2}}\right)+\theta_1^+-\beta_w^+$$
$$+\frac{\beta_w^+}{\sqrt{2\pi}}\left(\frac{\sqrt{2}\mathit{erfinv}(2\frac{1-\theta_2^+}{\beta_w^+}-1)}{e^{(\mathit{erfinv}(2\frac{1-\theta_2^+}{\beta_w^+}-1))^2}}\right)+\theta_2^+-1+\beta_w^+$$

$$R(\theta_2^+)=\lim_{n\rightarrow\infty}\frac{Er_{dep+}}{\sqrt{n}}=r_{socp+}^{(sc)}+x_{mag}^{(sc)}\left(\beta_w^+\sqrt{\frac{1}{2\pi}}e^{-(\mathit{erfinv}(2\frac{1-\theta_2^+}{\beta_w^+}-1))^2}\right)$$

$$\begin{aligned}
A(\theta_1^+,\theta_2^+) &= \lim_{n\rightarrow\infty}\frac{Ea_{dep+}}{\sqrt{n}}=\frac{\sqrt{\sigma^2+(1-\theta_2^+)(x_{mag}^{(sc)})^2}(\alpha-D(\theta_1^+,\theta_2^+))}{R(\theta_2^+)}\\
B(\theta_1^+,\theta_2^+) &= \lim_{n\rightarrow\infty}\frac{Eb_{dep+}}{\sqrt{n}}=\frac{\sqrt{\sigma^2+(1-\theta_2^+)(x_{mag}^{(sc)})^2}S(\theta_1^+,\theta_2^+)}{R(\theta_2^+)}\\
F(\theta_1^+) &= \sqrt{2}\mathit{erfinv}(2\frac{1-\theta_1^+}{1-\beta_w^+}-1)\\
G(\theta_2^+) &= \sqrt{2}\mathit{erfinv}(2\frac{1-\theta_2^+}{\beta_w^+}-1).
\end{aligned}\tag{83}$$

Set

$$N(\theta_1^+,\theta_2^+)=\frac{-(A(\theta_1^+,\theta_2^+)B(\theta_1^+,\theta_2^+)-S(\theta_1^+,\theta_2^+))}{A(\theta_1^+,\theta_2^+)^2-\alpha+D(\theta_1^+,\theta_2^+)}$$
$$-\frac{\sqrt{(A(\theta_1^+,\theta_2^+)B(\theta_1^+,\theta_2^+)-S(\theta_1^+,\theta_2^+))^2-(B(\theta_1^+,\theta_2^+)^2+\theta_1^++\theta_2^+-1)(A(\theta_1^+,\theta_2^+)^2-\alpha+D(\theta_1^+,\theta_2^+))}}{A(\theta_1^+,\theta_2^+)^2-\alpha+D(\theta_1^+,\theta_2^+)}.$$

Let the pair $(\widehat{\theta_1^+}, \widehat{\theta_2^+})$ be the solution of the following two equations

$$\begin{aligned} N(\theta_1^+,\theta_2^+)G(\theta_2^+) + \frac{x_{mag}^{(sc)}\sqrt{N(\theta_1^+,\theta_2^+)^2(\alpha - D(\theta_1^+,\theta_2^+)) + 2N(\theta_1^+,\theta_2^+)S(\theta_1^+,\theta_2^+) - (\theta_1^+ + \theta_2^+ - 1)}}{\sqrt{\sigma^2 + (1-\theta_2^+)(x_{mag}^{(sc)})^2}} &= 1 \\ F(\theta_1^+)N(\theta_1^+,\theta_2^+) &= 1. \end{aligned} \tag{84}$$

Then the concentrating points of ν_{dep+}, $\|\mathbf{w}_{dep+}\|_2$, and $\xi_{prim+}^{(dep)}(\sigma,\mathbf{g},\mathbf{h},x_{mag},r_{socp+})$ can be determined as

$$E\nu_{dep+} = N(\widehat{\theta_1^+},\widehat{\theta_2^+})$$

$$E\|\mathbf{w}_{dep+}\|_2 = \sigma\frac{\sqrt{N(\widehat{\theta_1^+},\widehat{\theta_2^+})^2(\alpha(1-\widehat{\theta_2^+})\frac{(x_{mag}^{(sc)})^2}{\sigma^2} + D(\widehat{\theta_1^+},\widehat{\theta_2^+})) - 2N(\widehat{\theta_1^+},\widehat{\theta_2^+})S(\widehat{\theta_1^+},\widehat{\theta_2^+}) + (\widehat{\theta_1^+} + \widehat{\theta_2^+} - 1)}}{\sqrt{N(\widehat{\theta_1^+},\widehat{\theta_2^+})^2(\alpha - D(\widehat{\theta_1^+},\widehat{\theta_2^+})) + 2N(\widehat{\theta_1^+},\widehat{\theta_2^+})S(\widehat{\theta_1^+},\widehat{\theta_2^+}) - (\widehat{\theta_1^+} + \widehat{\theta_2^+} - 1)}}$$

$$\begin{aligned} \lim_{n\to\infty}\frac{E\xi_{prim+}^{(dep)}(\sigma,\mathbf{g},\mathbf{h},x_{mag},r_{socp+})}{\sqrt{n}} = \sigma\frac{\sqrt{N(\widehat{\theta_1^+},\widehat{\theta_2^+})^2(\alpha - D(\widehat{\theta_1^+},\widehat{\theta_2^+})) + 2N(\widehat{\theta_1^+},\widehat{\theta_2^+})S(\widehat{\theta_1^+},\widehat{\theta_2^+}) - (\widehat{\theta_1^+} + \widehat{\theta_2^+} - 1)}}{\sqrt{1 + (1-\widehat{\theta_2^+})\frac{(x_{mag}^{(sc)})^2}{\sigma^2}}} \\ - N(\widehat{\theta_1^+},\widehat{\theta_2^+})r_{socp+}^{(sc)}. \end{aligned} \tag{85}$$

Proof. Follows from Theorem 3 based on the discussion presented above and a combination of (67), (72), (73), and (75). □

The results from the above theorem can be used to compute parameters of interest in our derivation for particular values of β_w^+, α, σ, x_{mag}, and r_{socp+}. In the following subsections we will present a collection of such results. However, before doing so in the next subsection we take a look back and discuss the feasibility of (47) in a bit more detail.

3.2.1 Feasibility of (47)

As we have mentioned at the beginning of this section the optimization problem in (47) is not necessarily feasible for all possible choices of $A, \mathbf{v}, \sigma, \tilde{\mathbf{x}}$, and r_{socp+}. Analogously, (51) and (57) are not necessarily bounded for all choices of $\alpha, \beta_w^+, \sigma, \mathbf{g}, \mathbf{h}, \tilde{\mathbf{x}}$, and r_{socp+}. Below we provide a brief discussion on potential unboundedness of (51) and (57). We will split the discussion into two parts. First we focus on a couple of scenarios where the objective of (51) and (57) is bounded. Afterwards we present a procedure that can be used to determine $x_{mag}^{(sc)}$ for which (57) becomes unbounded and (47) infeasible.

1) Universally feasible scenarios

Clearly, the most critical case for (57) to be unbounded is that $x_{mag}^{(sc)} = 0$. Even if $x_{mag}^{(sc)} = 0$ one can distinguish two important scenarios for parameters $\alpha, \beta_w^+, \sigma$, and r_{socp+} such that the objective in (57) is bounded with overwhelming probability.

a) $r_{socp+} > \sigma\sqrt{m}$

The first scenario assumes $r_{socp+} > \sigma\sqrt{m}$. Then for any combination of (α, β_w^+) that lies on or below

the signed fundamental characterization (50) and any σ one has that

$$\sigma\sqrt{\|\mathbf{g}\|_2^2\nu^2-\|\nu\bar{\mathbf{h}}^+-\mathbf{z}+\lambda\|_2^2}-\nu r_{socp+}=\nu(\sigma\sqrt{\|\mathbf{g}\|_2^2-\|\bar{\mathbf{h}}^+-\frac{\mathbf{z}}{\nu}+\frac{\lambda}{\nu}\|_2^2}-r_{socp+}). \tag{86}$$

Let $\epsilon_1^{(feas)}>0$ be an arbitrarily small constant and let $\epsilon_2^{(feas)}$ be a constant dependent on $\epsilon_1^{(feas)}$ but independent of n. Since

$$P(\|\mathbf{g}\|_2\leq(1+\epsilon_1^{(feas)})\sqrt{m})\geq 1-e^{-\epsilon_2^{(feas)}n}$$

one has that with overwhelming probability

$$\sigma\sqrt{\|\mathbf{g}\|_2^2\nu^2-\|\nu\bar{\mathbf{h}}^+-\mathbf{z}+\lambda\|_2^2}-\nu r_{socp+}\leq 0$$

which implies that the objective in (57) is indeed bounded with overwhelming probability.

b) $\alpha\leq 0.5$

The second scenario that we consider assumes that $\alpha\leq 0.5$. Then for any combination of (α,β_w^+) that lies on or below the signed fundamental characterization (50) and any σ one again has that the objective in (57) is bounded with overwhelming probability. To show this we will look at the expression on the right hand side of (86) instead of looking at the objective of (57). Clearly, to have that expression unbounded one must have $\nu\rightarrow\infty$ and the term in the parenthesis must be positive. Also the term under the square root must be nonnegative. Since $\mathbf{z}_i=1$ for any i one easily has that $\mathbf{z}/\nu$ would have to converge to 0. Let us therefore look at the following function $\zeta(\lambda)$

$$\zeta(\lambda)=\|\mathbf{g}\|_2^2-\|\bar{\mathbf{h}}^+-\frac{\lambda}{\nu}\|_2^2. \tag{87}$$

Furthermore let

$$\widehat{\zeta}=\max_{\lambda}\zeta(\lambda)=\max_{\lambda}\|\mathbf{g}\|_2^2-\|\bar{\mathbf{h}}^+-\frac{\lambda}{\nu}\|_2^2. \tag{88}$$

Then it is not that hard to see that

$$\widehat{\zeta}=\|\mathbf{g}\|_2^2-\|\bar{\mathbf{h}}^+_{c_1^{f+}+1:c_2^{f+}}\|_2^2, \tag{89}$$

for certain $c_1^{f+}+1\leq n-k$ and $n-k+1\geq c_2^{f+}\leq n$. For any arbitrarily small constants $\epsilon_3^{(feas)}>0$ and $\epsilon_5^{(feas)}>0$ and constants $\epsilon_4^{(feas)}$, $\epsilon_6^{(feas)}$ dependent on $\epsilon_3^{(feas)}$ and $\epsilon_5^{(feas)}$, respectively but independent of n one easily has

$$P(\bar{\mathbf{h}}^+_{((1+\epsilon_3^{(feas)})\frac{n-k}{2})}\geq 0)\geq 1-e^{-\epsilon_4^{(feas)}n}$$

and

$$P(\bar{\mathbf{h}}^+_{((1-\epsilon_5^{(feas)})\frac{2n-k}{2})}\geq 0)\geq 1-e^{-\epsilon_5^{(feas)}n}.$$

One then with overwhelming probability has that $c_1^{f+}<(1+\epsilon_3^{(feas)})\frac{n-k}{2}$ and $c_2^{f+}>(1-\epsilon_5^{(feas)})\frac{2n-k}{2}$. From (89) it then easily follows that with overwhelming probability

$$\widehat{\zeta}=\|\mathbf{g}\|_2^2-\|\bar{\mathbf{h}}^+_{c_1^{f+}+1:c_2^{f+}}\|_2^2<m-\frac{n}{2}. \tag{90}$$

On the other hand if $\alpha<0.5$ then $m<\frac{n}{2}$ and from (87), (89), and (90) one has that with overwhelming probability $\zeta(\lambda)$ can not be positive for $\nu\rightarrow\infty$. This in return implies that with overwhelming probability the objective in (57) is not unbounded.

We also mention that the feasibility of (47) in the above mentioned scenarios could be deduced by

looking directly at (47). For example, if $r_{socp+} > \sigma m$ then $\mathbf{x} = \tilde{\mathbf{x}}$ is with overwhelming probability feasible in (47). On the other hand if $\alpha < 0.5$ then based on results of [58] (and earlier [23]) one has that the norm-2 in the constraint of (47) can with overwhelming probability be made zero (this is in fact exactly the inverse problem of the one considered in [23, 58]). We will present this small exercise in one of our forthcoming papers since it fits better the topic there.

Also, we should mention that one can define many other scenarios where (57) is bounded. However, we restricted only to the above two since they are relatively simple to describe and have a nice connection to already known results.

2) Finding the feasibility breaking point

In the rest of this subsection we will present a general mechanism that can be used to determine a critical $x_{mag}^{(sc)}$ for which the objective in (57) becomes unbounded and (47) infeasible. We start by rewriting the objective of (57) in the following way

$$\nu(\sigma\sqrt{\|\mathbf{g}\|_2^2 - \|\bar{\mathbf{h}}^+ - \frac{\mathbf{z}}{\nu} + \frac{\lambda}{\nu}\|_2^2} - x_{mag}\sum_{i=n-k+1}^{n}\frac{\lambda_i}{\nu} - r_{socp+}).$$

To have the above expression unbounded one needs $\lambda_i = \nu\lambda_i^{(\nu)}$, $\nu \to \infty$, and the expressions under the square root and in the parenthesis to be positive. Let us then consider

$$\begin{aligned} \max_{\lambda^{(\nu)}} \quad & \sigma\sqrt{\|\mathbf{g}\|_2^2 - \|\bar{\mathbf{h}}^+ + \lambda^{\nu}\|_2^2} - x_{mag}\sum_{i=n-k+1}^{n}\lambda_i^{(\nu)} - r_{socp+} \\ \text{subject to} \quad & \lambda_i^{(\nu)} \geq 0, 1 \leq i \leq n. \end{aligned} \tag{91}$$

Let $\lambda^{(feas)}$ be the solution of (57). Following the line of thought presented in Sections 2 and 3.2 there will be parameters $c_1^{(feas)}$ and $c_2^{(feas)}$ such that

$$\lambda^{(feas)} = [\lambda_1^{(feas)}, \lambda_2^{(feas)}, \ldots, \lambda_{c_1^{(feas)}}^{(feas)}, 0, 0, \ldots, 0, \lambda_{c_2^{(feas)}+1}^{(feas)}, \lambda_{c_2^{(feas)}+2}^{(feas)}, \ldots, \lambda_n^{(feas)}]$$

and obviously $c_1^{(feas)} \leq n-k$ and $n-k \leq c_2^{(feas)} \leq n$. At this point let us assume that these parameters are known and fixed. Then following what was presented in Sections 2 and 3.2 the optimization problem from (91) can be rewritten in the following way

$$\begin{aligned} \max_{\lambda_{c_1^{(feas)}+1:n}} \quad & \sigma\sqrt{\|\mathbf{g}\|_2^2 - \|\bar{\mathbf{h}}_{c_1^+ +1:n}^+ + \lambda_{c_1^{(feas)}+1:n}\|_2^2} - x_{mag}\sum_{i=n-k+1}^{n}\lambda_i - r_{socp+} \\ \text{subject to} \quad & \lambda_i \geq 0, c_2^{(feas)} + 1 \leq i \leq n \\ & \lambda_i = 0, c_1^{(feas)} + 1 \leq i \leq c_2^{(feas)}. \end{aligned} \tag{92}$$

Based on the arguments just above (91) one has that if the optimal value of the objective in (91) is positive then the optimization problem in (57) is unbounded. We will then call the largest $x_{mag}^{(sc)}$ for which the optimal value of the objective in (91) is positive the feasibility breaking point. To determine such an $x_{mag}^{(sc)}$ we proceed by solving the above optimization problem. To make writing of what will follow easier we set

$$\xi^{(feas)} = \sigma\sqrt{\|\mathbf{g}\|_2^2 - \|\bar{\mathbf{h}}_{c_1^+ +1:n}^+ + \lambda_{c_1^{(feas)}+1:n}\|_2^2} - x_{mag}\sum_{i=n-k+1}^{n}\lambda_i - r_{socp+}, \tag{93}$$

and

$$\begin{aligned}\widehat{\xi^{(feas)}} = \max_{\lambda_{c_1^{(feas)}+1:n}} \quad & \xi^{(feas)} \\ \text{subject to} \quad & \lambda_i \geq 0, c_2^{(feas)} + 1 \leq i \leq n \\ & \lambda_i = 0, c_1^{(feas)} + 1 \leq i \leq c_2^{(feas)}. \end{aligned} \tag{94}$$

Similarly to what was done in Section 3.2 we then proceed by solving the optimization in (92) (or the one in (94)) over $\lambda_{c_1^{(feas)}+1:n}$. To do so we look at the derivatives with respect to $\lambda_i, c_2^{(feas)} + 1 \leq i \leq n$, of the objective in (92). Computing the derivatives and equalling them to zero gives

$$\begin{aligned} & \frac{d\xi^{(feas)}}{d\lambda_i} = 0, c_2^{(feas)} + 1 \leq i \leq n \\ \iff \quad & \sigma \frac{-(\bar{\mathbf{h}}_i^+ + \lambda_i)}{\sqrt{\|\mathbf{g}\|_2^2 - \|\bar{\mathbf{h}}^+_{c_1^{(feas)}+1:n} + \lambda_{c_1^{(feas)}+1:n}\|_2^2}} - x_{mag} = 0, c_2^{(feas)} + 1 \leq i \leq n \\ \iff \quad & \lambda_i + \bar{\mathbf{h}}_i^+ = -\frac{x_{mag}}{\sigma}\sqrt{\|\mathbf{g}\|_2^2 - \|\bar{\mathbf{h}}^+_{c_1^{(feas)}+1:n} + \lambda_{c_1^{(feas)}+1:n}\|_2^2}, c_2^{(feas)} + 1 \leq i \leq n. \end{aligned} \tag{95}$$

From the second to line in the above equation one then has

$$(\lambda_i + \bar{\mathbf{h}}_i^+)^2 = \frac{x_{mag}^2}{\sigma^2}(\|\mathbf{g}\|_2^2 - \|\bar{\mathbf{h}}^+_{c_1^{(feas)}+1:c_2^{(feas)}} + \lambda_{c_1^{(feas)}+1:c_2^{(feas)}}\|_2^2 - \|\bar{\mathbf{h}}_{c_2^{(feas)}+1:n} + \lambda_{c_2^{(feas)}+1:n}\|_2^2)$$

and after an easy algebraic transformation

$$(\lambda_i + \bar{\mathbf{h}}_i^+)^2 = \frac{x_{mag}^2}{\sigma^2 + (n - c_2^{(feas)})x_{mag}^2}(\|\mathbf{g}\|_2^2 - \|\bar{\mathbf{h}}^+_{c_1^{(feas)}+1:c_2^{(feas)}}\|_2^2). \tag{96}$$

Using (96) we further have

$$\sqrt{\|\mathbf{g}\|_2^2 - \|\bar{\mathbf{h}}^+_{c_1^{(feas)}+1:n} + \lambda_{c_1^{(feas)}+1:n}\|_2^2} = \frac{\sigma}{\sqrt{\sigma^2 + (n - c_2^{(feas)})x_{mag}^2}}\sqrt{\|\mathbf{g}\|_2^2 - \|\bar{\mathbf{h}}^+_{c_1^{(feas)}+1:c_2^{(feas)}}\|_2^2}. \tag{97}$$

Plugging the value for λ_i from (96) in (93) gives

$$\begin{aligned} \xi^{(feas)} &= \sigma\sqrt{\|\mathbf{g}\|_2^2 - \|\bar{\mathbf{h}}^+_{c_1^{(feas)}+1:n} + \lambda_{c_1^{(feas)}+1:n}\|_2^2} - x_{mag}\sum_{i=n-k+1}^{n}\lambda_i - r_{socp+} \\ &= \frac{\sigma^2 + (n - c_2^{(feas)})x_{mag}^2}{\sigma}\sqrt{\|\mathbf{g}\|_2^2 - \|\bar{\mathbf{h}}^+_{c_1^{(feas)}+1:n} + \lambda_{c_1^{(feas)}+1:n}\|_2^2} \\ &+ x_{mag}\sum_{i=c_2^{(feas)}+1}^{n}\bar{\mathbf{h}}_i^+ - r_{socp+}. \end{aligned} \tag{98}$$

Combining (97) and (98) we finally obtain

$$\xi^{(feas)} = \sqrt{\sigma^2 + (n - c_2^{(feas)})x_{mag}^2}\sqrt{\|\mathbf{g}\|_2^2 - \|\bar{\mathbf{h}}^+_{c_1^{(feas)}+1:c_2^{(feas)}}\|_2^2} - (r_{socp+} - x_{mag}\sum_{i=c_2^{(feas)}+1}^{n}\bar{\mathbf{h}}_i^+). \tag{99}$$

Following what was done in Sections 2 and 3.2 we have that a combination of (96) and (98) (together with the fact that the elements of λ are nonnegative) gives the following two equations that can be used to determine $c_1^{(feas)}$ and $c_2^{(feas)}$

$$\begin{aligned}\bar{\mathbf{h}}^+_{c_2^{(feas)}} + \frac{x_{mag}}{\sqrt{\sigma^2 + (n - c_2^{(feas)})x_{mag}^2}}\sqrt{\|\mathbf{g}\|_2^2 - \|\bar{\mathbf{h}}^+_{c_1^{(feas)}+1:c_2^{(feas)}}\|_2^2} &= 0 \\ \bar{\mathbf{h}}^+_{c_1^{(feas)}} &\leq 0.\end{aligned} \tag{100}$$

Let $\widehat{c_1^{(feas)}}$ and $\widehat{c_2^{(feas)}}$ be the solution of (100). Then from (99) we have

$$\widehat{\xi^{(feas)}} = \sqrt{\sigma^2 + (n - \widehat{c_2^{(feas)}})x_{mag}^2}\sqrt{\|\mathbf{g}\|_2^2 - \|\bar{\mathbf{h}}^+_{\widehat{c_1^{(feas)}}+1:\widehat{c_2^{(feas)}}}\|_2^2} - (r_{socp+} - x_{mag}\sum_{i=\widehat{c_2^{(feas)}}+1}^{n}\bar{\mathbf{h}}_i^+). \tag{101}$$

Combination of (100) and (101) is conceptually enough to determine the feasibility breaking point for $x_{mag}^{(sc)}$. The part that remains is a computation of all unknown quantities that appear in (100) and (101). To do it we will as usual substantially rely on what was shown in previous section and basically in [53, 57].

The first thing to resolve is (100). Since all random quantities concentrate we will again deal with the expected values. To compute the solution of (100), $\widehat{c_1^{(feas)}}$ and $\widehat{c_2^{(feas)}}$, we will need the following expected values

$$E\|\mathbf{g}\|_2^2, E\|\bar{\mathbf{h}}^+_{c_1^{(feas)}+1:n-k}\|_2^2, E\|\bar{\mathbf{h}}^+_{n-k+1:c_2^+}\|_2^2, E\sum_{i=c_2^{(feas)}+1}^{n}\bar{\mathbf{h}}_i^+. \tag{102}$$

As in previous sections we easily have

$$E\|\mathbf{g}\|_2^2 = m. \tag{103}$$

Let $c_1^{(feas)} = (1 - \theta_1^{(feas)})n$ and $c_2^{(feas)} = \theta_2^{(feas)}n$ where $\theta_1^{(feas)}$ and $\theta_2^{(feas)}$ are constants independent of n. Then as shown in [53, 57]

$$\lim_{n\to\infty}\frac{E\|\bar{\mathbf{h}}^+_{c_1^{(feas)}+1:n-k}\|_2^2}{n} = \frac{1-\beta_w^+}{\sqrt{2\pi}}\left(\frac{\sqrt{2}(\text{erfinv}(2\frac{1-\theta_1^{(feas)}}{1-\beta_w^+}-1))}{e^{(\text{erfinv}(2\frac{1-\theta_1^{(feas)}}{1-\beta_w^+}-1))^2}}\right) + \theta_1^{(feas)} - \beta_w^+. \tag{104}$$

where we of course recall that $\beta_w^+ = \frac{k}{n}$. Also, as in Section 2 and earlier in [53, 57] we have

$$\lim_{n\to\infty}\frac{E\|\bar{\mathbf{h}}^+_{n-k+1:c_2^{(feas)}}\|_2^2}{n} = \frac{\beta_w^+}{\sqrt{2\pi}}\left(\frac{\sqrt{2}\text{erfinv}(2\frac{1-\theta_2^{(feas)}}{\beta_w^+}-1)}{e^{(\text{erfinv}(2\frac{1-\theta_2^{(feas)}}{\beta_w^+}-1))^2}}\right) + \theta_2^{(feas)} - 1 + \beta_w^+. \tag{105}$$

Following further what was established in [53, 57] we also have

$$\lim_{n\to\infty}\frac{E(\sum_{i=c_2^{(feas)}+1:n}^{n}\bar{\mathbf{h}}_i^+)}{n}=-\left(\beta_w^+\sqrt{\frac{1}{2\pi}}e^{-(\text{erfinv}(2\frac{1-\theta_2^{(feas)}}{\beta_w^+}-1))^2}\right). \tag{106}$$

The only other thing that we will need in order to be able to compute $\widehat{c_1^{(feas)}}$ and $\widehat{c_2^{(feas)}}$ (besides the expectations from (102)) are the following inequalities related to the behavior of $\bar{\mathbf{h}}^+_{c_1^{(feas)}}$ and $\bar{\mathbf{h}}^+_{c_2^{(feas)}}$. Again, as shown in [53, 57]

$$\begin{aligned}
P(\sqrt{2}\text{erfinv}((1+\epsilon_1^{\bar{\mathbf{h}}^+_{c_1^{(feas)}}})(2\frac{1-\theta_1^{(feas)}}{1-\beta_w^+}-1))\leq\bar{\mathbf{h}}^+_{c_1^{(feas)}}) &\leq e^{-\epsilon_2^{\bar{\mathbf{h}}^+_{c_1^{(feas)}}}n}\\
P(\sqrt{2}\text{erfinv}((1+\epsilon_1^{\bar{\mathbf{h}}^+_{c_2^{(feas)}}})(2\frac{1-\theta_2^{(feas)}}{\beta_w^+}-1))\leq\bar{\mathbf{h}}^+_{c_2^{(feas)}}) &\leq e^{-\epsilon_2^{\bar{\mathbf{h}}^+_{c_2^{(feas)}}}n}.
\end{aligned} \tag{107}$$

where $\epsilon_1^{\bar{\mathbf{h}}^+_{c_1^{(feas)}}}>0$ and $\epsilon_1^{\bar{\mathbf{h}}^+_{c_2^{(feas)}}}>0$ are arbitrarily small constants and $\epsilon_2^{\bar{\mathbf{h}}^+_{c_1^{(feas)}}}$ and $\epsilon_2^{\bar{\mathbf{h}}^+_{c_2^{(feas)}}}$ are constants dependent on $\epsilon_1^{\bar{\mathbf{h}}^+_{c_1^{(feas)}}}$ and $\epsilon_1^{\bar{\mathbf{h}}^+_{c_2^{(feas)}}}$, respectively, but independent of n. Also, we find it useful for what follows to introduce the following definitions

$$\begin{aligned}
s_{feas} &= \sum_{i=c_2^{(feas)}+1}^{n}\bar{\mathbf{h}}_i^+\\
d_{feas} &= \sum_{i=c_1^{(feas)}+1}^{c_2^{(feas)}}(\bar{\mathbf{h}}_i^+)^2\\
r_{feas} &= r_{socp+}-x_{mag}\sum_{i=c_2^{(feas)}+1}^{n}\bar{\mathbf{h}}_i^+.
\end{aligned} \tag{108}$$

At this point we have all the necessary ingredients to determine $\widehat{c_1^{(feas)}}$ and $\widehat{c_2^{(feas)}}$ and consequently $\widehat{\xi^{(feas)}}$, or to be more precise their concentrating points. The following theorem then provides a systematic way of doing so.

Theorem 5. *Assume the setup of Theorem 3. Let the nonzero components of $\tilde{\mathbf{x}}$ have magnitude x_{mag} and let $\bar{\mathbf{h}}^+$ be as defined in (55). Further, let $r_{socp+}^{(sc)}=\lim_{n\to\infty}\frac{r_{socp+}}{\sqrt{n}}$ and $x_{mag}^{(sc)}=\lim_{n\to\infty}\frac{x_{mag}}{\sqrt{n}}$. Also, let $\widehat{\xi^{(feas)}}$ be as defined in (94). Let $\alpha=\frac{m}{n}$ and $\beta_w^+=\frac{k}{n}$ be fixed. Consider the following*

$$S(\theta_1^{(feas)},\theta_2^{(feas)})=\lim_{n\to\infty}\frac{Es_{dep+}}{n}=-\left(\beta_w^+\sqrt{\frac{1}{2\pi}}e^{-(\textit{erfinv}(2\frac{1-\theta_2^{(feas)}}{\beta_w^+}-1))^2}\right)$$

$$D(\theta_1^{(feas)},\theta_2^{(feas)}) = \lim_{n\to\infty}\frac{Ed_{dep+}}{n} = \frac{1-\beta_w^+}{\sqrt{2\pi}}\left(\frac{\sqrt{2}(\mathit{erfinv}(2\frac{1-\theta_1^{(feas)}}{1-\beta_w^+}-1))}{e^{(\mathit{erfinv}(2\frac{1-\theta_1^{(feas)}}{1-\beta_w^+}-1))^2}}\right)+\theta_1^{(feas)}-\beta_w^+$$
$$+\frac{\beta_w^+}{\sqrt{2\pi}}\left(\frac{\sqrt{2}\mathit{erfinv}(2\frac{1-\theta_2^{(feas)}}{\beta_w^+}-1)}{e^{(\mathit{erfinv}(2\frac{1-\theta_2^{(feas)}}{\beta_w^+}-1))^2}}\right)+\theta_2^{(feas)}-1+\beta_w^+$$

$$R(\theta_2^{(feas)}) = \lim_{n\to\infty}\frac{Er_{dep+}}{\sqrt{n}} = r_{socp+}^{(sc)} - x_{mag}^{(sc)}S(\theta_1^{(feas)},\theta_2^{(feas)}) + x_{mag}^{(sc)}(1-\theta_2^{(feas)})$$
$$= r_{socp+}^{(sc)} + x_{mag}^{(sc)}\left(\beta_w^+\sqrt{\frac{1}{2\pi}}e^{-(\mathit{erfinv}(2\frac{1-\theta_2^{(feas)}}{\beta_w^+}-1))^2}\right)$$

$$\begin{aligned} F(\theta_1^{(feas)}) &= \sqrt{2}\mathit{erfinv}(2\frac{1-\theta_1^{(feas)}}{1-\beta_w^+}-1) \\ G(\theta_2^{(feas)}) &= \sqrt{2}\mathit{erfinv}(2\frac{1-\theta_2^{(feas)}}{\beta_w^+}-1). \end{aligned} \tag{109}$$

Let the pair ($\widehat{\theta_1^{(feas)}}$, $\widehat{\theta_2^{(feas)}}$) be the solution of the following two equations

$$\begin{aligned} G(\theta_2^{(feas)}) + \frac{x_{mag}^{(sc)}\sqrt{(\alpha - D(\theta_1^{(feas)},\theta_2^{(feas)}))}}{\sqrt{\sigma^2+(1-\theta_2^{(feas)})(x_{mag}^{(sc)})^2}} &= 0 \\ F(\theta_1^{(feas)}) &= 0. \end{aligned} \tag{110}$$

Then the feasibility breaking point for $x_{mag}^{(sc)}$ can be determined as the solution of

$$\lim_{n\to\infty}\frac{E\widehat{\xi^{(feas)}}}{\sqrt{n}} = \sqrt{\sigma^2+(1-\widehat{\theta_2^{(feas)}})(x_{mag}^{(sc)})^2}\sqrt{(\alpha - D(\widehat{\theta_1^{(feas)}},\widehat{\theta_2^{(feas)}}))} - R(\widehat{\theta_2^{(feas)}})$$
$$= -(\sigma^2+(1-\widehat{\theta_2^{(feas)}})(x_{mag}^{(sc)})^2)\frac{G(\widehat{\theta_2^{(feas)}})}{x_{mag}^{(sc)}} - R(\widehat{\theta_2^{(feas)}}) = 0. \tag{111}$$

Proof. Follows from Theorem 3 based on the discussion presented above and a combination of (94), (100), and (108). □

Remark 1: It is relatively easy to see that $\widehat{\theta_1^{(feas)}} = \frac{1+\beta_w^+}{2}$ which somewhat simplifies the expression for $D(\theta_1^{(feas)},\theta_2^{(feas)})$. For the completeness though we chose to present the results in the above theorem in a general form.

Remark 2: Another way to deal with the unboundedness (infeasibility) is to look at (68) and recognize that $(a_{dep+}^2 - \|\mathbf{g}\|_2^2 + d_{dep+})$ needs to be negative so that (57) is bounded. We presented the results in

Theorem 3 by assuming that all relevant parameters are such that (57) is bounded. Instead one could actually characterize them through one of the above approaches. However, we thought that it would complicate the presentation and opted for the current exposition.

The results from the above theorem can be used to compute the breaking feasibility point for $x_{mag}^{(sc)}$ for particular values of β_w^+, α, σ, and r_{socp+}. In a part of the following subsection we will present a subset of such results.

3.2.2 Theoretical predictions

In this subsection we present the theoretical predictions one can get based on the result of the previous sections. Similarly to what was done in Section 2.2.1 we will split the presentation of the results into several parts.

1) $\frac{E\|\mathbf{w}_{dep+}\|_2}{\sigma} = \frac{E\|\mathbf{w}_{socp+}\|_2}{\sigma}$ ***as a function of*** $x_{mag}^{(sc)}$

To present this portion (as well as several others that will follow) of theoretical results we will as in Section 2.2.1 look at three regimes: 1) low α-, medium α-, and high α-regime. For each of the regimes we will show the theoretical results for $\frac{E\|\mathbf{w}_{dep+}\|_2}{\sigma} = \frac{E\|\mathbf{w}_{socp+}\|_2}{\sigma}$ as a function of $x_{mag}^{(sc)}$. We will again take $\alpha = 0.3$ as a representative of the low α-regime, $\alpha = 0.5$ as a representative of the medium α-regime, and $\alpha = 0.7$ as a representative of the high α-regime. We will consider $r_{socp+} = r_{socp+}^{(opt)} = \sigma\sqrt{\frac{\alpha n}{1+\rho^2}}$. For each of the α-regimes we will look at two different sub-regimes: low β_w^+- and high β_w^+-regime (which based on results from [53] is equivalent to low ρ- and high ρ-regimes). For each of these two sub-regimes β_w^+ will be selected based on the curves obtained in [53] (or those obtained in [52]) in the following way. In the low β_w^+ sub-regime we will set $\rho = 2$ and $r_{socp+} = r_{socp+}^{(opt)} = \sigma\sqrt{\frac{\alpha n}{5}}$ whereas in the high β_w^+ sub-regime we will set $\rho = 3$ and $r_{socp+} = r_{socp+}^{(opt)} = \sigma\sqrt{\frac{\alpha n}{10}}$. At the same time from [53] we will have $r_{socp+} = r_{socp+}^{(opt)} = \sigma\sqrt{(\alpha - \alpha_w^+)n}$ where α_w^+ and β_w^+ are such that (50) holds (we also recall on [53] where it was reasoned that the low β regime is selected so that the pair (α, β_w^+) is well below the fundamental characterization (50) whereas the high β regime is selected so that the pair (α, β_w^+) is closer to the fundamental characterization (50)). The values for $\frac{E\|\mathbf{w}_{dep+}\|_2}{\sigma} = \frac{E\|\mathbf{w}_{socp+}\|_2}{\sigma}$ one can then get through the results of Theorem 4 for such (α, β_w^+) pairs and $r_{socp+}^{(opt)}$ are shown in Figure 13 as functions of $x_{mag}^{(sc)}$. As can be seen from Figure 13, the values of $\frac{E\|\mathbf{w}_{dep+}\|_2}{\sigma} = \frac{E\|\mathbf{w}_{socp+}\|_2}{\sigma}$ converge to ρ as $x_{mag}^{(sc)}$ increases.

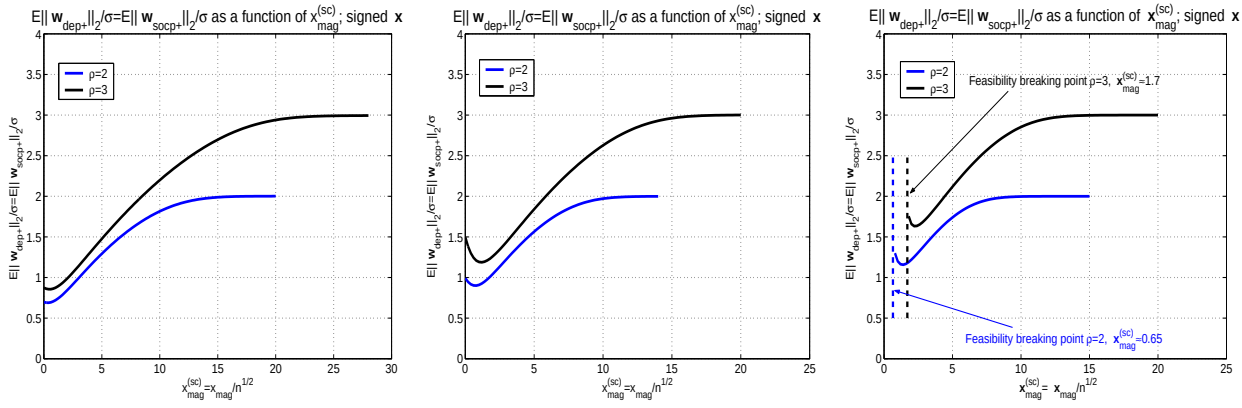

Figure 13: $\frac{E\|\mathbf{w}_{dep+}\|_2}{\sigma} = \frac{E\|\mathbf{w}_{socp+}\|_2}{\sigma}$ as a function of $x_{mag}^{(sc)}$; $r_{socp+} = \sqrt{\frac{\alpha n}{1+\rho^2}}$; left — $\alpha = 0.3$, center — $\alpha = 0.5$, right — $\alpha = 0.7$

This is of course in agreement with [53] where it was demonstrated that for $r_{socp+}^{(opt)}$ one has $\rho = \frac{\|\mathbf{w}_{socp+}\|_2}{\sigma}$ with overwhelming probability. Also, this is in a agreement with a similar conclusion made in Section 2.2.1. Furthermore, as it was the case in Section 2.2.1, the convergence is "faster" (or happens for smaller $x_{mag}^{(sc)}$) for larger α.

On the other hand one should observe from Figure 13 that for $\alpha = 0.7$ the optimization problem in (57) is infeasible with overwhelming probability for $x_{mag}^{(sc)}$ below ≈ 1.7 in high β_w^+ regime and for $x_{mag}^{(sc)}$ below ≈ 0.65 in low β_w^+ regime.

2) $\frac{Ef_{obj+}}{\sqrt{n}} = \frac{E\xi_{prim+}^{(dep)}(\sigma,\mathbf{g},\mathbf{h},x_{mag},r_{socp+})}{\sqrt{n}}$ ***as a function of*** $x_{mag}^{(sc)}$

Similarly to what was discussed above (and is related to $\|\mathbf{w}_{socp+}\|_2$ and $\|\mathbf{w}_{dep+}\|_2$) one can determine the concentrating points of f_{obj+} and $\xi_{prim+}^{(dep)}$ also as functions of $x_{mag}^{(sc)}$. As in Section 2.2.1, to present these results we restrict ourselves to the medium α-regime, or in other words to $\alpha = 0.5$. As in part 1) above we again choose $r_{socp+} = r_{socp+}^{(opt)} = \sigma\sqrt{\frac{\alpha n}{1+\rho^2}}$ and consider low $\rho = 2$- and high $\rho = 3$- regime. The obtained results are shown in Figure 14. As can be seen from Figure 14 $\frac{Ef_{obj+}}{\sqrt{n}}$ is larger for larger ρ.

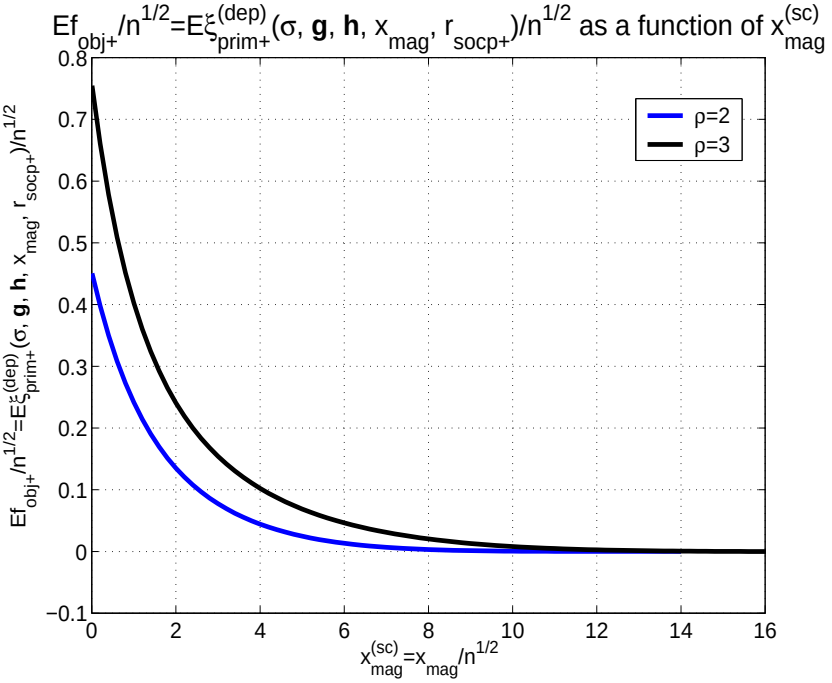

Figure 14: $\frac{Ef_{obj+}}{\sqrt{n}} = \frac{E\xi_{prim+}^{(dep)}(\sigma,\mathbf{g},\mathbf{h},x_{mag},r_{socp+})}{\sqrt{n}}$ as a function of $x_{mag}^{(sc)}$; $r_{socp+} = \sqrt{\frac{\alpha n}{1+\rho^2}}$; $\alpha = 0.5$

3) $\frac{E\|\mathbf{w}_{dep+}\|_2}{\sigma} = \frac{E\|\mathbf{w}_{socp+}\|_2}{\sigma}$ ***as a function of*** $x_{mag}^{(sc)}$***; varying*** r_{socp+}

Another interesting set of results relates to possible variations in the r_{socp+} that can be used in (4). The results that we presented above assume an optimal choice for r_{socp+} (in a sense defined in [53]). Namely, they assume that for a fixed pair (α, β_w^+) one chooses $r_{socp+} = r_{socp+}^{(opt)} = \sigma\sqrt{(\alpha - \alpha_w^+)n}$ where α_w^+ and β_w^+ are such that (50) holds. In the worst-case scenario (or in the generic scenario as we referred to it in [53]) one has that choice $r_{socp+}^{(opt)}$ offers the minimal norm-2 of the error vector. However, such a scenario assumes particular $\tilde{\mathbf{x}}$'s which leaves a possibility that for a wide range of other $\tilde{\mathbf{x}}$'s the performance of the SOCP from (4) in the ℓ_2 norm of the error vector sense can be more favorable. Of course as shown in Figure (13) this indeed happens to be the case. On the other hand that also leaves an option that one can possibly choose

a different r_{socp+} and get say a smaller norm-2 of the error vector for various different $\tilde{\mathbf{x}}$. Below we present a few results in this direction.

We will consider again only the medium or $\alpha = 0.5$ regime. For two sets of different values of ρ, $r_{socp+} = r_{socp+}^{(opt)}$, and β_w^+ we presented the results for $\frac{E\|\mathbf{w}_{dep+}\|_2}{\sigma} = \frac{E\|\mathbf{w}_{socp+}\|_2}{\sigma}$ in Figure 13. In addition to that we now in Figure 15 show similar results one can get through Theorem 4 for two different choices of r_{socp+}. To be more precise, for $\rho = 2$ we choose the same α and β_w^+ as in Figure and only vary r_{socp+} over $\{\sigma\sqrt{0.05\alpha n}, \sigma\sqrt{0.2\alpha n}\sigma\sqrt{0.6\alpha n}\}$. Clearly, choice $\sigma\sqrt{0.05\alpha n}$ is smaller than $r_{socp+}^{(opt)} = \sigma\sqrt{0.2\alpha n}$ whereas choice $\sigma\sqrt{0.6\alpha n}$ is larger than $r_{socp+}^{(opt)} = \sigma\sqrt{0.2\alpha n}$. On the other hand for $\rho = 3$ we choose the same α and β_w^+ as we have chosen for $\rho = 3$ in Figure 13 and vary r_{socp+} but this time over $\{\sigma\sqrt{0.05\alpha n}, \sigma\sqrt{0.1\alpha n}\sigma\sqrt{0.5\alpha n}\}$. Again, clearly, choice $\sigma\sqrt{0.05\alpha n}$ is smaller than $r_{socp+}^{(opt)} = \sigma\sqrt{0.1\alpha n}$ whereas choice $\sigma\sqrt{0.6\alpha n}$ is larger than $r_{socp+}^{(opt)} = \sigma\sqrt{0.2\alpha n}$. It is rather obvious but we mention for the completeness that the middle r_{socp+} choices for both, $\rho = 2$ and $\rho = 3$, cases correspond to the center plot in Figure 13. Based on the results presented in Figure 15 one can then make the same two

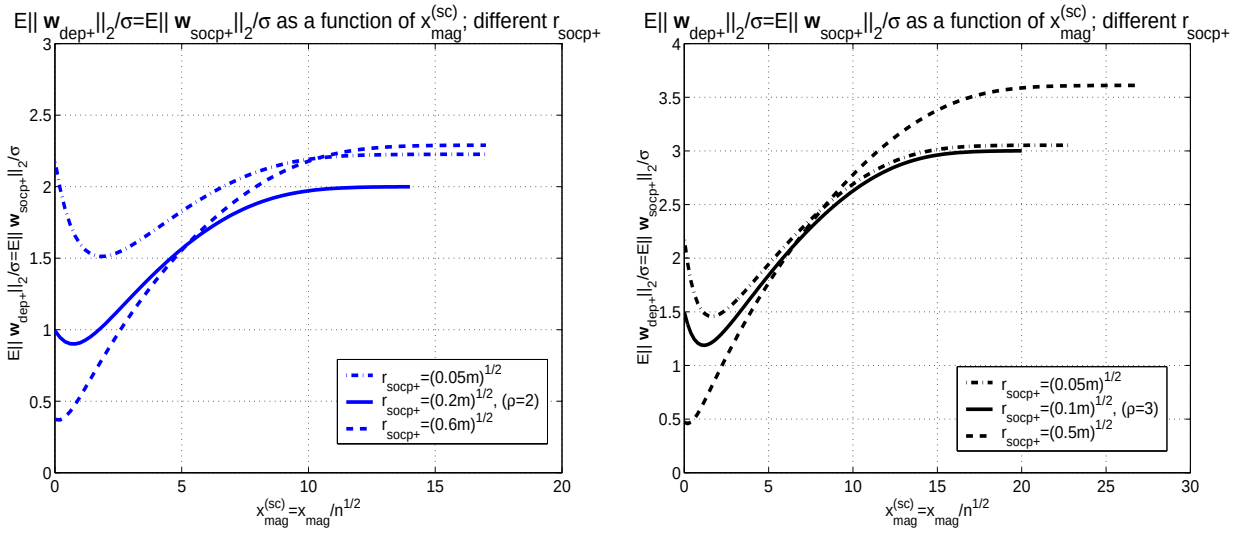

Figure 15: $\frac{E\|\mathbf{w}_{dep+}\|_2}{\sigma} = \frac{E\|\mathbf{w}_{socp+}\|_2}{\sigma}$ as a function of $x_{mag}^{(sc)}$ for different r_{socp+}; left — $\rho = 2$, $r_{socp+} \in \{\sigma\sqrt{0.05\alpha n}, \sigma\sqrt{0.2\alpha n}\sigma\sqrt{0.6\alpha n}\}$; right — $\rho = 3$, $r_{socp+} \in \{\sigma\sqrt{0.05\alpha n}, \sigma\sqrt{0.1\alpha n}\sigma\sqrt{0.5\alpha n}\}$

observations that we made earlier related to the results presented in Figure 5. The first one is that Figure 15 suggests that if r_{socp+} is smaller than $r_{socp+}^{(opt)}$ then $\frac{E\|\mathbf{w}_{socp+}\|_2}{\sigma}$ could be larger than the one that can be obtained for $r_{socp+}^{(opt)}$. This actually happens to be the case. As in Section 2.2.1 we skip the details of this simple exercise. The second observation is that if r_{socp+} is larger than $r_{socp+}^{(opt)}$ then for certain $\tilde{\mathbf{x}}$ $\frac{E\|\mathbf{w}_{socp+}\|_2}{\sigma}$ could be smaller than the one that can be obtained for $r_{socp+}^{(opt)}$. This of course suggests that a choice of r_{socp+} larger than $r_{socp+}^{(opt)}$ could be more favorable in certain applications and for a particular measure of performance. However, if one has no a priori available knowledge about $\tilde{\mathbf{x}}$ then adapting r_{socp+} beyond $r_{socp+}^{(opt)}$ would be hard.

4) $\frac{Ef_{obj+}}{\sqrt{n}} = \frac{E\xi_{prim+}^{(dep)}(\sigma,\mathbf{g},\mathbf{h},x_{mag},r_{socp+})}{\sqrt{n}}$ ***as a function of*** $x_{mag}^{(sc)}$***; varying*** r_{socp+}

Similarly to what was done above in part 2) one can also determine the theoretical predictions for $\frac{Ef_{obj+}}{\sqrt{n}} = \frac{E\xi_{prim+}^{(dep)}}{\sqrt{n}}$ for a varying r_{socp+}. As in parts 2) and 3) above, we restrict our attention only to the medium $\alpha = 0.5$ regime. We also assume exactly the same scenarios as in part 3). The obtained results are

shown in Figure 6. As in part 2) Figure 16 shows that $\frac{Ef_{obj+}}{\sqrt{n}}$ is larger for larger ρ. On the other hand it also

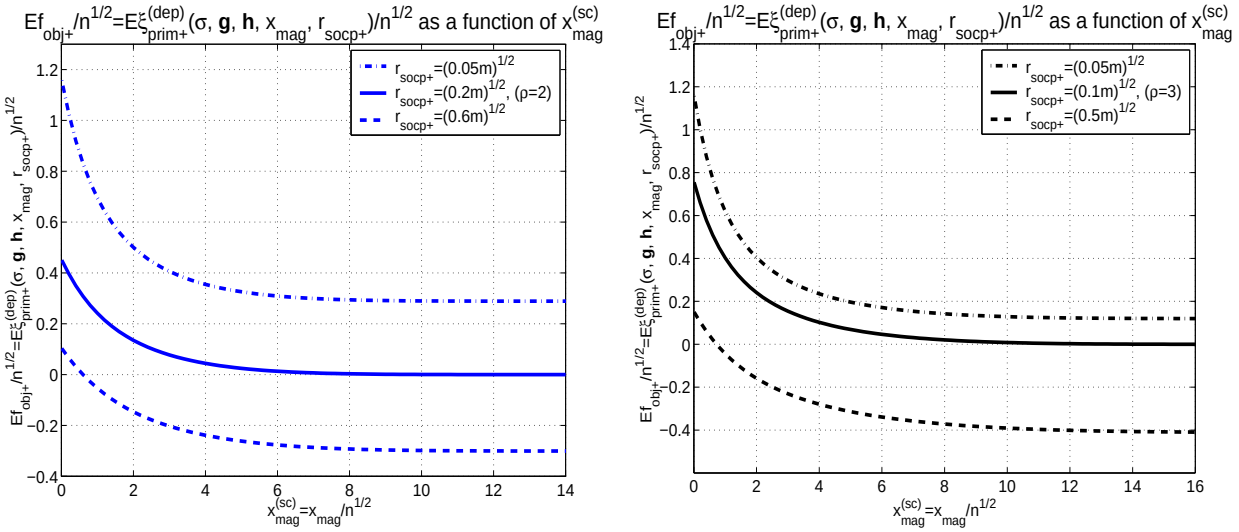

Figure 16: $\frac{Ef_{obj+}}{\sqrt{n}} = \frac{E\xi^{(dep)}_{prim+}(\sigma,\mathbf{g},\mathbf{h},x_{mag},r_{socp+})}{\sqrt{n}}$ as a function of $x^{(sc)}_{mag}$ for different r_{socp+}; left — $\rho = 2$, $r_{socp+} \in \{\sigma\sqrt{0.05\alpha n}, \sigma\sqrt{0.2\alpha n}\sigma\sqrt{0.6\alpha n}\}$; right — $\rho = 3$, $r_{socp+} \in \{\sigma\sqrt{0.05\alpha n}, \sigma\sqrt{0.1\alpha n}\sigma\sqrt{0.5\alpha n}\}$

shows that $\frac{Ef_{obj+}}{\sqrt{n}}$ decreases as r_{socp+} increases. This also follows rather trivially from the structure of (47) or in a way discussed in the corresponding part of Section 2.2.1.

As in Section 2.2.1 we conducted massive numerical experiments and again found that the results one can get through them are in a firm agreement with what the presented theory predicts. In the next subsection we present a sample of the results obtained through the conducted numerical experiments.

3.2.3 Numerical experiments

As in earlier subsection we will split the presentation of the numerical results in several parts. The numerical results that we will present below are obtained by running the SOCP from (47). To demonstrate the precision of our technique we will in parallel show the results obtained by running (57). To make scaling simpler in all our numerical experiments we again set $\sigma = 1$.

1) $\frac{E\|\mathbf{w}_{dep+}\|_2}{\sigma}$ and $\frac{E\|\mathbf{w}_{socp+}\|_2}{\sigma}$ as functions of $x^{(sc)}_{mag}$

In this part we will show the numerical results that correspond to the theoretical ones given in part 1) in the previous subsection. We will restrict our attention again only on the medium or $\alpha = 0.5$ regime (in a later section we will show the results one can get for $\alpha = 0.7$ regime). We then set all other parameters as in the center plot of Figure 13 (these parameters are of course different depending if we are considering $\rho = 2$ or $\rho = 3$; below we will consider both of them).

a) Low (α, β^+_w) regime, $\rho = 2$

We first consider the $\rho = 2$ scenario. As mentioned above in our experiments we set $\alpha = 0.5$, $r_{socp+} = \sqrt{\frac{\alpha n}{1+\rho^2}} = \sqrt{0.2\alpha n}$, and (as shown in [53]) β^+_w such that (α^+_w, β^+_w) satisfy (50) and $\alpha^+_w = \frac{\rho^2}{1+\rho^2}\alpha$. We then ran (47) 300 times with $n = 600$ for various $x^{(sc)}_{mag}$. In parallel we ran (16) for the exact same parameters with only one difference; namely we ran (57) with $n = 2000$. The obtained results for $\frac{E\|\mathbf{w}_{socp+}\|_2}{\sigma}$ and $\frac{E\|\mathbf{w}_{dep+}\|_2}{\sigma}$ are shown on the left-hand and right-hand side of Figure 23, respectively (given our assumption that $\sigma = 1$ $\frac{E\|\mathbf{w}_{dep+}\|_2}{\sigma}$ and $\frac{E\|\mathbf{w}_{socp+}\|_2}{\sigma}$ are of course just $E\|\mathbf{w}_{dep+}\|_2$ and $E\|\mathbf{w}_{socp+}\|_2$, respectively). We

also show in Figure 23 the corresponding theoretical predictions obtained in the previous subsection.

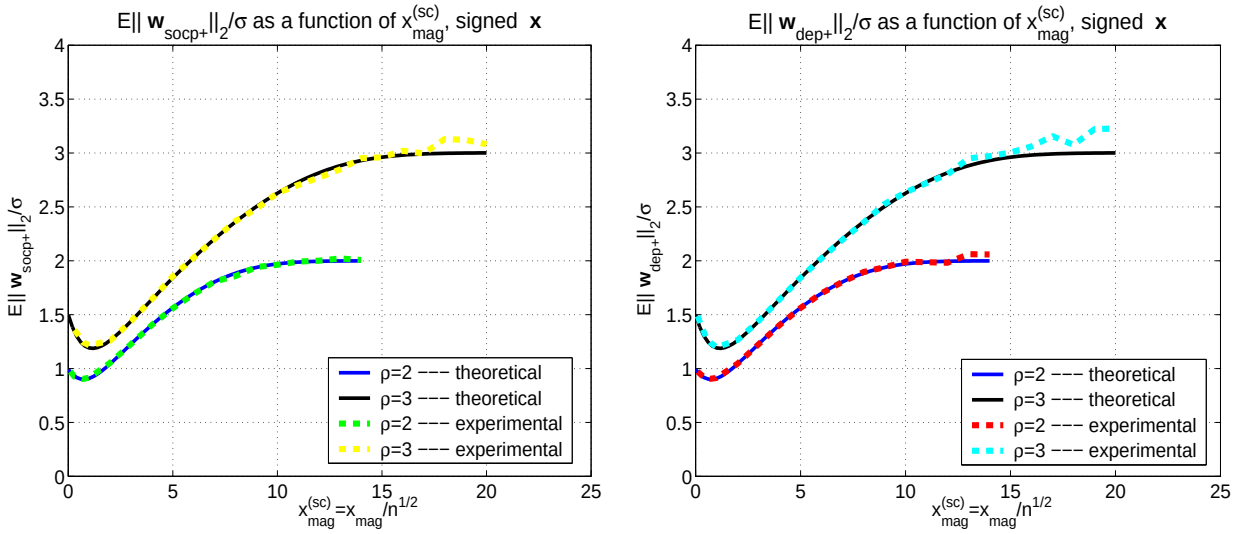

Figure 17: Experimental results for $\frac{E\|\mathbf{w}_{socp+}\|_2}{\sigma}$ and $\frac{E\|\mathbf{w}_{dep+}\|_2}{\sigma}$ as a function of $x_{mag}^{(sc)}$; $\rho = 2$, $r_{socp+} = \sqrt{0.2\alpha n}$; $\rho = 3$, $r_{socp+} = \sqrt{0.1\alpha n}$; left — SOCP from (47), right — (57)

b) High (α, β_w^+) regime, $\rho = 3$

We also conducted a set of experiments in the so-called "high" (α, β_w^+) regime. We used exactly the same parameters as in low (α, β_w^+) except that we changed ρ from 2 to 3. Consequently we chose $r_{socp+} = \sqrt{0.1\alpha n}$ and β_w^+ such that (α_w^+, β_w^+) satisfy (50) and $\alpha_w^+ = \frac{\rho^2}{1+\rho^2}\alpha$. As above we ran 300 times each (47) and (57). We ran (47) with $n = 600$ and (57) with $n = 2000$. The numerical results obtained for $\rho = 3$ together with the theoretical predictions are again shown in Figure 23. From Figure 23 we observe a solid agreement between the theoretical predictions and the results obtained through numerical experiments.

2) $\frac{Ef_{obj+}}{\sqrt{n}}$ and $\frac{E\xi_{prim+}^{(dep)}(\sigma,\mathbf{g},\mathbf{h},x_{mag},r_{socp+})}{\sqrt{n}}$ as functions of $x_{mag}^{(sc)}$

In this part we will show the numerical results that correspond to the theoretical ones given in part 2) in the previous subsection. We then set all parameters as in Figure 13 (these parameters are exactly the same as in experiments whose results we just presented above). Of course we again distinguish two cases: $\rho = 2$ and $\rho = 3$. For both $\rho = 2$ and $\rho = 3$ we ran 300 times each, (47) and (57) and again we ran (47) with $n = 600$ and (57) with $n = 2000$. The numerical results that we obtained for $\frac{Ef_{obj+}}{\sqrt{n}}$ and $\frac{E\xi_{prim+}^{(dep)}(\sigma,\mathbf{g},\mathbf{h},x_{mag},r_{socp+})}{\sqrt{n}}$ are shown in Figure 18. We again observe a solid agreement between the theoretical predictions and the results obtained through numerical experiments.

3) $\frac{E\|\mathbf{w}_{dep+}\|_2}{\sigma}$ and $\frac{E\|\mathbf{w}_{socp+}\|_2}{\sigma}$ as functions of $x_{mag}^{(sc)}$; varying r_{socp+}

In this part we will show the numerical results that correspond to the theoretical ones given in part 3) in the previous subsection. These results relate to possible variations in the r_{socp+} that can be used in (47). We then set all other parameters as in Figure 15 (these parameters are of course again different depending if we are considering $\rho = 2$ or $\rho = 3$).

a) Low (α, β_w^+) regime, $\rho = 2$

We first consider the $\rho = 2$ scenario. As in part 1) of this subsection we set $\alpha = 0.5$ and choose β_w^+ as in part 1). However, differently from part 1) we now consider two different possibilities for r_{socp+}, namely $r_{socp+} = \sqrt{0.05\alpha n}$ and $r_{socp+} = \sqrt{0.6\alpha n}$. We then ran (47) 300 times with $n = 600$ for various $x_{mag}^{(sc)}$. In parallel we ran (57) with $n = 2000$. The obtained results for $\frac{E\|\mathbf{w}_{socp+}\|_2}{\sigma}$ and $\frac{E\|\mathbf{w}_{dep+}\|_2}{\sigma}$ are shown on

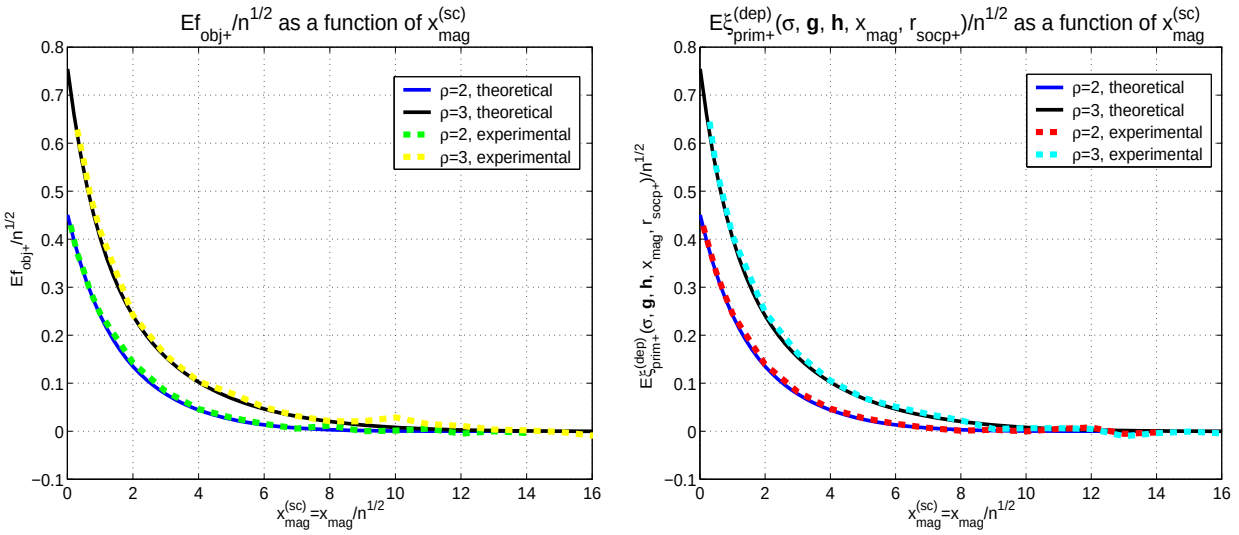

Figure 18: Experimental results for $\frac{Ef_{obj+}}{\sqrt{n}}$ and $\frac{E\xi^{(dep)}_{prim+}(\sigma,\mathbf{g},\mathbf{h},x_{mag},r_{socp+})}{\sqrt{n}}$ as a function of $x^{(sc)}_{mag}$; $\rho=2$, $r_{socp+}=\sqrt{0.2\alpha n}$; $\rho=3$, $r_{socp+}=\sqrt{0.1\alpha n}$; left — SOCP from (47); right — (57)

the left-hand and right-hand side of Figure 19, respectively. We also show in Figure 19 the corresponding theoretical predictions obtained in the previous subsection.

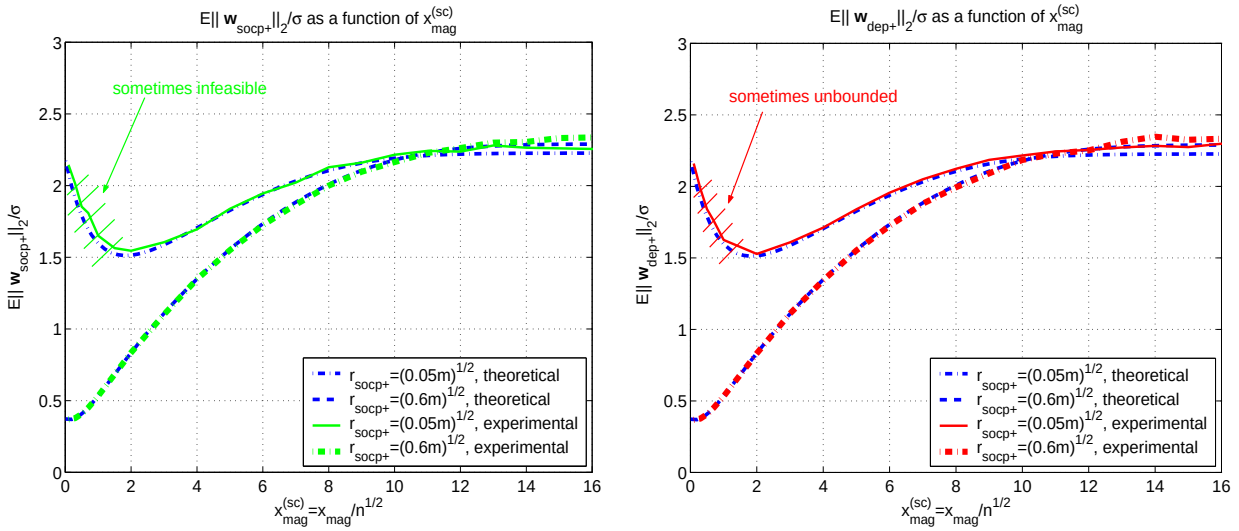

Figure 19: Experimental results for $\frac{E\|\mathbf{w}_{socp+}\|_2}{\sigma}$ and $\frac{E\|\mathbf{w}_{dep+}\|_2}{\sigma}$ as a function of $x^{(sc)}_{mag}$; $\rho=2$; $r_{socp+}\in\{\sqrt{0.05\alpha n},\sqrt{0.6\alpha n}\}$; left — SOCP from (47), right — (57)

b) High (α,β^+_w) regime, $\rho=3$

We also consider the $\rho=3$ scenario. As above, we set $\alpha=0.5$ and choose β^+_w as in part 1) of this subsection. Everything else remain the same as in $\rho=2$ case except the way we vary r_{socp+}. This time we consider (as in part 3) of the previous section when $\rho=3$ case was considered) $r_{socp+}=\sqrt{0.05\alpha n}$ and $r_{socp+}=\sqrt{0.5\alpha n}$. As usual (47) was run 300 times with $n=600$ for various $x^{(sc)}_{mag}$. In parallel we ran (57) 300 times with $n=2000$. The obtained numerical results for $\frac{Ef_{obj+}}{\sqrt{n}}$ and $\frac{E\xi^{(dep)}_{prim+}(\sigma,\mathbf{g},\mathbf{h},x_{mag},r_{socp+})}{\sqrt{n}}$ as well

Table 1: Experimental results for the noisy recovery through SOCP; $r_{socp+} = \sqrt{0.05m}$, $\sigma = 1$; (47) was run 300 times with $n = 600$; (57) was run 300 times with $n = 2000$

		$x_{mag}^{(sc)}$	0.1	0.3	0.5	0.7	1	2
$\rho = 2$	$r_{socp+} = \sqrt{0.05n}$	# of successes (47)	269	274	286	294	296	300
$\rho = 2$	$r_{socp+} = \sqrt{0.05n}$	# of successes (57)	268	278	281	287	299	299
$\rho = 3$	$r_{socp+} = \sqrt{0.05n}$	# of successes (47)	277	287	292	296	299	300
$\rho = 3$	$r_{socp+} = \sqrt{0.05n}$	# of successes (57)	270	274	288	294	299	299

as the corresponding theoretical predictions obtained in the previous subsection are shown on the left-hand and right-hand side of Figure 20, respectively. We again observe a solid agreement between the theoretical

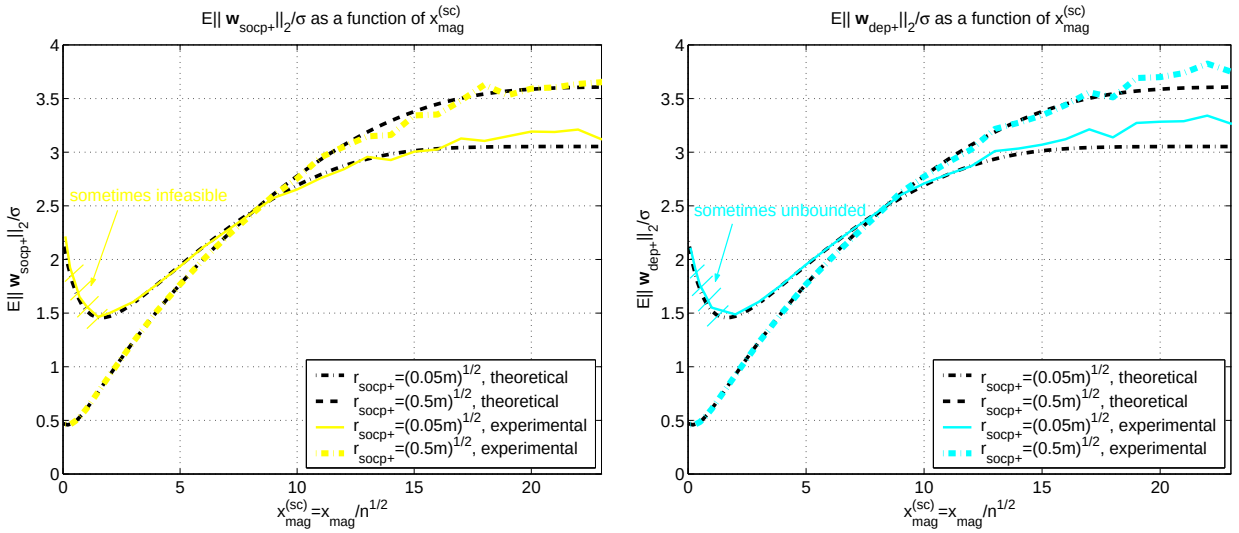

Figure 20: Experimental results for $\frac{E\|\mathbf{w}_{socp+}\|_2}{\sigma}$ and $\frac{E\|\mathbf{w}_{dep+}\|_2}{\sigma}$ as a function of $x_{mag}^{(sc)}$; $\rho = 3$; $r_{socp+} \in \{\sqrt{0.05\alpha n}, \sqrt{0.5\alpha n}\}$; left — SOCP from (47), right — (57)

predictions and the results obtained through numerical experiments. As in Section 2.2.2 small glitches that happen in large $x_{mag}^{(sc)}$ regime could have been fixed by choosing a larger n. We again purposely chose a smaller n to show that results are fairly good even when n is not very large. In fact, even a smaller n than the one that we have chosen would work quite fine.

Another observation related to Figures 19 and 20 (and several figures that will follow) is in place. For $r_{socp+} = \sqrt{0.05\alpha n}$ and roughly speaking $x_{mag}^{(sc)} \leq 2$ it may happen that (47) is on occasion infeasible and that (57) is unbounded. From a theoretical point of view this should not happen for any $x_{mag}^{(sc)}$. However, as discussed in Section 3.2.1, $\alpha = 0.5$ is in a sense a border line choice for universal feasibility. On the other hand, since all these claims are of "with overwhelming probability" type it may sometimes happen that even when $\alpha = 0.5$ (47) is infeasible and (57) is unbounded. In Table 1 we show the number of our experiments for which everything worked fined, i.e. for which (47) turned out to be feasible and (57) turned out to be bounded (we restrict only to what we call interesting region, which for this example we found to be roughly $x_{mag}^{(sc)} \leq 2$). We refer to such a number as the number of successes. The results in $r_{socp+} = \sqrt{0.05\alpha n}$ regime shown in Figures 19 and 20 are averaged over the feasible instances of (47) and the bounded instances of (57).

4) $\frac{Ef_{obj+}}{\sqrt{n}}$ ***and*** $\frac{E\xi^{(dep)}_{prim+}(\sigma,\mathbf{g},\mathbf{h},x_{mag},r_{socp+})}{\sqrt{n}}$ ***as functions of*** $x^{(sc)}_{mag}$***; varying*** r_{socp+}

In this part we will show the numerical results that correspond to the theoretical ones given in part 4) in the previous subsection. These results relate to behavior of $\frac{Ef_{obj+}}{\sqrt{n}}$ and $\frac{E\xi^{(dep)}_{prim+}(\sigma,\mathbf{g},\mathbf{h},x_{mag},r_{socp+})}{\sqrt{n}}$ when one varies r_{socp+} in (47). We again consider $\rho = 2$ or $\rho = 3$. The observations made above that relate to the occasional feasibilities do apply to the results presented in this part as well.

a) Low (α, β^+_w) *regime,* $\rho = 2$

The setup that we consider is exactly the same as the one considered in part 3a) of this subsection. We set $\alpha = 0.5$, chose β^+_w as in part 1), and considered two different possibilities for r_{socp+}, namely $r_{socp+} = \sqrt{0.05\alpha n}$ and $r_{socp+} = \sqrt{0.6\alpha n}$. The obtained results for $\frac{Ef_{obj+}}{\sqrt{n}}$ and $\frac{E\xi^{(dep)}_{prim+}(\sigma,\mathbf{g},\mathbf{h},x_{mag},r_{socp+})}{\sqrt{n}}$ are shown on the left-hand and right-hand side of Figure 21, respectively. The corresponding theoretical predictions obtained in the previous subsection are also shown in Figure 21.

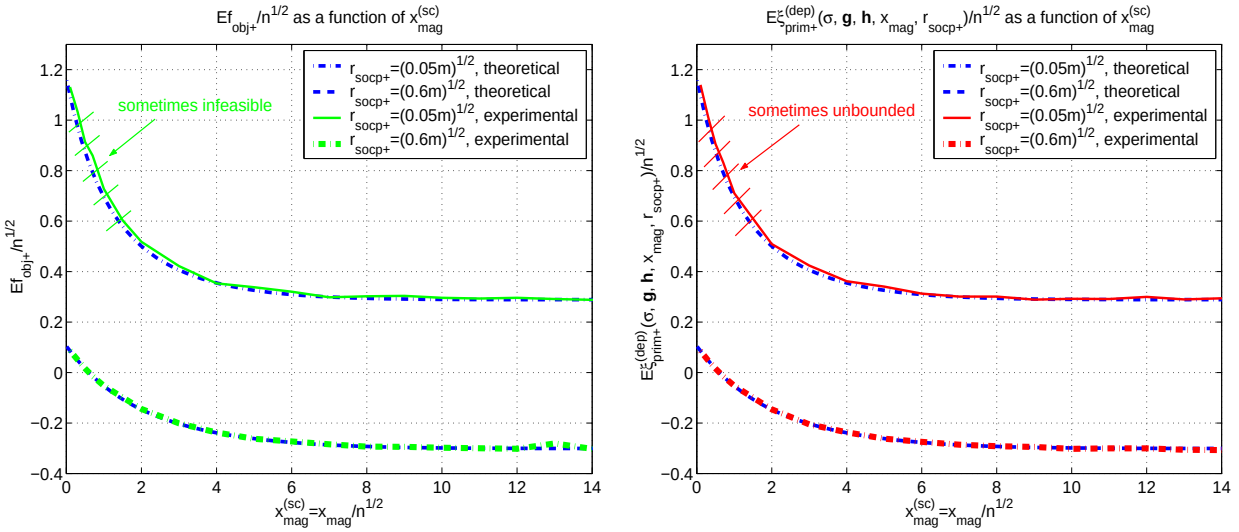

Figure 21: Experimental results for $\frac{Ef_{obj+}}{\sqrt{n}}$ and $\frac{E\xi^{(dep)}_{prim+}(\sigma,\mathbf{g},\mathbf{h},x_{mag},r_{socp+})}{\sqrt{n}}$ as a function of $x^{(sc)}_{mag}$; $\rho = 2$; $r_{socp+} \in \{\sqrt{0.05\alpha n}, \sqrt{0.6\alpha n}\}$; left — SOCP from (47), right — (57)

b) High (α, β^+_w) *regime,* $\rho = 3$

The setup that we consider is exactly the same as the one considered in part 3b) of this subsection. We set $\alpha = 0.5$, chose β^+_w as in part 1), and considered two different possibilities for r_{socp+}, namely $r_{socp+} = \sqrt{0.05\alpha n}$ and $r_{socp+} = \sqrt{0.5\alpha n}$. The obtained results for $\frac{E\|\mathbf{w}_{socp+}\|_2}{\sigma}$ and $\frac{E\|\mathbf{w}_{dep+}\|_2}{\sigma}$ are shown on the left-hand and right-hand side of Figure 22, respectively. The corresponding theoretical predictions obtained in the previous subsection are also shown in Figure 22. We again observe a solid agreement between the theoretical predictions and the results obtained through numerical experiments.

3.2.4 Numerical experiments — feasibility

In this section we will present a couple of numerical results that relate to the feasibility of (47) or unboundedness of (57).

1) $\frac{E\|\mathbf{w}_{dep+}\|_2}{\sigma}$ ***and*** $\frac{E\|\mathbf{w}_{socp+}\|_2}{\sigma}$ ***as functions of*** $x^{(sc)}_{mag}$

In this part we will show the numerical results that correspond to the theoretical ones given in part 1) in the previous subsection. We will restrict our attention to $\alpha = 0.7$ regime (we recall that earlier in Section

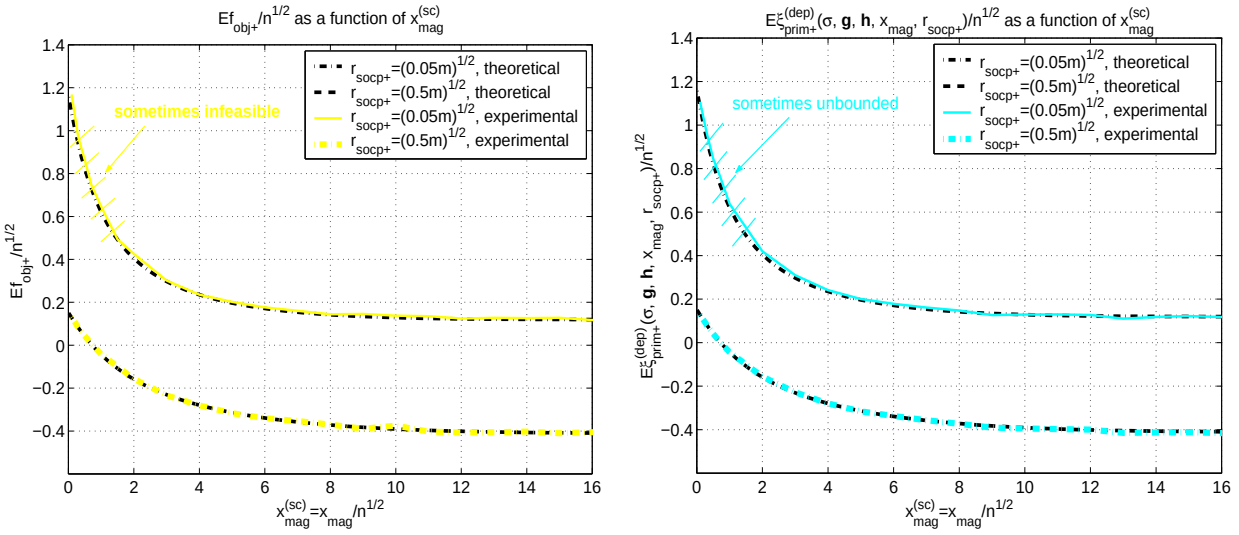

Figure 22: Experimental results for $\frac{Ef_{obj+}}{\sqrt{n}}$ and $\frac{E\xi_{prim+}^{(dep)}(\sigma,\mathbf{g},\mathbf{h},x_{mag},r_{socp+})}{\sqrt{n}}$ as a function of $x_{mag}^{(sc)}$; $\rho=3$; $r_{socp+}\in\{\sqrt{0.05\alpha n},\sqrt{0.5\alpha n}\}$; left — SOCP from (47), right — (57)

3.2.3 we showed the corresponding results one can get for $\alpha=0.5$ regime). We then set all other parameters as in the plot on the right hand side of Figure 13 (these parameters are of course different depending if we are considering $\rho=2$ or $\rho=3$; below we will consider both of them).

a) Low (α,β_w^+) regime, $\rho=2$

We first consider the $\rho=2$ scenario. We set $\alpha=0.7$, $r_{socp+}=\sqrt{\frac{\alpha n}{1+\rho^2}}=\sqrt{0.2\alpha n}$, and (as shown in [53]) β_w^+ such that (α_w^+,β_w^+) satisfy (50) and $\alpha_w^+=\frac{\rho^2}{1+\rho^2}\alpha$. We then ran (47) 100 times with $n=800$ for various $x_{mag}^{(sc)}$. In parallel we ran (57) for the exact same parameters with only two differences; namely we ran (57) 200 times with $n=4000$. The obtained results for $\frac{E\|\mathbf{w}_{socp+}\|_2}{\sigma}$ and $\frac{E\|\mathbf{w}_{dep+}\|_2}{\sigma}$ are shown on the left-hand and right-hand side of Figure 23. We also show in Figure 23 the corresponding theoretical predictions obtained earlier.

b) High (α,β_w^+) regime, $\rho=3$

We also conducted a set of experiments in the so-called "high" (α,β_w^+) regime. We used exactly the same parameters as in low (α,β_w^+) except that we changed ρ from 2 to 3. Consequently we chose $r_{socp+}=\sqrt{0.1\alpha n}$ and β_w^+ such that (α_w^+,β_w^+) satisfy (50) and $\alpha_w^+=\frac{\rho^2}{1+\rho^2}\alpha$. As above we ran 100 times (47) and 200 times (57). Also as above, we ran (47) with $n=800$ and (57) with $n=4000$. The numerical results obtained for $\rho=3$ together with the theoretical predictions are again shown in Figure 23. From Figure 23 we observe a solid agreement between the theoretical predictions and the results obtained through numerical experiments.

Remark: We do mention that in a range of $x_{mag}^{(sc)}$ close to the theoretical "breaking feasibility point" not all instances of (47) were feasible and not all instances of (57) were bounded (instead an overwhelming majority of them was). The results that are shown in Figure 23 are obtained by averaging over the feasible instances of (47) and the bounded instances of (57).

2) Feasibility/boundedness probability

In this part we show how the number of feasible instances of (47) and the number of bounded instances of (57) change as $x_{mag}^{(sc)}$ changes. We set $\alpha=0.7$ and considered the $\rho=3$ regime or in other words "high" (α,β_w^+) regime. As above we chose $r_{socp+}=\sqrt{0.1\alpha n}$ and β_w^+ such that (α_w^+,β_w^+) satisfy (50)

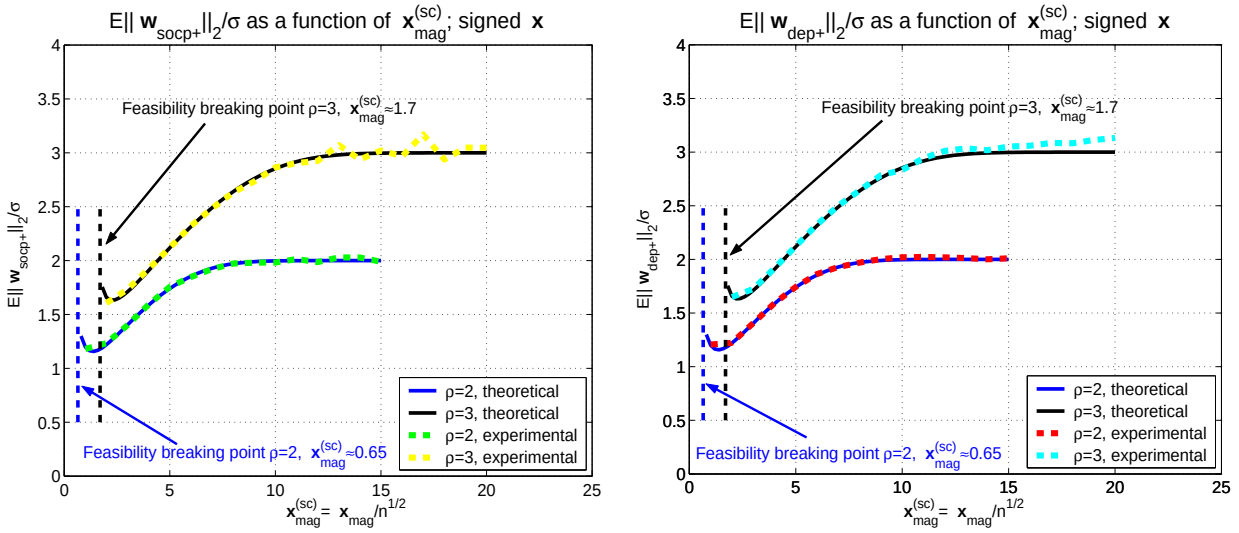

Figure 23: Experimental results for $\frac{E\|\mathbf{w}_{socp+}\|_2}{\sigma}$ and $\frac{E\|\mathbf{w}_{dep+}\|_2}{\sigma}$ as a function of $x_{mag}^{(sc)}$; $\alpha = 0.7$; $\rho = 2$, $r_{socp+} = \sqrt{0.2\alpha n}$; $\rho = 3$, $r_{socp+} = \sqrt{0.1\alpha n}$; left — SOCP from (47), right — (57)

and $\alpha_w^+ = \frac{\rho^2}{1+\rho^2}\alpha$. We then ran each of (47) and (57) 200 times. We ran (47) with $n = 1000$ and (57) with $n = 10000$. For a range of $x_{mag}^{(sc)}$ we recorded the fraction of instances where (47) was feasible. We refer to such a fraction as p_{socp+}. Simultaneously, for the same range of $x_{mag}^{(sc)}$ we recorded the fraction of instances where (57) was bounded. We refer to such a fraction as p_{prim+}. The numerical results along with the theoretical prediction for the feasibility breaking point are shown in Figure 24. From Figure 24 we observe a solid agreement between the theoretical predictions and the results obtained through numerical experiments.

4 Discussion

In this paper we considered "noisy" under-determined systems of linear equations with sparse solutions. We looked from a theoretical point of view at polynomial-time second-order cone programming (SOCP) algorithms. More precisely, we looked at a general framework developed for characterization of such algorithms in [53]. Within the framework we then considered what we referred to as the SOCP's *problem dependent* performance. We established the precise values of the norm-2 of the error vector for a wide class of unknown sparse vectors. We also provided a characterization of several important parameters that appear in solving of an SOCP.

Many further developments are possible (one can make essentially the same conclusion for the general framework developed in [53] as well as for the analysis of the LASSO algorithms presented in [52]). Any problem dependent scenario that can be solved in the so-called noiseless case through the mechanisms developed in [57] and [55] can now be handled in the noisy case as well. For example, quantifying performance of SOCP or LASSO optimization problems in solving "noisy" systems with special structure of the solution vector (block-sparse, box- and binary-sparse, partially known locations of nonzero components, low-rank matrix, just to name a few), "noisy" systems with noisy (or approximately sparse)) solution vectors can then easily be handled to an ultimate precision. In several forthcoming papers we will present some of these applications.

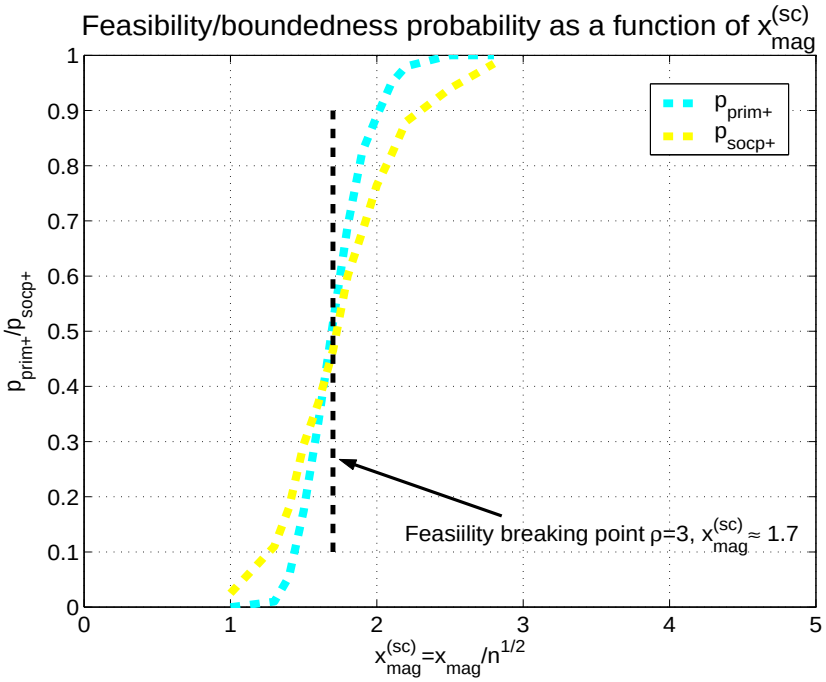

Figure 24: p_{socp+} and p_{prim+} as functions of $x_{mag}^{(sc)}$; $\rho = 3$; $\alpha = 0.7$; $r_{socp+} = \sqrt{\frac{\alpha n}{1+\rho^2}}$

References

[1] M. Akcakaya and V. Tarokh. A frame construction and a universal distortion bound for sparse representations. *IEEE Trans. on Signal Processing*, 56(6), June 2008.

[2] M. S. Asif and J. Romberg. On the lasso and dantzig selector equivalence. *44th Annual Conference on Information Sciences and Systems (CISS)*, pages 1–6, March 2010.

[3] R. Baraniuk, V. Cevher, M. Duarte, and C. Hegde. Model-based compressive sensing. available online at http://www.dsp.ece.rice.edu/cs/.

[4] M. Bayati and A. Montanari. The lasso risk of gaussian matrices. *Preprint*. available online at arXiv:1008.2581.

[5] R. Berinde, A. C. Gilbert, P. Indyk, H. Karloff, and M. J. Strauss. Combining geometry and combinatorics: A unified approach to sparse signal recovery. 2008. available online at http://www.dsp.ece.rice.edu/cs/.

[6] P. J. Bickel, Y. Ritov, and A. B. Tsybakov. Simultaneous analysis of lasso and dantzig selector. *The Annals of Statistics*, 37(4):1705–1732, 2009.

[7] F. Bunea, A. B. Tsybakov, and M. H. Wegkamp. Sparsity oracle inequalities for the lasso. *Electronic Journal of Statistics*, 1:169–194, 2007.

[8] E. Candes. Compressive sampling. *Proc. International Congress of Mathematics*, pages 1433–1452, 2006.

[9] E. Candes, J. Romberg, and T. Tao. Robust uncertainty principles: exact signal reconstruction from highly incomplete frequency information. *IEEE Trans. on Information Theory*, 52:489–509, December 2006.

[10] E. Candes, J. Romberg, and T. Tao. Stable signal recovery from incomplete and inaccurate measurements. *Comm. Pure Appl. Math.*, 59:1207–1223, 2006.

[11] E. Candes and T. Tao. Decoding by linear programming. *IEEE Trans. on Information Theory*, 51:4203–4215, Dec. 2005.

[12] E. Candes, M. Wakin, and S. Boyd. Enhancing sparsity by reweighted l1 minimization. *J. Fourier Anal. Appl.*, 14:877–905, 2008.

[13] E. Cands and T. Tao. The dantzig selector: statistical estimation when p is much larger than n. *Ann. Statist.*, 35(6):2313–2351, 2007.

[14] S.S. Chen and D. Donoho. Examples of basis pursuit. *Proceeding of wavelet applications in signal and image processing III*, 1995.

[15] S.S. Chen, D. L. Donoho, and M. A. Saunders. Atomic decomposition by basis pursuit. *SIAM, JOurnal on Scientific Computing*, 20:33–61, 1998.

[16] S. Chretien. An alternating ell-1 approach to the compressed sensing problem. 2008. available online at http://www.dsp.ece.rice.edu/cs/.

[17] G. Cormode and S. Muthukrishnan. Combinatorial algorithms for compressed sensing. *SIROCCO, 13th Colloquium on Structural Information and Communication Complexity*, pages 280–294, 2006.

[18] S. F. Cotter and B. D. Rao. Sparse channel estimation via matching pursuit with application to equalization. *IEEE Trans. on Communications*, 50(3), 2002.

[19] W. Dai and O. Milenkovic. Subspace pursuit for compressive sensing signal reconstruction. *Preprint*, page available at arXiv:0803.0811, March 2008.

[20] W. Dai and O. Milenkovic. Weighted superimposed codes and constrained integer compressed sensing. *IEEE Trans. on Information Theory*, 55(9):2215–2219, September 2009.

[21] D. Donoho. High-dimensional centrally symmetric polytopes with neighborlines proportional to dimension. *Disc. Comput. Geometry*, 35(4):617–652, 2006.

[22] D. Donoho, A. Maleki, and A. Montanari. The noise-sensitiviy thase transition in compressed sensing. *Preprint*, Apr. 2010. available on arXiv.

[23] D. Donoho and J. Tanner. Counting the face of randomly projected hypercubes and orthants with application. 2008. available online at http://www.dsp.ece.rice.edu/cs/.

[24] D. L. Donoho, M. Elad, and V. Temlyakov. Stable recovery of sparse overcomplete representations in the presence of noise. *IEEE Transactions on Information Theory*, 52(1):6–18, Jan 2006.

[25] D. L. Donoho, Y. Tsaig, I. Drori, and J.L. Starck. Sparse solution of underdetermined linear equations by stagewise orthogonal matching pursuit. *2007*. available online at http://www.dsp.ece.rice.edu/cs/.

[26] M. Duarte, M. Davenport, D. Takhar, J. Laska, T. Sun, K. Kelly, and R. Baraniuk. Single-pixel imaging via compressive sampling. *IEEE Signal Processing Magazine*, 25(2), 2008.

[27] B. Efron, T. Hastie, and R. Tibshirani. Discussion: The dantzig selector: statistical estimation when p is much larger than n. *Ann. Statist.*, 35(6):2358–2364, 2007.

[28] S. Foucart and M. J. Lai. Sparsest solutions of underdetermined linear systems via ell-q minimization for $0 < q \leq 1$. available online at http://www.dsp.ece.rice.edu/cs/.

[29] M. P. Friedlander and M. A. Saunders. Discussion: The dantzig selector: statistical estimation when p is much larger than n. *Ann. Statist.*, 35(6):2385–2391, 2007.

[30] A. Gilbert, M. J. Strauss, J. A. Tropp, and R. Vershynin. Algorithmic linear dimension reduction in the l1 norm for sparse vectors. *44th Annual Allerton Conference on Communication, Control, and Computing*, 2006.

[31] A. Gilbert, M. J. Strauss, J. A. Tropp, and R. Vershynin. One sketch for all: fast algorithms for compressed sensing. *ACM STOC*, pages 237–246, 2007.

[32] R. Gribonval and M. Nielsen. Sparse representations in unions of bases. *IEEE Trans. Inform. Theory*, 49(12):3320–3325, December 2003.

[33] J. Haupt and R. Nowak. Signal reconstruction from noisy random projections. *IEEE Trans. Information Theory*, pages 4036–4048, September 2006.

[34] P. Indyk and M. Ruzic. Fast and effective sparse recovery using sparse random matrices. 2008. avialable on arxiv.

[35] S. Jafarpour, W. Xu, B. Hassibi, and R. Calderbank. Efficient compressed sensing using high-quality expander graphs. available online at http://www.dsp.ece.rice.edu/cs/.

[36] G. James, P. Radchenko, and J. Lv. Dasso. Dasso: Connections between the dantzig selector and lasso. *J. Roy. Statist. Soc. Ser. B*, 71:127142, 2009.

[37] V. Koltchinskii. The dantzig selector and sparsity oracle inequalities. *Bernoulli*, 15(3):799–828, 2009.

[38] J. Mairal, F. Bach, J. Ponce, Guillermo Sapiro, and A. Zisserman. Discriminative learned dictionaries for local image analysis. *IEEE Conf. on Computer Vision and Pattern Recognition (CVPR)*, 2008.

[39] I. Maravic and M. Vetterli. Sampling and reconstruction of signals with finite rate of innovation in the presence of noise. *IEEE Trans. on Signal Processing*, 53(8):2788–2805, August 2005.

[40] N. Meinshausen, G. Rocha, and B. Yu. Discussion: A tale of three cousins: Lasso, l2boosting and dantzig. *Ann. Statist.*, 35(6):2373–2384, 2007.

[41] N. Meinshausen and B. Yu. Lasso-type recovery of sparse representations for high-dimensional data. *Ann. Statist.*, 37(1):246270, 2009.

[42] O. Milenkovic, R. Baraniuk, and T. Simunic-Rosing. Compressed sensing meets bionformatics: a new DNA microarray architecture. *Information Theory and Applications Workshop*, 2007.

[43] D. Needell and J. A. Tropp. CoSaMP: Iterative signal recovery from incomplete and inaccurate samples. *Applied and Computational Harmonic Analysis*, 26(3):301–321, 2009.

[44] D. Needell and R. Vershynin. Unifrom uncertainly principles and signal recovery via regularized orthogonal matching pursuit. *Foundations of Computational Mathematics*, 9(3):317–334, 2009.

[45] F. Parvaresh and B. Hassibi. Explicit measurements with almost optimal thresholds for compressed sensing. *IEEE ICASSP*, Mar-Apr 2008.

[46] F. Parvaresh, H. Vikalo, S. Misra, and B. Hassibi. Recovering sparse signals using sparse measurement matrices in compressed dna microarrays. *IEEE Journal of Selected Topics in Signal Processing*, 2(3):275–285, June 2008.

[47] B. Recht, M. Fazel, and P. A. Parrilo. Guaranteed minimum-rank solution of linear matrix equations via nuclear norm minimization. 2007. available online at http://www.dsp.ece.rice.edu/cs/.

[48] F. Rodriguez and G. Sapiro. Sparse representations for image classification: Learning discriminative and reconstructive non-parametric dictionaries. 2008. available online at http://www.dsp.ece.rice.edu/cs/.

[49] J. Romberg. Imaging via compressive sampling. *IEEE Signal Processing Magazine*, 25(2):14–20, 2008.

[50] R. Saab, R. Chartrand, and O. Yilmaz. Stable sparse approximation via nonconvex optimization. *ICASSP, IEEE Int. Conf. on Acoustics, Speech, and Signal Processing*, Apr. 2008.

[51] V. Saligrama and M. Zhao. Thresholded basis pursuit: Quantizing linear programming solutions for optimal support recovery and approximation in compressed sensing. 2008. available on arxiv.

[52] M. Stojnic. A framework for perfromance characterization of *LASSO* algortihms. available at arXiv.

[53] M. Stojnic. A performance analysis framework for *SOCP* algorithms in noisy compressed sensing. available at arXiv.

[54] M. Stojnic. A rigorous geometry-probability equivalence in characterization of ℓ_1-optimization. available at arXiv.

[55] M. Stojnic. Upper-bounding ℓ_1-optimization weak thresholds. available at arXiv.

[56] M. Stojnic. Block-length dependent thresholds in block-sparse compressed sensing. *submitted to IEEE Trans. on Information Theory*, 2009. available at arXiv:0907.3679.

[57] M. Stojnic. Various thresholds for ℓ_1-optimization in compressed sensing. *submitted to IEEE Trans. on Information Theory*, 2009. available at arXiv:0907.3666.

[58] M. Stojnic. Recovery thresholds for ℓ_1 optimization in binary compressed sensing. *ISIT, International Symposium on Information Theory*, June 2010.

[59] M. Stojnic, W. Xu, and B. Hassibi. Compressed sensing of approximately sparse signals. *ISIT, International symposium on information theory*, July 2008.

[60] R. Tibshirani. Regression shrinkage and selection with the lasso. *J. Royal Statistic. Society*, B 58:267–288, 1996.

[61] J. Tropp. Just relax: Convex programming methods for identifying sparse signals in noise. *IEEE Transactions on Information Theory*, 52(3):1030–1051, March 2006.

[62] J. Tropp and A. Gilbert. Signal recovery from random measurements via orthogonal matching pursuit. *IEEE Trans. on Information Theory*, 53(12):4655–4666, 2007.

[63] J. A. Tropp. Greed is good: algorithmic results for sparse approximations. *IEEE Trans. on Information Theory*, 50(10):2231–2242, 2004.

[64] S. van de Geer. High-dimensional generalized linear models and the lasso. *Ann. Statist.*, 36(2):614–645, 2008.

[65] H. Vikalo, F. Parvaresh, and B. Hassibi. On sparse recovery of compressed dna microarrays. *Asilomor conference*, November 2007.

[66] M. J. Wainwright. Sharp thresholds for high-dimensional and noisy recovery of sparsity. *Proc. Allerton Conference on Communication, Control, and Computing*, September 2006.

[67] J. Wright and Y. Ma. Dense error correction via ell-1 minimization. available online at http://www.dsp.ece.rice.edu/cs/.

[68] W. Xu and B. Hassibi. Efficient compressive sensing with determinstic guarantees using expander graphs. *IEEE Information Theory Workshop*, September 2007.